CHAPTER 4 – TABLE OF CONTENTS

LIST OF TABLES

List of Figures

4 REACTOR DESCRIPTION

4.1 Summary Description

The NBSR is a heavy water (D_2O) moderated and cooled, enriched fuel, tank-type reactor designed to operate at a thermal power level of 20 MW. There is no pulsing capability. The core is immersed in heavy water to thermalize fast neutrons to sustain the nuclear chain reaction, remove heat created by the reaction and serve as the first stage of shielding. Major reactor parameters are provided in Table 4.1.1.

The core is located in the lower section of an aluminum tank. Thirty-seven fuel element locations in addition to four semi-permanent irradiation thimble tubes are provided. Seven of the fuel element locations are specially adapted for thimble tubes, leaving only 30 positions available for fuel element assemblies. The fuel element is a MTR plate type element consisting of U_3O_8 mixed with aluminum powder contained in aluminum clad plates. Each fuel element contains an upper and lower fuel section separated by a gap resulting in a split core design. This "split-core" design, with uranium fuel placed above and below the mid-plane of the reactor, results in the thermal neutron flux reaching a peak in the center of the gap.

The large volume in the core provides very flexible capabilities for thermal neutron irradiation. Insertion of nine radial beam tubes and the "cold neutron source" into the gap allows high intensity beams, with low "background" from unwanted fast neutrons and gamma rays, to be extracted for thermal neutron scattering research. A pneumatic rabbit system provides researchers with the ability to automatically inject samples into the core region of the reactor while thimbles provide for their manual loading.

Routine operation of the reactor uses forced circulation of the primary coolant. Analysis has shown that the reactor may be operated at power levels of up to 500 kW (see App. A) without forced flow, for short times such that the temperature of the primary coolant does not exceed 45°C/113°F. Operations up to 10 kW without forced flow are permitted for any length of time since the heat generated by the core is insufficient to cause significant heating of the reactor coolant.

Two D_2O hold-up tanks ensure an adequate cooling water supply to the core in the event of a major rupture of the subpile piping. The inner reserve tank, located in the top reflector, can only be drained through two non-isolable pipes at the bottom of the tank. These pipes feed a distribution pan which routes emergency cooling water to the individual elements in the core. A second hold-up tank, which extends upward from the lower grid plate to a level above the lower fueled portions of the elements, keeps the lower core submerged in water and serves to collect any of the water from the inner reserve tank that splashes over the top of the distribution pan or runs down the outside of the fuel elements.

Heavy water acts as coolant, moderator and reflector. The side reflector is 20 inches (50.8 cm) thick, and the top reflector is approximately 118 inches (300 cm) thick. The top reflector is a

variable thickness reflector controlled by the operator. During normal operations, this level is 118 inches (300 cm) above the top of the core (the height of the inlet to the 3 inch (7.62 cm) overflow pipe). During fuel transfers, water is maintained at a level slightly above the core at the height of the upper grid plate elevation by the low-level overflow pipe, concentric with the 3 inch (7.62 cm) overflow pipe. During abnormal operations, a third overflow pipe concentric with the fuel element transfer chute, serves as a moderator dump to drop the water level to 1 inch (2.54 cm) above the core for emergency shutdown of the reactor.

4.2 Reactor Core

The reactor core is located in the lower section of an aluminum tank, 7 feet (2.13 m) in diameter by 16 feet (4.87 m) in height. The fuel elements are held in place by upper and lower grid plates. The grid plates provide for 37 fuel element positions and four 2.5 inch (6.35 cm) semi-permanent irradiation thimbles. Seven of the fuel element locations are especially adapted for 3.5 inch (8.89 cm) experimental thimbles, leaving 30 positions for fuel element assemblies. The 37 positions are placed in 7 rows to form a hexagonal pattern with the rows oriented east to west in the core. The fuel is contained in three rings within this hexagonal pattern, with the inner two rings having 6 fuel elements each and the outer ring having the remaining 18 fuel elements. The 7 experimental thimble positions form a circular pattern about the center location. The fuel element assemblies are located on 6.9 inch (17.5 cm) centers in the NBSR core. Each of the 30 fuel elements fits into a unit cell; the cell locations are fixed by openings in the grid plates. Figures 4.2.1 and 4.2.2 provide cross-sectional views of the reactor, including the core.

Control of the reactor is achieved by four semaphore-type shim safety arms and one automatic regulating rod. Primary control of the reactor is accomplished by use of the four shim arms. They are used to attain criticality on start up, make major changes in the power level of the reactor, and compensate for reactivity changes that occur as a result of xenon, temperature, and fuel burnup. Fine control of the reactor is accomplished by the use of the regulating rod. The four-shim arms are mounted on hanger brackets just under the upper grid plate. The regulating rod is located in a 3.5-inch (8.89 cm) vertical thimble. The locations of the shim arms and the regulating rod are shown in Figure 4.2.1.

Normally, sufficient photoneutrons are available for startup. After extended shutdowns, the strength of this neutron source may be insufficient to provide indication on the nuclear instrument channels and for reactor startup. On these rare occasions, a 2-curie Americium/Beryllium neutron source is inserted into the core region to provide sufficient source neutrons for reactor startup.

Heat generated by fission is removed from the core by means of the primary coolant system. Coolant enters through a plenum at the bottom of the fuel, passes up through the fuel and into the reactor vessel, and then out through two outlet pipes in the bottom of the vessel. A certain amount of freedom in the arrangement of the fuel elements within the core is made possible by the use of the double plenum, system. The inner six fuel positions and the central thimble are fed by one plenum while the remaining fuel and thimbles are fed by a concentric plenum. The primary coolant passes out of the reactor and flows through pumps and plate-type heat

exchangers before returning to the reactor vessel, in a closed loop. The helium blanket system keeps a small pressure of helium of about 4 inches of water (1kPa) on the reactor and allows for the recovery of any D_2O lost from the system due to evaporation. A detailed description of the primary coolant system and the helium sweep system are given in Sections 5.2 and 9.5 respectively.

Seven of the fuel element locations are especially adapted for 3.5 inch (8.89 cm) experimental thimbles. A pneumatic rabbit system provides the ability to automatically inject samples into the core region of the reactor for irradiation. Nine radial beam tubes, a 'cold' neutron source, and a thermal column extract thermal neutrons from the reactor core region for the numerous experimental stations.

4.2.1 Reactor Fuel

At the present, the NBSR reactor utilizes only the MTR plate type fuel element. No plans exist for the use of partial elements, shim arm elements, instrumented elements, or special elements for experimental facilities.

Compliance with NBSR safety limits applicable to reactor power, and reactor coolant flow and temperature will ensure fuel cladding integrity and prevent the release of fission products into the primary coolant.

4.2.1.1 Fuel Composition

The nuclear fuel is a U_3O_8 plus aluminum powder dispersion fuel, enriched to 93±1% ^{235}U. All materials used in the NBSR fuel element contain less than 10 ppm of boron and 30 ppm of cadmium. The fuel core is a slug type design, and the U_3O_8 - Al fuel contains 35 weight percent enriched uranium. Each element has two fuel sections with seventeen fuel plates per section. The ^{235}U content of each element is 350 ± 3.4 grams. Each fuel plate contains 10.294 ± 0.20 grams of ^{235}U. The aluminum powder used as a melting stock for the fuel is ATA 101 (or equivalent). The chemical requirements for the powder is provided in Table 4.2.1. Hot rolling ensures metallurgical bonding between the clad and fuel materials. After blister testing, the plates receive a final cold reduction of not less than 15%. Final curving is accomplished over a warm die. No burnable poisons or neutron moderators are added to any of the fuel elements. Table 4.2.2 provides the material and physical properties of the NBSR fuel. A typical NBSR fuel plate contains about 13 g of U_3O_8 and 19 g of Al in the 8.9 cm^3 available for the fuel meat. The resulting volume fractions are approximately 18% U_3O_8, 78% Al, and about 4% void.

4.2.1.2 Fuel Element Description

Figure 4.2.3 illustrates a typical fuel element assembly. The fuel is contained in curved fuel plates approximately 13 inches in length by 2.793 inches in width by 0.050 inches in thickness (33 cm length by 7.094 cm width by 0.127 cm thick). The dimensions of the core, or fuel meat, in each plate is 11 inches in length by 2.436 inches in width by 0.020 inch thick (27.94 cm by 6.187 cm by 0.0508 cm), and the cladding thickness is 0.015 inches (0.0381 cm). The radius of

curvature is 5 .5 inches (13.97 cm). Figure 4.2.4 illustrates top and bottom flat short fuel plates. Each fuel element contains an upper and a lower fuel section separated by a 7 inch (17.78 cm), non-fueled gap. Each plate has a half-inch (1.27 cm) unfueled region in this gap, and a 1½ inch (3.81 cm) unfueled region at its opposite end. The overall length of the fuel element assembly is approximately 68.8 inches (1.75 m).

Support for the fuel is provided by two curved outside plates, unfueled, and two flat side plates which form a box section for the full length of the assembly between the upper and the lower adapters. The thickness of the two unfueled outside plates is 0.065 inches (0.165 cm) (slightly thicker than a fuel plate). The thickness of the two side plates is 0.188 inches (0.478 cm). The side plates have 19 slots 0.095 inches (0.241 cm) deep to receive the 17 fuel plates and two end plates. The fuel plates and the curved outside plates are held in place by the two side plates by swaged mechanical connections. By utilizing curved fuel plates, the effects of heating on the mechanical joints of a fuel assembly are minimized. The fuel elements are located in a hexagonal array on 6.9-inch (17.5 cm) centers in the NBSR core. Each element fits into a unit cell of 3.20 inches by 3.89 inches (8.13 cm by 9.88 cm), defined by rectangular openings in the top grid plate and holes in the bottom grid plate. This arrangement provides sufficient space between elements, such that tolerances on the outer configuration of the fuel element assemblies are not of primary importance.

The fuel plate core frames and cladding are aluminum Alloy 6061-Temper 0 (ASTM B209). The unfueled curved outside plates and the side plates are fabricated from Alloy 6061-T6 aluminum (ASTM B209). The upper and lower castings are A356.0-T6 aluminum (ASTM B618, Class/Grade 3/C).

The upper and lower end castings are welded to the box section formed by the two unfueled outside curved plates and two side plates. The lower adapter is attached with a full seam weld to form a watertight joint. The upper adapter is welded to the two side plates. The bottom adapter serves as both an inlet nozzle and a ‘check’ valve. Coolant enters the internal passage of the bottom adapter, flows up through the internal conical transition section to the lower portion of the box section, through the 18 channels defined by the curved fuel plates and curved outside plates of the lower fuel section, into the unfueled region, 6 inches (15 cm) of which contains no fuel plates, into the 18 channels of the upper fuel section, and then through the upper box section and out the top adapter. A small amount of coolant, 4%, bypasses the external surface of the lower nozzle, creating a .012-inch (0.030 cm) gap, preventing bulk stagnation in the moderator. This bypass flow is possible only when the exterior conical section of the lower adapter is lifted from a mating conical seat in the lower grid plate. The fuel element is spring loaded down by a latching mechanism. The lifting force necessary to achieve this bypass flow results from the hydraulic drag of the coolant on the fuel assembly. Should flow cease for any reason, the fuel elements will be forced down on the seats and retain a portion of the bulk coolant in a pan-like structure that surrounds the core up to mid-fuel height (Section 7.1). Thus the bottom adapters act as check valves, allowing the upward bypass flow when the primary coolant pumps are operating, but preventing the draining of the holdup pan if there is no flow.

The upper adapter contains the spring loaded cross bar lock mechanism that locks the fuel elements into the grid plate structure (Figure 4.2.5). When the fuel element has been fully inserted through the upper grid plate into the lower grid plate, additional pressure on the handling head will compress the spring bringing the cross bar down inside the upper adapter, to a position just under the upper grid plate. Counter-clockwise rotation of the handling head rotates the cross bar such that the ends of the cross bar project through the side windows of the upper adapter and pass under the bottom surface of the upper grid plate. Release of the downward force allows the spring to pull the cross bar up into small notches in the bottom surface of the upper grid plate, thus locking the fuel assembly between the grid plates.

Fresh NBSR fuel assemblies are shipped to the NBSR prior to the start of refueling shutdowns. For the brief time between arrival and insertion into the reactor, the assemblies are stored in the fuel vault (Section 9 discusses new fuel storage). Upon discharge from the core, spent fuel assemblies are transferred to the fuel storage pool by the fuel handling system. Storage of new and spent fuel is discussed in Section 9.2.

4.2.1.3 Fabrication

Fabrication of NBSR fuel elements is in accordance with standard industry techniques for the manufacture of MTR plate type fuel elements and the NIST specification for aluminum clad fuel elements (NIST, 2004a). Prior to insertion into the core, new fuel element assemblies are subjected to stringent quality assurance. The manufacturer inspects the fuel assemblies, in accordance with U.S. Department of Energy requirements.

After each fuel plate is hot rolled bonded, it is blister tested by being heated to 900°F (482 °C) and held at that temperature for one hour. Any plate exhibiting evidence of blistering or lamination is rejected. After blister testing, each plate is ultrasonically tested for voids, inclusions, or other discontinuities; any such irregularities are cause of rejection. Cladding thickness and grain growth are verified microscopically by destructively testing a randomly selected plate from each batch of 100 rolled plates. If cladding thickness less than 0.0105 inch (0.0267 cm) or grain growth of less than 20% across all boundaries is found, three additional randomly selected plates from the batch are sampled and analyzed. If any sample value from these three additionally tested plates fails, the entire batch of 100 plates is rejected.

Prior to forming, each fuel plate is examined by x-ray procedures (e.g., fluoroscope, radiographic or homogeneity scanner) to ensure that the location of the fuel core and aluminum edging around the fuel core meet the design requirements. The surface density for any 0.080-in (0.20 cm) spot within the fuel shall not exceed 27% that of a standard, using an x-ray beam transmission technique. Prior to assembly, the surface of the aluminum cladding on the fuel bearing section is examined for pits, scratches and dents. Pits or scratches greater than .005 inch deep (.013 cm) over fuel or .006 inch (0.015 cm) on any other surface will result in rejection of the plate. Dents greater than 0.250 inch (0.06 cm) in diameter and/or greater than .006 inch (0.015 cm) deep will also result in rejection of the plate. Welds are inspected for evidence of cracks, inclusions, and inadequate penetration. Unsatisfactory welds are repaired to meet the specifications. The efficiency of the roll swaging assembly technique is tested by determining the force which is

necessary to fail test sections. A minimum joint strength of 150 lbs. per linear inch (26.8 kg per linear cm.) of roll swaged joint is required. The assembly of fuel elements in the production run is done in the same manner and by the same operations used in the fabrication of satisfactory pull test specimens.

After assembly of the fuel element, the water channel spacing is measured along the element centerline for each channel of each element. These measurements, together with the other dimensional measurements are submitted as part of the inspection data on each fuel element. Certified copies of reports identifying all materials used in the fabrication of the fuel assembly are also required. Before accepting fuel element assemblies, a full dimensional check, including water channels, as well as a complete visual check for surface defects on fuel plates are made for each fuel element at the manufacturer's facility by NIST personnel.

Each fuel element is assigned a unique serial number, which is recorded along with the melt serial number, the U-235 enrichment fraction for that melt, and the U-235 content of the core based on the melt chemical analysis and core weight. Each core plate is assigned a unique serial number, which is recorded along with the core numbers. These fuel plate numbers are then recorded, along with their position in a serial numbered fuel element. The serial number for the fuel element is engraved on both side plates, one each adjacent to each half of the split fuel core. Thus, when a cut is made through the gap for disposal purposes, both ends will have unique identifying numbers.

4.2.1.4 Development History of MTR Fuel

The enriched uranium fueled plate type element with aluminum or a structural cladding material has a long and trouble-free history in research and test reactor technology. All of the variations in the basic plate type element derive from the MTR design and development work done circa-1950. The MTR commenced operation in 1952. Since then, a variety of reactors using the same general type of element have been built and operated in this country and abroad. The NBSR has been operating since 1967. This basic plate type fuel element, operating at coolant conditions and power densities far more severe than those of the NBSR, has many hundreds of megawatt years of successful operating experience. There have been only two changes of significance to the original NBSR fuel element design: the elimination of unfueled interior plates, and step-wise increases in the U-235 fuel loading (170 grams to the current 350 grams).

The outer shell of the NBSR fuel element represents the only major variation from the classic MTR plate type fuel element. Since this outer shell controls the establishment of the proper hydraulic regime for heat transfer purposes, confirmation of the structural and hydraulic design objectives was accomplished on a hydraulic stand, using a fuel element assembly fitted with dummy plates. Flow rates of 30 ft/sec which are over two times those seen in operation, (9.1 m/sec) were employed to measure flow conditions in each channel and across typical channels as well as the total pressure drop, drag forces, bypass flow around the lower nozzle, and the vibration characteristics of the spring loaded element lock. The predicted performance of the NBSR fuel element design was confirmed. The primary features of uniform flow delivered to all channels, lack of structural deformation and absence of vibration were all proven. Operating

experience with NBSR fuel elements has been excellent. The design and manufacturing of the fuel element assemblies has been proven to be extremely reliable and durable. Table 4.2.3 provides a comparison of key reactor parameters to other similar high power density research and test reactors.

The corrosion history of aluminum MTR type fuel elements has been studied extensively. Fuel plates of the same basic configuration and the same material as those used in the NBSR fuel elements have been operated at higher flows, higher temperatures and at much higher heat fluxes than are achieved in the NBSR. All of these factors generally increase the corrosion rate and yet corrosion of the fuel elements during lifetimes comparable to those in the NBSR has not been a problem from the standpoint of structural integrity. No NBSR element has exhibited significant signs of corrosion or symptoms of corrosion damage. The lifetime of the NBSR fuel element is typically one year (burn up limited).

The U_3O_8 – Al dispersion fuels have been in widespread use for over forty years; extensive testing of fuel plates to determine the limits on fission density as a function of fuel loading has been performed. Since the fuel loading is about 10.3 g per plate, the ^{235}U density is 3.0×10^{27} atoms/m^3. Assuming all the fuel was consumed, the maximum possible fission density would be 2.6×10^{27} fissions/m^3 (14% of the neutrons absorbed produce ^{236}U). With a burnup of 73% in the 8-cycle fuel elements, the typical fission density is 1.9×10^{27} fissions/m^3.

Figure 4.2.6 shows the results of several measurements of swelling in fuel plates (Snelgrove, 1994). The curve represents the maximum burnup for a given fuel loading; MTR type plates with U_3O_8 fuel mixtures below the curve had acceptable levels of swelling. Upon irradiation, some of the fuel meat is transformed into U_4O_9, and a mixed UAl_4-Al_2O_3 phase. Though fission gas bubbles are observed in the Al_2O_3, so long as the reacted fuel particles remain largely isolated, as in a moderately loaded dispersion, swelling will be modest and predictable. NBSR fuel is moderately loaded at 18%, and the 8-cycle fission density is well below the curve. In general, dispersion fuels swell at a rate of 3 ± 1 % per 10^{27} fissions/m^3, so the expected swelling in the NBSR fuel plates would be between 4 and 9%.

Irradiated fuel plates have also been subjected to high temperatures in order to determine limits for fission product release. Blistering of the U_3O_8 plates occurs between 450 and 550 ºC (842-1022 °F). Since breaking of the fuel particles often precedes blistering, fission gasses are first released through microcracks that develop as blisters form. The maximum allowable fuel clad temperature is therefore 450 ºC (842 °F) (Snelgrove, 1994).

4.2.1.5 Technical Specifications

There is one technical specification concerning the fuel elements:

Technical Specification 5.3, Reactor Core and Fuel:

(1) The reactor core may consist of up to 30 (3.0 x 3.3 inch) MTR curved plate type fuel elements. The NBSR MTR-type fuel elements shall be such that the central seven (7)

inches of the fuel element contains no fuel. The middle six (6) inches of the aluminum in the unfueled region may be removed.

(2) the side plates, unfueled outer plates, and end adaptor castings of the fuel element shall be aluminum alloy .

(3) the fuel plates shall be uranium-aluminum alloy ; aluminum-uranium oxide or uranium-aluminum clad with aluminum.

Basis:

The neutronic and thermal hydraulic analysis (SAR, NBSR 14, Chapter 4) was based on the use of the NBSR MTR-type thirty-four (34) plate fuel element. The NBSR fuel element has a seven (7) inch centrally located unfueled area, in the open lattice array. The middle six (6) inches of aluminum in the unfueled region has been removed. The analysis requires that the fuel be loaded in a specific pattern (SAR, NBSR 14, Chapters 4 and 13). Significant changes in core loading patterns require a recalculation of the power distribution to ensure that burnout ratios shall be within acceptable limits.

4.2.2 Control Rods

The NBSR employs two emergency shutdown mechanisms. The primary one uses the shim safety arms. The second (or backup system) is called the moderator dump system which dumps the top reflector to a level 1 inch (2.54 cm) above the core. The NBSR has two types of control rods. Primary control of the reactor is accomplished by use of four semaphore type shim safety arms. Fine control of the reactor is accomplished by the use of a regulating rod. The location of the shim arms and the regulating rod are shown in Figures 4.2.1 and 4.2.2. NBSR shutdown using the shim arms can be accomplished by: rundown (electrical driven insertion of all shim safety arms and the regulating rod at normal operating speed), scram (spring-assisted gravity insertion of all shim safety arms) and major scram (same as scram plus the automatic isolation of the confinement building).

4.2.2.1 Shim Safety Arms

The detailed design of the NBSR shim safety arms is shown in Figures 4.2.7 through 4.2.10. These shim safety arms are identical to those used in the CP-5 reactor with the exception of a slight increase in length. The reactor operator manually controls the shim safety arms, either individually or as a bank. A scram signal automatically inserts all four shim safety arms into the core to shutdown the reactor and to place it in a subcritical mode.

The shim safety arms contain 0.040 inch (0.102 cm) thick cadmium poison plates (99.9% pure) clad with 1100 series aluminum on both sides. Each shim arm is 1 inch thick by 5 inches wide (2.54 by 12.7 cm) with a 52 inch (132.1 cm) poison length. The shim safety arms have a hollow interior filled with helium. Figure 4.2.7 shows the detailed design of the shim safety arm. Each shim arm is mounted on hanger brackets just under the grid plate. The shim safety arms are located between the inner five rows of fuel elements with an east to west orientation symmetrical

about the center row of the core (as shown in Figure 4.2.2). The drive shafts penetrate the reactor vessel below the water level and drive the shim arms directly. The vessel penetrations are sealed and made leak tight with rotating seals and the drive mechanisms are mounted in recesses in the biological shield. Figure 4.2.8 shows the shim safety arm assembly while Figure 4.2.9 shows the shim safety arm drive shaft assembly.

The blade portion of the NBSR shim safety blades is rough formed by assembling three concentric tubes to form an aluminum-cadmium-aluminum sandwich. The aluminum tubes are seamless extrusions and the cadmium tube is rolled to the needed diameter. This sandwich section is then collapsed to the approximate configuration of the completed arm. The ends of the section are seal-welded to prevent entry of lubricants or other foreign matter. The section is then mounted on a draw bench where roughing and finishing dies are drawn through the inside of the section. Small inelastic strains occur which bring the section to its final dimension and, more importantly, ensure contact between the cadmium and the aluminum at all points.

The components of the shim safety blades and the final assembly are inspected for adherence to all design requirements and tolerances. Radiography of completed blades is performed and the results compared to representative standards to ensure extrusion of Cd into any voids that existed before the drawing operation and for the absence of new voids or inclusions. After complete assembly of each unit, all welds are radiographed and visually examined for cracks, checks, and absence of penetration or undercut.

The void in the blade section is then repeatedly evacuated and purged with helium and seal welded shut. Helium at just slightly above atmospheric pressure (15 psig) is left in the void.

Each NBSR shim safety arm has an operational travel of 41^{o} and a maximum travel of 50^{o}. The full-in position is when the blade centerline is 41^{o} below horizontal. Full retraction brings the blade to its horizontal position in the top reflector above the core just below the upper grid plate.

The blades are supported by a hub-unit that rides on two ball bearings. These bearings are mounted in a hanger bracket. Each hanger bracket is inserted into one of two mounting brackets and bolted in place. The mounting brackets are the same ones used to support the grid plate. The hanger brackets are bolted to the reinforcing ring that is welded to the vessel. Beneath these hanger brackets, shim arm guides are welded to the vessel wall to position the shim arms at the proper angle for installation. Shim arm guide extensions, or ‘catchers’, were added to prevent an arm from falling out of the core in the event of a broken shim arm or shaft. The catchers are located just below the down positions of the arms.

The drive systems and shock absorbers are mounted on the biological shield. A stainless steel, splined shaft connects the drive units to the arm assemblies. The drive shafts are inserted into the hub of the shim arms from the side, through the vessel wall. An outer bearing assembly supports the shaft and an inner bearing-seal assembly, both of which are accessible from the shim arm cavities in the biological shield.

The shim arm drive (Figure 4.2.10) essentially consists of a large compression spring that is compressed by a ball nut and screw jack when the shim arm is raised. The shim arm shaft is connected to the housing that holds the ball nut. As a result, the shim arm is raised or lowered as the nut rides up and down the screw.

The ball screw jack is driven, in turn, by an electric motor, through a high ratio gear case and finally through an electromagnetic clutch. When the arm is raised, the compressed spring is pushing on the very low friction ball nut, attempting to force it back down to its rest position. This would require the screw to turn, but it cannot turn because it is connected through the clutch to the output shaft of the high ratio gearbox. Should the clutch be disengaged, however, the screw is free to turn and the spring will ram the nut, and so the shim arm, back to the "in" position.

The reactor operator manually controls the drive motor. The power to move the shim arm in or out comes from the Rod Drive Power. Power for the clutch comes from the output units of the Nuclear Instrumentation. Digital position indication is provided to the operator on the reactor control panel by a potentiometer coupled to the shim safety arm drive shaft. All electrical power for control and indication comes from the Critical Power Panel.

The energy of the shim safety arms due to a rapid return or scram is absorbed by a hydraulic shock absorber. This shock absorber is mounted on the biological shield, adjacent to the drive package. A mechanical stop, to prevent over travel of the arm should the shock absorber bottom out, is located on the linkage that connects the shim arm shaft lever to the shock absorber. All impact loads are, therefore, borne by the biological shield.

To prevent over travel during normal operation of the shim arm, installed upper and lower limit switches are set to approximately 41^{o} and 2^{o}, respectively. This ensures that the shim arm is not driven over the full range of its travel and into the upper grid plate or the shim arm catcher.

The shaft connecting the drive package and the shim arm must be sealed where it passes through the vessel wall. This is accomplished with a mechanical bellows type seal. The original seal units were tested at 50 psi (3.4 atmospheres) water pressure both by the manufacturer before shipment and when installed at the NBSR. Since the seals are exposed to a maximum operating pressure of 3.5 psi (0.24 atmospheres), no leakage is expected. Bearing-seal assemblies installed after 1984 are of stainless steel, replacing the original carbon steel units.

The total reactivity worth of the four shim safety arms is approximately 26.4 % (at end of cycle). The maximum reactivity insertion rate using all four shim safety arms is 4.5×10^{-4} $\Delta\rho$/sec (5.0×10^{-4} $\Delta\rho$/sec is the Technical Specification limit, see Section 4.2.2.6). A shim arm withdrawal accident for the NBSR is analyzed in Chapter 13 and in Appendix A using the technical specification for the maximum insertion rate. The analysis showed that the most severe accident is bounded by the maximum reactivity insertion accident, and will not result in core damage.

The design of the NBSR core is such that it is possible to shut the reactor down from its most reactive state with the most reactive shim safety arm stuck in the fully withdrawn position.

Although the NBSR could maintain a substantial shutdown margin with less than four shim arms, flux and shim arm worth distortions could occur by operating in this manner. Redundancy is achieved by the use of four separate shim arms instead of using a single arm for shutdown. The moderator dump (discussed in section 5.2.6) provides additional redundancy by providing a second, independent method of shutting down the reactor and maintaining it in a shutdown condition.

The lifetime of the shim arms is affected by poison burnup, corrosion and radiation damage. Under normal operating conditions, shim safety arms have a lifetime of approximately 21,000 MW-days. As will be discussed below, the latter two effects are not nearly as limiting as the poison burnup rate. The poison in each shim arm consists of a total thickness of 0.080 inches (0.20 cm) of cadmium. The burnup rate during shutdown, when the shim arms are fully inserted, is negligible compared to the burnup rate during operation. In the presence of the shim arms, the flux will fall rapidly with distance above the core so the shim arms will burnup much more rapidly along their bottom edges. Due to the effect of the shim arms, the flux is significant only to the bottom 2 inches (5.08 cm) of the arm. It will take in excess of four years of 250 days per year full power operation to reduce the shutdown margin below an acceptable level, with one shim arm fully withdrawn. Even a very thin section of cadmium is just as black to thermal neutrons as a thick sheet, so the shutdown margin is only changed by complete cadmium burnup in a large fraction of the arm.

The fact that corrosion does not limit the shim arm lifetime is demonstrated by the fact that similar arms remained in the CP-5 reactor for approximately 8 years until poison burnup required their replacement. Over thirty years of operation of the NBSR reactor have shown this to also be true for the NBSR shim arms.

The radiation damage to the shim safety arms is not significant during reactor operation since the shim arms are in the top reflector above the core where the fast neutron flux is relatively low. Shim arm sets have been replaced at the NBSR reactor three times, with no radiation damage apparent in the shims removed.

4.2.2.2 Regulating Rod

The regulating rod consists of a solid aluminum cylinder, 2½ inches in diameter by 29 inches long (6.35 by 74 cm). It is located in the 3½-inch (8.9 cm) vertical thimble (Figure 4.2.1 and 4.2.2). The rod is driven by a standard commercial design vertical drive mechanism mounted in the top plug. The regulating rod acts as a poison designed with a reactivity worth approximately 0.58 $\Delta\rho$ (see Section 4.5.1.5.3 for additional details). The low absorption cross-section of the poison ensures the long life of the absorbing atoms and the spreading out of the poison over a large volume minimizes the local thermal flux depression. The regulating rod with these features, combined with the location of the rod near the center of the reactor, causes only a 1-2% perturbation of the thermal flux at the beam holes as the rod is moved.

The drive train consists of two 2-phase electric servo motors in parallel which drive an extremely accurate lead-screw nut combination. An extension shaft mounted on the nut at one end carries

the regulating rod at the other. As the screw revolves, the nut, and thus the regulating rod, moves up or down at a fixed rate. The nominal rate of movement, 29 inches (74 cm) per 15 seconds, is determined by the motor speed and the pitch of the lead screw. Drive power for the two servo motors comes from the flux controller card in the NC-5 channel of the Nuclear Instrumentation.

Analog position indication is provided to the operator on the reactor control panel by a servo-synchro. Position indication servos are connected to the motor shaft through servo gear trains. Regulating rod position indicator synchros mounted on the main control panel show the rod position accurate to 0.02 inches (0.05 cm).

The total rod travel is 29 inches (74 cm). Limit switches mounted in the drive package are used to indicate and limit the extremes of travel as well as to signal the operator when the rod is within 7 inches (18 cm) of the fully inserted or the fully withdrawn positions. Knowing this, the operator adjusts the shim arms to keep within the lower and upper limits of the regulating rod travel. On a scram or rundown signal, the regulating rod is also driven to its fully inserted position.

Since the regulating rod poison is the aluminum that the rod is fabricated from, poison burnup presents no problem. The half life of an aluminum atom in a flux of 10^{14} n/cm^2-sec is approximately 1000 years. Since the rod is made of the same material as the rest of the core structure, it suffers minimal corrosion (similar to other core components). Regulating rod lifetime is greater than 20 years.

The regulating rod operates in a shroud of approximately 3.5 inches I.D (8.9 cm). The shroud has the same configuration as the 3.5-inch (8.9 cm) experimental thimbles. A fixed orifice in the nozzle of the shroud delivers a coolant water flow of 8 gpm from the outer plenum. This flow passes up around the regulating rod and then out into the bulk coolant. At a calculated heating rate of 5 watts per square centimeter, at 20 MW, this coolant flow will result in a maximum regulating rod wall temperature of 140 $^{\circ}$F.

4.2.2.3 Kinetic Behavior of Control Devices

Section 4.5.1.5 provides additional details relating to the worth of the shim safety arms and the regulating rod.

The shutdown margin requirement for the NBSR reactor is that it be possible to make the reactor subcritical in a cold, xenon-free condition with the most reactive shim arm stuck in the fully withdrawn position. Shutdown margin calculations are discussed in Section 4.5 and Appendix A).

4.2.2.4 Scram Logic and Circuitry

The Output Cards of the Nuclear Instrumentation provide the current required to keep the clutches of each shim safety arm energized. Each channel of the process instrumentation is connected to the scram system control redundant scram relays (K-104). A scram signal, whether

generated from the Nuclear Instrumentation, one of the process instruments or a manual scram, de-energizes the clutches causing the shim safety arms to be inserted into the core by gravity and spring force, thus shutting down the reactor. The scram signal also drives the regulating rod into the core to its full "in" position. Detailed discussion and description of operation of the scram circuitry, the rod withdrawal permit circuitry and the rundown circuitry are provided in Chapter 7, Instrumentation and Control Systems.

4.2.2.5 Special Features of Control Devices

The NBSR shim safety arm control system is designed to ensure operability and provide safe reactor operation and shutdown under all operating conditions including that of a single failure or malfunction in the control system itself. This is achieved by using a design that relies on a passive feature (gravity) to achieve the safety function. All four shim safety arms are coupled to their drive motors by electromagnetic clutches. Thus, the only action required to effect a safe and rapid shutdown is to de-energize the electromagnets, driving the arms to their fully inserted positions in the core. The shim safety arms are considered operable for a scram if they drop the top 5 degrees of travel within 220 milliseconds. The system is fail-safe in that:

a. No power source is required to initiate a shutdown.
b. Loss of electrical power automatically results in a shutdown.
c. No mechanical action, such as the release of a latch, is required in order to insert a shim arm.
d. There are four shim safety arms. Insertion of any three will result in a reactor shutdown under the most reactive core conditions.

Per NBSR technical specifications, the reactivity worth of each shim and regulating rod is determined annually, the withdrawal and insertion speeds determined semi-annually, and the scram times of each shim arm drive are measured semi-annually. In addition, verification tests are performed to ensure continued operability following maintenance on any portion of the reactor control or reactor safety systems.

4.2.2.6 Technical Specifications

The following Technical Specifications apply to the operability and surveillance requirements of the shim safety arms and the regulating control rod. Related specifications regarding excess reactivity and shutdown margin are given in Section 4.5.

<u>Technical Specifications 3.4, Reactor Control and Safety Systems</u>

The reactor shall not be operated unless :

(1) all four shim safety arms are operable
(2) the reactivity insertion rate, using all four shim safety arms, does not exceed 5.0 x 10^{-4} $\Delta\rho$ / sec

(3) the Scrams and Major Scrams are operable in accordance with Table 3.1 of the Technical Specifications.
(4) the moderator dump system is operable

Basis : Although the NBSR could operate and could maintain a substantial shutdown margin with less than the four installed shim safety arms, flux and rod worth distortions could occur by operating in this manner. Furthermore, operation of the reactor with one shim arm known to be inoperable would further reduce the shutdown margin that would be available if one of the remaining three shim arms were to suffer a mechanical failure that prevented its insertion.

A rod withdrawal accident for the NBSR is analyzed (SAR, NBSR 14, Chapter 13 and Appendix A) using the maximum insertion rate, corresponding to the maximum beginning-of-life rod worths with the rods operating at the design speed of their constant speed mechanisms. The analysis showed that the most severe accident, a startup from source level, is bounded by the maximum reactivity insertion accident, and will not result in core damage.

In the unlikely event that the shim safety arms cannot be inserted, an alternate means of shutting down the reactor is provided by the moderator dump. The moderator dump provides a shutdown capability for any core configuration. Hence, it is also considered necessary for safe operation. It is shown (Section 4.5.1.3.3) that the moderator dump provided sufficient negative reactivity to make the normal Start-Up (SU) core subcritical even with all four shim arms fully withdrawn.

Technical Specification 4.3, Reactor Control and Safety Systems:

This specification applies to reactor control and safety system operation. The objective is to ensure proper operation of reactor control and safety systems.

The reactor shall not be operated unless

(1) reactivity worth of each shim and regulating rod shall be determined at least annually.
(2) the withdrawal and insertion speeds of each shim arm and the regulating rod shall be determined at least semiannually.
(3) scram times of each shim arm drive shall be measured at least semiannually.
(4) reactor safety system channels shall be tested for operability before each reactor startup following a shutdown in excess of 24 hours, or at least quarterly. This test shall include a verification of proper safety system channel trip settings. The safety channels shall be calibrated annually.
(5) a comparison of power range indication with flow time's ΔT shall be performed weekly when the reactor is operating above 5 MWt.
(6) Following maintenance on any portion of the reactor control or reactor safety systems, the repaired portion of the system shall be satisfactorily tested before the system is considered operable.

Basis: Measurements of reactivity worths of the shim arms have been shown (over many years of operation) to vary slowly as a result of absorber burnup and only slightly with respect to operational core loading and experimental changes. An annual check shall ensure adequate reactivity margins.

A channel calibration of the reactor safety channels has been shown to be adequate for the present operating cycle.

The shim arm drives are constant speed mechanical devices. Scram is aided by a spring that opposes drive motion during arm withdrawal. Withdrawal and insertion speeds or scram time should not vary except as a result of mechanical wear. The surveillance frequency is chosen to provide a significant margin over the expected failure or wear rates of these devices. The shim arms shall be considered operable if they drop the top five (5^{o}) within 220 msec. This value is consistent with the amount and rate of reactivity insertion assumed in analyzing the accident requiring the most rapid scram (SAR, NBSR 14, Chapter 13).

Because redundancy of all important safety channels is provided, random failures should not jeopardize the ability of these systems to perform their required functions. However, to ensure that failures do not go undetected, frequent surveillance is required and specified.

Because various experiments require precise operating conditions, the NBSR has been designed to ensure that accurate recalibration of power level channels can be easily and frequently achieved. The calibration is performed by comparison of nuclear channels with the thermal power measurement channel (flow times Δ T). Because of the small Δ T in the NBSR (about 15 ^{o}F at 20 MW) these calibrations will not be performed below 5 MW for 10 MW operation or below 10 MW for 20 MW operation. However, to ensure that no gross discrepancies between nuclear instruments and the flow ΔT indicators occur, comparisons (but not necessarily calibrations) are made above 5 MW.

4.2.3 Neutron Moderator and Reflector

The NBSR is a D_2O moderated, reflected and cooled tank-type reactor design. The core is immersed in heavy water to thermalize fast neutrons to sustain the nuclear chain reaction, to remove heat created by the reaction and to serve as the first stage of shielding. No other material is used within or in the area immediately surrounding the core region to moderate the fast neutrons created by the fission process. All construction materials used in the reactor tank and primary coolant system are either aluminum or stainless steel. Additional information on the primary coolant system is provided in Chapter 5, Reactor Coolant Systems.

The side reflector is 20 inches (51 cm) thick and the top reflector thickness is normally maintained at 118 inches (3.0 m). While the thickness of the side reflector is fixed by the design and construction of the reactor core and tank, the reactor operator controls the thickness of the top reflector. During normal operation, the level of the heavy water in the reactor tank is maintained at 118 inches (3.0 m), the height of the inlet to the 3-inch (7.6 cm) overflow pipe.

Nearly all of the reactivity effect caused by the top reflector occurs over the first 2 feet (60 cm) of thickness. In the unlikely event that the shim safety arms cannot be inserted, the reactor operator can initiate a Moderator Dump to drop the water level to approximately 1 inch above the core to effect an emergency shutdown of the reactor. This provides a shutdown capability for the most reactive core configuration. The moderator dump system provides a fully redundant backup to the shim safety arms. Technical Specifications for the Reactor Control and Safety Systems require that the moderator dump system be operable for the reactor to be operated (see Section 4.5.1.7).

4.2.4 Neutron Startup Source

The normal operating cycle for the NBSR is 7 weeks, with continuous operation at its licensed power for approximately 38 days. The remaining 11 days are used for maintenance activities and refueling. With the exception of a 2-week summer shutdown and a 2-week end of year shutdown, this schedule continues unabated. As a result, the power history of the NBSR is more than sufficient to maintain a strong photoneutron source for reactor startup.

After extended shutdowns, the strength of the photoneutron source may be insufficient to provide indication on the nuclear instrument channels and for reactor startup. On these rare occasions, an encapsulated Americium/Beryllium neutron source (of nominal strength 2 curies) is inserted into the core region to provide sufficient source neutrons for reactor startup by utilizing any one of the vertical experimental thimbles. The current strength of this source is 1.9 Ci, and the half-life is 458 years. The source was manufactured by NUMEC of Apollo, PA, and is stored inside a shielded container in a source storage locker in Room C-200. The source is handled through the use of remote handling tools, following Good Work Processes. The neutron yield is 2.2×10^6 n/s/Ci. The source is positioned within the thimble to provide neutron indication on the Nuclear Instrumentation channels. The NBSR is then taken critical. Once the reactor is critical and prior to raising the power level to 20 MW, the startup source is removed from the reactor and placed in its shielded storage container.

Since the source is placed into one of the existing experimental thimbles it does not contact the coolant or other core components. The neutron source is not a normal component of the NBSR; it is almost never used, as sufficient photoneutrons are almost always present.

4.2.5 Core Support Structure

The NBSR core is designed not to be moved. The core support structure is designed to ensure that all fuel elements, reactivity control devices and in-core experimental facilities are properly secured against all anticipated loads including both the buoyant force of the coolant and the hydraulic forces associated with the primary coolant flow. The principal feature for achieving this is the heavy grid structure that is positioned at the top of the core combined with 10 hold down bolts fastening the upper grid to mounting brackets located on the vessel wall. This grid is designed to lock the fuel and other core components in place during reactor operation and to prevent movement of the core components by the hydraulic lifting force.

The mass of an NBSR fuel element is 8.84 kg (its weight is 19.4 lb). Each element has a downward force due to gravity of the mass times the acceleration due to gravity minus the buoyant force due to the displaced water of 61 N (11.5 lb). In addition to the force of gravity, each element is held in place by a locking mechanism located at the top of each assembly. This locking mechanism engages the underside of the upper grid plate to secure each assembly in place. A spring in the assembly allows each element to rise slightly due to forced primary coolant flow, creating a .012 in. gap (.031 cm) between the conical section of the lower adapter nozzle and the mating conical seat in the lower gird plate. At rated flows, the pressure drop across the fuel is 84 kPa (12.3 psi) and 48 kPa (7 psi) for elements in the inner and outer plenum respectively. These figures include the pressure drop due to gravity.

The internal structure of the reactor vessel supports the core, the shim safety arms and the inner reserve cooling tank. The fuel elements, experimental thimbles and regulating rod shroud are located between the upper and the lower grid plates. The grid plates fix the fuel element and the 3.5 inch (8.89 cm) experimental thimbles spacing at 6.928 inches (17.6 cm) center-to-center in a hexagonal pattern. The fixed pattern in the grid plates also aid in maintaining accurate positioning of the fuel elements, the reactivity control devices and the experimental thimbles. Fuel can only be loaded in predetermined locations in the grid plates with lateral movement severely limited by the dimensions of the openings in the grid plates.

The fueled portions of the elements extend from 9 inches (23 cm) above the bottom grid plate to 24 inches (61 cm) below the upper grid plate with a 7 inch (18 cm) unfueled section in the central plane. Coolant flow through the core structure comes from two concentric plenums located just below the lower grid plate. The D_2O coolant passes up through the fuel elements, experimental thimbles and regulating rod shroud. In addition, a small amount of coolant flows around the base of the fuel elements directly into the bulk coolant.

The upper and the lower grid plates are shown in Figures 4.2.11 and 4.2.12, and their relationship to other core components is shown on Figure 4.2.1. The selection of 6061-T6 aluminum alloy for the upper and lower grid plates makes them compatible with the materials of the vessel and primary piping. Aluminum is chemically compatible with the heavy water coolant and exhibits excellent resistance to corrosion and erosion. It has low induced radioactivity and is resistant to radiation damage.

With the exception of the 3.5 inch (8.89 cm) experimental thimbles, which are held down by poison tubes from the top plug, all of the core components are held down against the upward force of the water by the upper grid plate. The fuel elements are locked under the upper grid plate and the 3.5inch (8.89 cm) experimental thimbles are semi-permanently held down directly by the upper grid plate. Thus, the upper grid plate must resist the upward force of the core components caused by the flow of the primary coolant. The lower grid plate is loaded by the hydraulic pressure in the two plenums, the weight of the core components when water is not flowing and the thermal stresses resulting from radiation heating.

The lower grid plate is completely supported at the edges by a 1 inch (2.54 cm) plate (the outer plenum flange plate) welded to the outer plenum directly beneath it. The outer plenum is welded

to the vessel bottom, so the load of the lower grid plate is supported from below. The flange plate also has sections extending to the vessel wall where they are welded for further support. The grid plate is fastened to the flange plate by eighteen 1 inch (2.54 cm) diameter stainless steel bolts. The large number of bolts is employed to give a tight seal between the lower grid plate and its mounting surface. Their loading capacity far exceeds that required to handle the grid plate loading.

The upper grid plate is attached to four mounting brackets welded to the vessel wall. These brackets are further reinforced by quarter rings welded to them and to the vessel wall. Ten 0.750 inch diameter (1.91 cm) stainless steel bolts fix the grid plate to the mounting brackets. The upper grid plate mounting brackets also serve to support the inner reserve cooling tank. It stands on four legs, each resting on one bracket, and is bolted in place by one bolt passing through each leg into the mounting bracket. These features are also shown in Figure 4.3.1, a cut away view of the vessel internal structure.

4.3 Reactor Vessel

The NBSR reactor vessel contains the reactor core and its support structure, the heavy water (D_2O) as coolant/moderator/reflector, the D_2O helium blanket, D_2O plenums and their connections to inlet and outlet piping, control devices, fuel element transfer chute, inner reserve tank (IRT) for emergency cooling and its overflow piping connection, emergency cooling distribution pan, and D_2O holdup pan. Figure 4.2.1 is the elevation of the reactor while Figure 4.2.2 shows a cross-sectional view.

4.3.1 Design

The reactor vessel is an aluminum-alloy vessel 7 feet (2 meter) in diameter and 16 feet (5 meter) in height and is designed in accordance with the ASME Boiler and Pressure Vessel Code for Unfired Pressure Vessels, 1959 Edition of Section VIII, including all revisions, addenda, and applicable Code Cases in effect at that time.

Basically, the vessel is a vertical cylinder with an elliptical bottom (with penetration sleeves) and a flange at the top. The reactor vessel flange rests on top of the Thermal Shield Shim Ring and is bolted to it by twenty-four 1-inch (2.5-cm) bolts. The thermal shield is an iron-lead light water cooled structure that protects the biological shield from excessive radiation heating. This shielding structure surrounds the reactor vessel and rests on a concrete foundation supporting the weight of the vessel; a nominal gap of one-inch (2.5-cm) is maintained between the vessel and the shield. The top shield plug assembly rests on the vessel's flange. Both are independently fastened to the thermal shield's shim-ring. A stainless steel O-ring gasket forms a seal against helium or heavy water at the interface of the reactor's top plug assembly and the upper face of the reactor vessel's flange. A second such gasket forms a seal against carbon dioxide at the interface of the lower face of the reactor vessel's flange and the Thermal Shield Shim Ring.

As shown in Figure 4.3.1, the core is split into an upper section and a lower section, each section being 44 inches (112 cm) in diameter and 11 inches (28 cm) height, with an unfueled 7 inches (18 cm) high center section. Thus, the overall dimension of the core is 44 inches (112 cm) in diameter by 29 inches (74 cm) high. Two grid plates 62 inches (158 cm) apart support the fuel elements. The top of the lower grid plate is 9 inches (23 cm) below the bottom of the core and the bottom of the top grid plate is 24 inches (61 cm) above the top of the core.

One of the two D_2O inlet pipes, the outer plenum, is welded in the center of the vessel's bottom while the two outlet pipes are welded to the bottom on either side of the outer plenum pipe. The inner plenum is located within, and is concentric to, the outer plenum. The lower grid plate is bolted to both the inner and the outer plenums forming a watertight seal. The D_2O holdup pan surrounds the core to a height just above the lower fuel section of the core and is attached to the lower grid plate; this traps an inventory of cooling water during a loss of coolant accident.

The upper grid plate is bolted to four mounting brackets welded to the vessel wall. Both the emergency cooling distribution pan and the inner reserve tank for emergency cooling are attached to the upper grid plate. The emergency cooling distribution pan ensures an even distribution of coolant to each fuel assembly in the event of a loss of coolant accident. The inner reserve tank provides a reserve of cooling water to the distribution pan. Its 800-gallon (3,000-liter) capacity ensures approximately 28 minutes of emergency cooling, thereby providing time for the operator to act. An additional 3300-gallons (12,500-liters) of cooling water is available to cool the core from an external D_2O Emergency Cooling Tank.

The upper girth of the reactor vessel, made of 0.50 inches (1.3 cm) thick aluminum 6061-T6, extends down approximately 115 ¾ inches (294 cm) below the surface of the reactor vessel's flange. The lower girth and the reactor vessel bottom are made of 0.875 inches (2.2 cm) thick aluminum 5052. The lower girth extends down from the upper girth to approximately 166 inches (422 cm) below the reactor vessel's flange. The beam ports, grazing tubes, cold source and rabbit tubes all attach to the reactor vessel in the lower girth.

The design temperature for the reactor vessel is 250 $^{\circ}$F (121 ^{o}C), and the design pressure is 50 psig (345 kPa). The normal reactor outlet temperature is 114 $^{\circ}$F (45.5 ^{o}C) and the normal operating pressure is atmospheric. After fabrication, the vessel was hydrostatically tested at a pressure of 75 psig (517 kPa). The maximum hydrostatic pressure, which occurs at the bottom of the reactor vessel, is 7.2 psig (50 kPa). The hydrodynamic pressure at 8700 gpm (550 l/s) is minimal, as the water exits from the fuel elements at the hydrostatic pressure at that elevation. The only hydrodynamic forces are the upward force on the upper grid plate from the elements due to water flow. This force has been measured as 17.4 N (77.5 lb) at a flow of 25 l/s (400 gpm) per element ["Fuel Flow Tests," in Engineering Services Folder #7, NBSR records].

During the design of the vessel, the loads resulting from constraining forces or members were considered, along with those from steady state and transient thermal conditions, including emergencies.

The vessel's low heating rates experienced since its operation and the excellent thermal conductivity of the aluminum combine to yield negligible stresses from internal temperature gradients. Areas of distinct interest from the standpoint of thermal expansion are the grazing tube to shell joints, and the grazing tube column reactions resulting from end restraints. Both of these areas were investigated and the resulting stresses considered in the vessel's design. (NBS, 1966a)**.** These loads do not exceed the Code-allowable working stresses at any point. The NBSR vessel is fabricated entirely of aluminum alloys. Therefore, stresses resulting from differential expansion between dissimilar materials are negligible.

The very small temperature differentials between the coolant and the vessel components generate insignificant thermal transient loads (NBS, 1966a). Irradiation damage studies run on various aluminum alloys show that the changes in the engineering properties of these materials are not significant for NBSR vessel design (NBS, 1966a). The subject of irradiation damage is presented in Chapter 16, but a summary of that discussion is presented here.

The NBSR vessel is fabricated from aluminum alloys 5052 and 6061, which have been studied in radiation fields for many years. Heavily irradiated (4.2×10^{23} thermal, 2.0×10^{22} fast neutrons/cm^2) samples of the 6061-T6 alloy were taken from a control rod drive follower tube used in the HFBR at Brookhaven National Laboratory (Weeks et al, 1993). Analysis of the irradiation data indicates that, the ductility, while reduced, retains approximately 70% of the original value, although the Charpy energy has dropped by over a factor of 6. The most heavily irradiated portions of the NBSR vessel, the tips of the beam tubes, will have accumulated less than 2×10^{23} n-cm^{-2}-s^{-1} thermal neutron fluence by 2024. Thus, the tips remain a ductile material, with reduced impact strength and toughness.

The primary irradiation effects on the aluminum 6061-T6 properties will be reduced resistance to crack propagation under *tensile* stress, and reduced resistance to sudden pressure applications and impacts. Since the vessel is entirely closed, there is no credible mechanism of exerting such a tensile stress, or impact, on the beam tube tips during reactor operation. The D_2O does exert a compressive force (due only to the static head as there is no coolant pressure), which causes a compressive stress, but this stress will not create cracks that can propagate quickly. By analogy to the results of Weeks, embrittlement of the vessel creates no hazard to continued operation of the NBSR.

Since the vessel is an all-aluminum structure, and since the flow rates in the vessel and associated piping are small, only aluminum corrosion was considered in the design. A 125-mil (3-mm) corrosion allowance was allowed on all of the vessel's pressure containment surfaces. The maximum predicted corrosion for the design temperature of 250 ^{o}F (121 ^{o}C) and a coolant pH of 5 would be 0.87×10^{-4} mils/day (0.22×10^{-4} mm/day). The primary system's pH is maintained between 5 to 6 by the ion exchangers of the purification system, described in Section 9. Historically, its pH has ranged from 5.3 to 5.7. As the corrosion rate is extremely temperature sensitive and the vessel wall's temperature does not approach the design specification, the predicted corrosion rate is quite conservative (NBS, 1966a). A visual inspection of the vessel's internal components in 1994 revealed little corrosion.

The Helium Sweep System removes gases formed by radiolysis of the primary coolant and recovers any heavy water lost due to evaporation. To accomplish this, the primary system is a closed, pressure-tight system maintained at a slightly elevated pressure, approximately 3- to 5-inches (8- to 13-cm) of H_2O. The Helium gas supply consists of six bulk Helium gas tanks, with standard high-pressure bottles as a backup supply, connected through suitable pressure-regulating manifolds to a closed recirculating system.

The reactor vessel and its associated piping move freely under the influence of thermal expansion. Only the reactions from the bellows-type CO_2 seals are transmitted to the vessel. Sliding pad-type pipe supports absorb the major portion of all reaction forces resulting from primary system flow in the external piping. Hence, the resulting loads on the vessel are small, and in conjunction with all other loadings do not cause any stress levels above the maximum allowable working stress for various reactor sections (NBS, 1966a).

No impact loads are transmitted to the vessel. The shim safety-arm drive and shock absorbing systems are mounted on the biological shield so that only the extremely small reaction between the outer faces and the balls is transmitted to the vessel.

Pressure surges that might be generated in the vessel by reactor power transients are small and would not cause the vessel to exceed the 50-psi (0.35-kPa) design pressure. As a precaution, a safety relief valve, set at 50 psi (0.35 kPa), was installed in the reactor coolant system.

The vessel's design was checked for its ability to withstand seismic forces from horizontal accelerations of 0.1g. The resulting combined stress levels from this loading plus all other design loads were well within the allowable limits for the various sections of the vessel (NBS, 1966a). This horizontal acceleration is within the range of intensity VII to VIII earthquake on the Mercalli scale.

4.3.2 Shielding/Adequacy of Depth

The biological shield surrounding the vessel and the top shield plug assembly provide radiation shielding for personnel. The shielding of the core is described in Section 4.4 of this report. During normal operation, the level of the coolant in the reactor vessel is maintained by continuous spillover of D_2O from the inner reserve tank into the 3-inch (7.6-cm) overflow pipe. There are 118 inches (300 cm) from the top of the NBSR fuel to the overflow pipe. During refueling with the reactor shutdown, the D_2O level is manually maintained at a height of 23 inches (58 cm). In an emergency, the Moderator Dump System, consisting of an emergency dump line concentric with the fuel element transfer chute, can lower the level of the primary coolant to 1 inch (2.5 cm) above the core, shutting down the reactor.

The upper and lower shielding donuts and the center shield plug are an integral part of the pressure boundary of the reactor vessel. In addition to the installed shielding, the coolant inventory is maintained over the core during operations to aid in shielding the operators.

The core is refueled without removing the center shielding plug or either of the shielding donuts. The level of the coolant in the reactor vessel is lowered to just below the opening to the fuel-transfer chute. Fuel removed from the reactor is transferred to the storage pool through this chute. New fuel is loaded through an opening in the center shielding plug. A fuel pickup tool and fuel transfer arms remotely handle all the fuel in the reactor vessel.

4.4 Biological Shield

The shielding surrounding and often supporting the NBSR is an integral part of the confinement building, installed during the construction of the building. It was designed for 20-MW operation. Experience has demonstrated its adequacy. Chapter 10 of NBSR-9 (NBS, 1966a) contains a thorough description the design considerations and shielding calculations for the construction of the biological shield. This section is a summary of that chapter.

4.4.1 Biological Shield

The biological or bulk shield of heavy concrete surrounds the thermal shield and reduces the radiation that still remains at the outside of the thermal shield to acceptable levels at accessible areas in the shield's face. The bulk shield is designed to reduce the radiation to insignificant levels, namely on the order of instrument background. This requirement is more stringent than that set by personnel exposure limitations.

At the core elevation, the thermal shield, consisting of 2 inches (5 cm) of lead and 8 inches (20 cm) of steel, nearly surrounds the Reactor Vessel. (A large D_2O tank on the south side of the core, shown in Figures 4.2.1 and 4.2.2, fills an opening in the thermal shield, allowing thermal neutrons entry into the thermal column.) The shield, which extends to the top of the vessel and underneath it, is light water cooled (see Chapter 5). At full power, about 350 kW is deposited in the thermal shield, preventing the concrete in the biological shield from excessive heating. Calculations of the gamma-ray energy deposition versus depth in the shield show that energy absorption decreases from about 0.6 W/cm^3, in the lead adjacent to the vessel, to 0.03 W/cm^3, at the steel-concrete interface. Neutrons deposit very little energy in the thermal shield directly, but the high-energy capture gamma rays from neutron absorption in iron are a major component of the radiation entering the biological shield.

The bulk shielding completely surrounds the reactor, becoming an integral part of the first and second floors. The reactor can be accessed from the second floor on the top of the reactor. The top shield plug assembly consists of two doughnut shaped plugs, one above the other, and a stepped cylindrical plug that fits into the doughnut. The center plug is 5 feet (1.5 meter) thick which is thinner than the doughnut combination leaving a 2 feet (0.61 meter) deep well in the center of the floor over the reactor. This well is covered with a 6-inch (15.2-cm) thick removable steel plate.

Below the reactor, the large pipes of the reactor coolant system penetrate the shield. The area of these penetrations below the reactor is enclosed in the sub pile room with concrete walls of a minimum thickness of 3 feet (0.9 meter). The sub pile room is located in the much larger Process Room, also heavily shielded by 4 and 5 feet (1.2 and 1.5 meter) thick walls.

The bulk reactor shield is made of magnetite concrete with a minimum dry density of 240 lbs/ft^3 (3,844 kg/m^3). Its minimum thickness in the reactor's high-flux central plane region is 74 inches (188 cm). The concrete was formed directly against the thermal shield on the inside and has 0.5 inch (1.3 cm) thick steel faceplates on the outside. The three top plugs are made of stainless steel and filled with 3 inches (7.6 cm) of lead on the bottom in turn covered by magnetite concrete.

4.4.2 Radial Shielding Calculations

Table 4.4.1 gives the neutron and gamma fluxes entering the biological shield in the central plane. In addition to these incident fluxes, neutron capture in the concrete produces some additional gamma rays that must be shielded.

Table 4.4.2 lists the shielding properties of the magnetite concrete. Most of the gamma-ray flux is generated by neutron capture in either the steel of the thermal shield (on the inside face of the biological shield) or the iron in the magnetite concrete. Therefore, an average energy of 6 MeV was used to determine the proper gamma-ray attenuation coefficient and buildup factor. The results yield a fast neutron flux 2.8 x 10^{-3} n/cm^2-sec and a gamma flux of 2 x 10^{-7} mW/cm^2 at the outside face of the biological shield. The contribution to the exiting gamma-ray flux from neutron capture in the concrete is approximately 25%; and from the neutron capture in the thermal shield is approximately 75%. The gamma-ray flux corresponds to a dose rate of approximately 2 mrem/hr at the outside face of the biological shield; the direct dose from neutrons through the concrete is negligible.

No credit was taken for structural steel in the actual shield or allowance made for voids and streaming through cracks around beam plugs. In designing the shield, care was taken to minimize the effects of voids. Wherever a void was necessary due to some structural feature, such as a pipe or shutter well, enough lead was added to its inside to compensate for the gamma-stopping power of the concrete that was removed. The beam holes are designed to extract intense radiation beams from the reactor. Therefore, they require extensive individual shielding to meet individual requirements. Each beam line was specifically reviewed at the design stage, checked upon installation, and verified to have acceptable radiation dose rates during operation.

4.4.3 Top Plug Shielding Calculations

The top plug shielding presents no problem during operation since the reactor core is covered by 10-1/2 feet (3.2 meter) of heavy water that effectively reduces the fast neutron flux to negligible levels. The Cd poison hold down tubes in the top reflector efficiently reduces the thermal neutron flux. The major contribution to the gamma-ray flux during operation comes from neutron capture in the poison tubes in the top reflector.

The center plug is the thinnest part of the top plug system. This plug is 5-feet (1.5-meter) thick and filled with heavy concrete except for the bottom 3 inches (7.6cm), which is filled with lead. Many pick-up and transfer tools penetrate this plug. The bulk of the center plug shield, including the head, is more than adequate as shielding, reducing the gamma dose rate at the top of the center plug to about 0.1 mrem/hr (as documented in Health Physics logs). A greater source of radiation is that emerging from these penetrations. The center of each pick-up tool penetration consists largely of aluminum over a region of 2 inches (5 cm) diameter. Also, the requirements that the pick-up tools slide vertically introduce a small crack, which is only partially stopped by tight fitting bushings and a step in the aluminum pick-up tool.

Radiation measurements have shown that the fields near the top of the center plug in the immediate vicinity of a pick-up tool, holding an element in a helium atmosphere, is less than 0.5 mrem/hr.

The radiation near the top of the center plug constitutes no health risk since it is in the well in the top floor that is covered with a 6 inch (15.2 cm) steel plate. This plate, an integral part of the transfer system, is always in place when fuel elements are being moved. The plate over each pick-up tool is penetrated by openings up to 6 inches (15.2 cm) in diameter that normally are plugged.

4.5 Nuclear Design

Information on the core nuclear parameters, routine operation, and factors influencing the kinetic behavior of the NBSR are presented in this section. Some of the information is obtained from the long record of safe operation over the last 35 years. New computer models have also added to the understanding of both the normal operation of the reactor and postulated abnormal conditions. A summary of the major core nuclear parameters is listed in Table 4.5.1.

As part of the effort to prepare this report, the Energy Sciences and Technology Department at the Brookhaven National Laboratory (BNL) performed reactor physics and safety analyses using state-of-the-art computer codes. Their report, “Physics and Safety Analysis for the NIST Research Reactor” (Carew, 2003) will be cited in this section and in Chapter 13 and is Appendix A to this document.

4.5.1 Normal Operating Conditions

The major components of the NBSR core have been described in Section 4.1. This section contains a description of normal reactor operations, including the power distribution, excess reactivity, effects of burnup and resulting reactivity changes. A model of the core, used for Monte Carlo simulations of core performance, is presented, along with benchmarks needed to validate the model.

4.5.1.1 Core Configuration and Fuel Management

4.5.1.1.1 Fuel Element Configuration

Figure 4.5.1 shows the hexagonal grid arrangement of the fuel elements (FEs) in the core, and the normal fuel management scheme. There are 30 FEs arranged in seven rows as shown in Fig. 4.5.1(A), with letters and numbers used to identify the 30 locations. The rows of FEs are numbered 1 to 7, from north to south, and the locations within a row are lettered from 'A' to 'M', from west to east. There are also seven locations in the grid that are not loaded with fuel. Six of these are reserved for 3.5-inch (8.9-cm) diameter vertical experimental thimbles, denoted as "ex," and the seventh, in location G-6, contains the regulating control rod, labeled "reg." The cold neutron source is on the north end of the core denoted as "CNS." Reactivity is controlled by the four shim arms, located between the interior rows, 2 through 6, of the fuel.

The FEs are held in place between two grid plates, referred to as the upper and lower grid plates. The shim arms are in a semaphore arrangement so they are attached to the vessel and are not mounted to either grid plate. The FEs are loaded and unloaded through 30 rectangular holes in the upper grid plate. The holes are rectangular so that the plates of each FE must always run east-west. The lower grid plate has 37 tapered holes into which the 30 FEs, 6 vertical experimental thimbles, and the regulation rod guide tube fit. The FEs are held in place with latches that lock the FEs to the upper grid plate. The coolant is then forced upward through the FEs, exiting through the upper grid plate.

4.5.1.1.2 Fuel Management Scheme

Normally, FEs reside in the core for either seven or eight reactor cycles; a cycle being 38 days of operation at full power. After each cycle, four FEs are removed to the spent-fuel storage pool, and the remaining 26 elements are moved following the pattern shown in Fig. 4.5.1(B). In this figure each position has two numbers associated with it. The first number indicates how many cycles the FE will be irradiated. The second number indicates the FE's irradiation history. The *-1 representation is a FE in its first cycle, the *-2 representation is a FE in its second cycle, etc. As such, the 7-7 and the 8-8 FEs are in their seventh and eighth and hence final fuel cycles, respectively.

At the end of a cycle, the FEs in positions E-4 and I-4, which are the 7-7 FEs, and in positions F-5 and H-5, the 8-8 FEs, are removed from the reactor. A FE in the 8-1 position is moved to an 8-

2 position. A FE in the 8-2 is moved to an 8-3 position, and so forth. All remaining elements are moved accordingly with fresh FEs loaded into positions D-1, J-1, A-4, and M-4. Fuel migration is generally from the outside ring of elements toward the center, with fresher FEs located on the north side (rows 1 through 3), benefiting the cold neutron source. It will be shown later in this section, that since the thermal neutron flux peaks in the core center, the elements with the highest burnup have about the same power production as the freshest ones on the perimeter; that is, the radial power distribution is very flat, ± 15%, even though the thermal neutron flux may vary by nearly a factor of three.

While the fuel loading has increased over the years from 170 g to 350 g of high enrichment uranium (HEU) per element, the fuel management scheme shown in Fig. 4.5.1 has been in use for most of the life of the facility. This normal fueling pattern is analyzed in this chapter. The power distribution, excess reactivity, shutdown margin, reactivity coefficients, and core thermal-hydraulic behavior are calculated and compared to measurements. The consequences of a fuel loading accident are discussed in Chapter 13.

4.5.1.1.3 A Normal Reactor Cycle

As a normal cycle begins, following a pre-critical check of instrumentation and the reactor protection circuits, the NBSR is made critical by withdrawing the shim arms, according to established procedures. Power is increased in steps to 20 MW. At each step, reactor systems' checks and Health Physics surveys are completed as required before increasing power to the next step. At 1 MW, with the reactor critical, the positions of the shim arms and regulating rod are recorded before operating temperatures are reached, and before the short-lived fission products can affect reactivity. Logging this information tracks the depletion of the cadmium in the shim arms and has provided the criticality benchmarks for the computer simulations discussed below.

After approximately 40 hours of operation, as ^{135}Xe and other short-lived fission products reach equilibrium concentrations, the shim arms are withdrawn about 4.5° to offset the associated negative reactivity. At this point, just two days into a normal cycle, the concentrations of the major poisons reach equilibrium, and further reactivity changes are due to fuel depletion only. After equilibrium has been reached, the shim arms are withdrawn approximately 0.4° every two days. The shim arm positions are adjusted in discrete movements which are accompanied with the insertion of the regulating rod. Criticality is then maintained by automatically withdrawing this rod. When the regulating rod has reached it upper limit, the shim arms are again withdrawn and the regulating rod is inserted. As the end of the cycle nears, and their differential reactivity worth decreases (see Section 4.5.1.5), the shim arms must be moved further to offset the fuel depletion rate. Ideally, the reactor is maintained at 20 MW power level for the entire cycle, until, with the shim arms fully withdrawn, the regulating rod reaches its upper limit for the last time. At this point the cycle is ended because the reactor cannot continue to operate at full power.

4.5.1.2 Neutronic and Burnup Model of the NBSR

4.5.1.2.1 NBSR Modeling with MCNP

To analyze the reactor physics under numerous conditions, a model of the core has been developed for computer simulations using the code MCNP (Briesmiester, 1997). MCNP is a Monte Carlo neutron and photon transport code developed at LANL and is used for a wide variety of problems including criticality simulations. It features generalized surfaces and cells so that complex geometries can be defined along with continuous energy cross-section data. Criticality calculations with the code have been carefully benchmarked with respect to LANL critical experiments (Whalen, et al., 1991) and power reactors (Sitarman, 1992). Many research reactors have also been successfully modeled using MCNP to analyze the possibility of conversion to low enrichment uranium (LEU) fuel, and the performance of proposed experimental facilities, such as epithermal neutron beam converters for boron neutron capture therapy (BNCT), and cold neutron sources (as discussed below). MCNP has been used to meet reactor-licensing requirements (Ougouag, et al. 1993) (Bretscher, 1997). Hundreds of cross-section files with gamma-ray production data have been formatted for use with the code, including thermal neutron scattering kernels for all common reactor moderators, and four cold moderators.

A three-dimensional (3D) MCNP model of the NBSR was first used at the NIST CNR for the development of a liquid hydrogen cold neutron source (CNS), accurately predicting its performance and nuclear heat load. This model was provided to the Energy Sciences and Technology Department at BNL as a basis for their reactor physics and safety analysis study, Appendix A of this report. All of the major features of the NBSR that affect the reactivity of the core are represented in great detail in this model including:

1. A hexagonal array of the 30 FEs, 6 vertical thimbles, and the regulating control rod.
2. All 1020 fuel plates, their Al cladding and D_2O-filled coolant channels, positioned in hexahedral repeating structures for the upper and lower sections of the core.
3. Fifteen fuel material specifications representing each step in the fuel management pattern for the 7- and 8-cycle FEs.
4. The four shim arms, which can be positioned at any angle between their scram and fully withdrawn positions.
5. Nine radial beam tubes, two tangential beam tubes, the vertical beam tube, and the four in-core pneumatic ‘rabbit’ tubes.
6. The large cryogenic beam port and the liquid hydrogen cold source.
7. The reactor vessel, filled with D_2O, representing the moderator between the FEs, and the core reflector regions (the top reflector thickness can be varied to simulate a moderator dump).
8. Layers of lead and iron outside of the vessel, comprising the thermal shield, and a layer of concrete, for part of the biological shield.
9. A portion of the D_2O tank, providing neutronic coupling with the graphite in the thermal column.

Section 3 of Appendix A contains a thorough description of that MCNP model, including the FE geometry, fuel loading scheme, control elements, experimental facilities, etc. The 30 FEs are included in the model by using a hexagonal repeating lattice structure. Each FE has 17 fuel plates in both the upper and lower section of the core for a total of 1020 plates.

The MCNP model of the NBSR has undergone continuous upgrades during the BNL study. In this document the analyses that were performed for the BNL study will be referred to as the "BNL" model. Subsequent calculations will be referred to as the "updated" model. Most of the perturbations that were calculated in the BNL study are not significantly impacted by the modifications included in the updated model. The most significant differences arose in power distributions, for which the BNL model is more conservative.

4.5.1.2.2 Burnup

The FE by FE inventory and, hence the burnup, was determined iteratively with three computer codes, MCNP, ORIGEN2 (Croff, 1980), and MONTEBURNS (Trellue, 1998), with MONTEBURNS managing the interactions between MCNP and ORIGEN2. MCNP is used to generate localized neutron fluxes along with other neutronic parameters at user defined time steps. MONTEBURNS then uses ORIGEN2 to calculate one group cross sections for the localized spectra and then calculates the actinide and fission product inventories. MONTEBURNS extracts that information and changes the materials in MCNP accordingly. The process is started again until one cycle is completed. At the end of a cycle MONTEBURNS allows for rearrangement of the FEs, so the calculations can be performed over numerous cycles without human intervention.

A total of 15 different inventories were calculated for the NBSR, invoking symmetry between the FEs that experience the identical irradiation history. The inventories used in both of the MCNP models were determined after nine complete 38-day cycles. In this manner, all of the initial assumptions of FE inventories were eliminated. Figure 4.5.2 shows the ^{235}U mass in each FE at startup (SU) and at the end-of-cycle (EOC). While the length of normal cycles will always vary somewhat, there will be about 6.43 kg of ^{235}U in the core at EOC, as compared to about 7.40 kg at SU. Since each fission results in about 195 MeV deposited in the core, an average of 970 grams of ^{235}U is consumed per cycle. The average ^{235}U burnup in the 7-cycle FEs is 66%, and the burnup in the 8-cycle FEs is 73%.

There is very little plutonium production in the NBSR because the fuel is 93% ^{235}U. Based on the fuel constituents generated with MONTEBURNS, MCNP, and ORIGEN2, each FE at the end of its life in the core contains approximately: 0.09 g of ^{238}Pu, 0.44 g of ^{239}Pu, 0.13 g of ^{240}Pu, and 0.05 g of ^{241}Pu. Therefore the total Pu inventory at EOC is about 13.0 grams, and contributes just 0.3% of the fissions; hence plutonium has a negligible effect on reactivity.

About 50 individual fission products are listed among the fuel constituents. Most are the stable-isotope end products for the various mass decay chains, but several radioisotopes are included.

Most of the radioactive isotopes that are included in the materials have large neutron absorption cross sections and are referred to as poisons. Elements and isotopes used in MCNP are limited to only those contained in the ENDF/B or similar libraries. As such they are the only isotopes that can be used in the calculations. Fission products that are calculated by ORIGEN2, that are not included in the set of libraries, are not included in any further calculation. This "loss" of material was dealt with by adding elemental Zr and Sn, and ^{138}Ba, to mock up those fission products. This amounted to nearly half of the total mass of fission products. To account for decay during the 10-day shutdown between cycles, the equilibrium concentration of ^{135}Xe was replaced with ^{135}Cs, the ^{105}Rh was replaced with ^{105}Pd, and the ^{149}Pm was replaced with ^{149}Sm. When the fuel is rearranged during the shutdown, these modified inventories, along with four fresh FEs, become the next SU core. The long-lived fission products remain in the fuel materials as the FEs are moved to their next location.

4.5.1.3 Excess Reactivity, Moderator Dump and Shutdown Margin

This section and those that follow contain specific reactivity calculations and analyses. Table 4.5.2 lists the results of the reactivity calculations that will be discussed. This table has a label for each calculation, a short description, and the value of k_{eff} with the one standard deviation uncertainty along with the change in reactivity worth, as appropriate.

4.5.1.3.1 Reactivity Calculations

MCNP was used to calculate k_{eff} for the SU and EOC cores, along with the excess reactivity of the SU core, the shutdown margin (SDM) of the shim arm bank, and the SDM with the most reactive shim arm withdrawn. In addition, the worth of the moderator dump was determined for the excess reactivity case, with all control elements withdrawn. Since the components added to the updated MCNP model have been shown to be worth about 3% reactivity, the updated model was used for the calculations in this section.

The reactivity change, $\Delta\rho_X$, between a reference case with reactivity ρ_{ref} and some other configuration, ρ_X, is calculated as follows:

$$\Delta\rho_X = \rho_X - \rho_{ref} = (k_X - 1)/k_X \; - \; (k_{ref} - 1)/k_{ref}$$

$$= 1/k_{ref} - 1/k_X.$$

When expressed in the units of dollars of reactivity,

$$\Delta\rho_X(\$) = \Delta\rho_X/\beta_{eff}$$

where

$$\beta_{eff} = 0.00757.$$

4.5.1.3.2 Excess Reactivity and Shutdown Margin

In Table 4.5.2, the benchmark calculation for the SU is labeled "su183." This core is the most reactive because it has the most fuel, and because the short-lived fission products are not present. This reference case was calculated with the fuel and moderator at operating temperature. The shim arms are withdrawn to 22.7°. The resulting value of k_{eff} for this base case is 1.007. If the ambient temperature of 20°C is specified, as in the so-called cold, clean case of "sucold," there is an additional positive reactivity of 0.34 %Δk/k. Clean in this context does not imply the absence of fission products, but that short-lived poisons have decayed away, or in the case of ^{149}Sm, to its SU concentration.

The excess reactivity of the SU core, that is the reactivity difference between the reference case and the case with the shim arms and regulating rod fully withdrawn, "surefx," is 6.57 %Δk/k ($8.67), well below the 15% excess reactivity limit of the Technical Specifications. If all four shim arms are positioned at their lower limit, case "susdm," taking no credit for the regulating rod, the shutdown margin (SDM) is calculated to be –17.1 %Δk/k (-$22.6). The difference between the SDM and the excess reactivity is the total worth of the shim arm bank, which is 23.7 %Δk/k for the SU core, or $31.3.

For the EOC core, when the shim arms are fully withdrawn, the excess reactivity is zero by definition, at normal operating conditions. If the short-lived fission product poisons ^{135}Xe, ^{105}Rh, and ^{149}Pm are allowed to decay and the ambient temperature is specified, there is ample positive reactivity to restart the reactor, +2.7 %Δk/k ($3.61), but sustained operation at full power is impossible.

Another Technical Specification of the NBSR is that the reactor must not be loaded such that it cannot be shutdown with the highest worth shim arm withdrawn at ambient temperature. Starting with the "susdm" input file, four additional calculations were performed, using files "susdm1" through "susdm4," in which one of the shims was fully withdrawn, and the remainder were in their scram position. Table 4.5.2 shows that the absence of shim #2, the south-most shim arm, results in the highest value of k_{eff}, 0.9200, and that the SU core is at least 9.4% Δk/k ($12.4) subcritical with shim #2 fully withdrawn. Shim #3, the north-most shim arm, has nearly the same worth as #2. The reactor is still subcritical with two shim arms withdrawn and the other two inserted, as seen in the results of "susd12" and "susd34" in the Table 4.5.2. From north to south the shim safety arms are numbered 3, 4, 1, and 2.

4.5.1.3.3 Moderator Dump

As described in Section 4.2.3, the NBSR has a backup shutdown mechanism, the moderator dump. In this case the D_2O in the reactor vessel can be drained to a level 2.96 cm above the top of the fuel which is referred to as the "dump level." Figures 3-30 and 3-31 in Appendix A are plots of reactivity as a function of the upper reflector thickness for the SU and EOC cores, respectively. The worth of the moderator dump is clearly a function of the position of the shim arms. For the SU core, with the shim arms at 22.7°, draining the D_2O to the dump level, case

"dump18," inserts a reactivity of approximately –3.1 %Δk/k (-$4.1). For the EOC core, case "dumpec," this draining is worth is approximately –8.1 %Δk/k (-$10.7).

Comparing SU cases with the shim arms fully withdrawn at 41°, "surefx," the maximum reactivity case, and "dumpxs," the worth of the dump is –7.4%Δk/k (-$9.8). It is clear, therefore, that *the moderator dump will make the reactor subcritical even in its most reactive state.*

4.5.1.3.4 Fission Product Poisons and the Equilibrium Core

The three major fission product poisons treated explicitly in this analysis are listed in Table 4.5.3, along with some relevant nuclear characteristics.

As mentioned in Section 4.5.1.2, only the radioactive fission products with the highest cross sections are included in the fuel inventory. The EOC equilibrium core contains concentrations as calculated with ORIGEN2. During the ten day refueling between cycles many of the radioactive isotopes have decayed, therefore for the SU model those isotopes were manually removed from the concentrations and the masses added to their daughter products. There is also a beginning-of-cycle (BOC) equilibrium core model, where those isotopes have been built up. This occurs approximately two days into a new cycle. These are described in more detail in Appendix A. In order to complete the BOC composition, these isotopes were included in the four fresh FEs. The reactivity difference between the SU benchmark, "su183," and the BOC equilibrium core, "eqlib, " is k_{eff} = 0.97911, and Δρ = - 2.86 %k/k, or –$3.78. This calculation maintained the shim arm positions at the 22.7° withdrawn position.

With this equilibrium core, the shim arms need to be withdrawn another 5.3° in order to return the value of k_{eff} to the SU value of 1.007. This calculation is referred to as "eqi13." The 5.3° difference in the shim arm positions between the SU and the BOC cores is in good agreement with the operating experience of the NBSR, as stated in Section 4.5.1.1. This represents another benchmark for the updated MCNP model.

4.5.1.4 Power Distribution Calculations

Power distributions, calculated with both MCNP models, will be described below. The similarity of the results of the two models verifies that either may be used as a basis for the thermal-hydraulic analyses in later sections.

After the fuel constituents were determined, MCNP was used to determine power distributions, control element reactivity worths, and reactivity coefficients. The radial, axial, plate-wise, and transverse relative power distributions were then used to determine the hot spot factors needed in the core thermal analysis. Figures 3-8 and 3-11 of Appendix A show the radial power distributions of the FEs for the SU and EOC cores. A comparison of Figures 3-8 and 3-11 shows that for the SU core, the relative power in the outside rows, row 1 on the north and row 7 on the south, is generally greater than in the core interior. The FEs in rows 1 and 7 are the only FEs without shim arms adjacent to them. At EOC, the distribution shows the fuel loading bias to

the north half of the core, and a depression near the CNS. Figures 3-13 through 3-25 of Appendix A depict plate-wise, axial, and transverse power distributions. It is clear from both the axial and the plate-wise distributions at SU and EOC, that the presence of the shim arms in the core at SU causes a power distribution shift to the lower core. All of the plots show that the power peaks along the edges of the FEs, and adjacent to the unfueled region at the core mid-plane.

The radial, axial, and plate-wise power distributions were calculated using the updated MCNP model to demonstrate that the power peaking factors presented in the BNL report are equivalent to, or more conservative than, those determined using the updated model.

Figure 4.5.3 shows the relative radial (axially averaged) power distributions for the 30 FEs for the SU and EOC cores, and for the equilibrium BOC core described in Section 4.5.1.3. The uncertainties are 0.27%, or less. The underscore lines in Fig. 4.5.3 indicate the approximate position of the intersection of the shim arms and the plane at the top of the fuel. For example, shim arm #3, the north most, dips toward the east between rows 2 and 3. In the SU core, shim #3 passes part of element I-2 and passes even more of K-2; thus the power in K-2 is 9% lower than in I-2. There is more asymmetry in the power distribution in rows 2 and 6, because only one shim arm is adjacent to these two rows, whereas the center three rows have shim arms on both sides of the FEs, dipping in opposite directions. This asymmetry disappears in the EOC core, where the shim arms are well above the fuel.

In general, slightly more power is generated on the north side of the core than the south side, which is intentional to maximize the output of the CNS. Each FE in rows 1 through 3 has about 25 more grams of ^{235}U than its mirror image on the south side in rows 7 through 5. Power gradients are due to the cold neutron source, the location of the largest void in the reflector. The SU core evolves to the equilibrium BOC in about two days, so nearly the entire cycle has a radial power distribution that lies between the equilibrium BOC core and the EOC core.
A position-by-position comparison between Fig. 4.5.3 and Figs. 3-8, 3-9, and 3-11 in Appendix A shows that the power distributions calculated with the updated MCNP model and the BNL model are nearly the same. Not one of the relative fission power values calculated with the updated model exceeds 1.16, the power factor used in the BNL analysis for the BOC hot element (H-1).

The plate-wise and axial power distributions for the SU and EOC cores were also computed with the updated MCNP model to verify that that there was no increase in the hot spot factors over those reported in the BNL analysis. Plots of these distributions for the FEs, A-4, E-2, and D-1, are presented in Figs. 4.5.4 through 4.5.15 for comparison with the same elements in Figs. 3-13 through 3-24 of Appendix A. The most notable feature is that the fraction of fission power is considerably higher in the lower core than the upper core at SU. This imbalance is exaggerated in the BNL model because the shim arms are inserted further. For the BNL model, the fraction of power in the lower core is 63%, whereas it is 58% when the updated model is used. In the equilibrium BOC core, the lower core produces just 53% of the power. The axial power distribution gradually reverses so that the lower core produces 47% in the EOC core.

Figures 4.5.4, 4.5.5, and 4.5.6 show clearly the bottom-heavy power distribution among the fuel plates in the SU core. They show that the effect decreases from A-4, having shim arms on both sides, to E-2, with a shim on the south side only, to D-1, with no shim arm adjacent to it. The plate-wise power distributions are normalized to the entire core for comparison to the BNL analysis. Comparing these three plots with those in the BNL report shows that nearly all the individual values are lower in the updated model, and that the power ratio of the lower to upper cores is also smaller. The curves are nearly symmetric, an exception being the west side of A-4, which faces away from the core.

Figures 4.5.7, 4.5.8, and 4.5.9 show the plate-wise power distributions for the same FEs for the EOC core. These demonstrate a slightly higher power distribution in the upper half of the core for EOC conditions.

Inspection of the axial profiles in Figs. 4.5.10 through 4.5.15 shows the same features. The power peaks at the edges of the FEs and not in the center. The relative values are nearly always lower for the power calculated with the updated MCNP model.

In summary, the shift from the original BNL model, to the updated model, used to calculate the power distributions shown in this chapter, tends to reduce the peaks and valleys in the calculated power distributions. The qualitative features are clearly the same. The hot spot factors used in the BNL core thermal analysis are therefore valid, and indeed conservative. The updated model did not show any hot channels or hot stripes that would produce a greater heat flux or higher temperatures than those of Appendix A.

4.5.1.5 Shim Safety Arms and Reactor Kinetic Behavior

4.5.1.5.1 The Shim Safety Arms

Reactivity control of the NBSR is achieved primarily through the movement of the four shim safety arms, described in Section 4.2.2.3, during the course of the reactor cycle. During a normal cycle, the shim safety arms would need to be withdrawn more than 20° above their shutdown positions for the reactor to reach criticality. After the initial criticality, the shim safety arms are further withdrawn approximately 5° in the first two days of a cycle to offset fission product poisoning. For the remainder of the cycle, the shim safety arms are raised to offset the burnup of fuel, as stated in Section 4.5.1.1. This is demonstrated in Fig. 4.5.16a, a plot of the shim arm bank position as a function of time into the cycle. This figure shows the large change in the first two days as the reactor poisons increase. After the initial shim arm movement, there is a gradual withdrawal until the shim safety arms are above the core and larger withdrawal steps are needed to achieve the same negative reactivity insertion. In the fully withdrawn, horizontal position, the shim safety arms are approximately 34 cm above the fuel. The withdrawal of the shim safety arms is to compensate for the smaller excess reactivity in the core as the ^{235}U is burned. The data in Figure 4.5.16 can be restated in terms of excess reactivity and this is shown in Figure 4.5.17. *Half of the initial excess reactivity is offset by the buildup of fission products in the first 2 days.*

There is an uncertainty associated with each point of ±0.2% Δρ because the exact position of the regulating rod and the temperature varied somewhat.

The integral and differential reactivity worths of the shim arm bank, measured with new shim safety arms in 1995, are shown in Figs. 4.5.18 and 4.5.19, respectively. Multiplying the differential shim bank reactivity worth by the speed of the shim arm drives, 0.0445 °/s, one obtains the reactivity insertion rate vs. position, shown in Fig. 4.5.19. The maximum calculated rate is 4.5×10^{-4} (%Δk/k)/s. Technical specifications limit the rate to 5.0×10^{-4} (%Δk/k)/s.

MCNP was also used to determine k_{eff} at 25 different shim arm positions, for both the SU and EOC cores, as discussed in Sections 3.5.3 and 4.2.3.5 in Appendix A. The data were fit to fifth-order polynomials to generate the shim arm worth curves in Fig. 4.5.20. These curves were later used for the transient analyses in Chapter 13. Using the BNL model, the calculated integral worths of the shim arm bank are 23.1 %Δk/k ($30.5), for the SU core, and 26.8 %Δk/k, at EOC ($35.4). The updated model has nearly the same results, as seen in Section 4.5.1.3.2.

4.5.1.5.2 Reactivity Worths of Individual Shim Safety Arms

MCNP was used to calculate the reactivity worth of each individual shim arm, when the remaining shim safety arms are fully withdrawn. For the EOC core, the input files "ecsdm1" through "ecsdm4" have just one shim arm inserted, and are compared to the reference case. For the SU core, the files "drop1" through "drop4" are compared to "surefx," in which all the shim safety arms are fully withdrawn. The shim arm worths so calculated are shown in Table 4.5.4.

The insertion worths are the reactivity insertions from the shutdown margin case by fully withdrawing one shim arm. As expected, the shim safety arms in the center of the core, numbers 1 and 4, are worth more than the outer ones, if just one is inserted. The outside shim safety arms are worth more if just one is withdrawn because if either shim arm 2 or 4 is absent, there will be three rows of FEs without poison. It is often the case that the worth of one control element depends on the location of the others. The measured values for the individual shim safety arms are necessarily made with the remaining three shims at some other position to keep the reactor close to critical.

4.5.1.5.3 The Regulating Control Rod

A description of the regulating rod is presented in Section 4.2.2.2. Its measured reactivity worth is about 0.58 %Δk/k, and, since its maximum speed is 1.9 in/s (4.8 cm/s), its average reactivity insertion rate is 3.8×10^{-4} Δρ/sec. Figure 3-28 of Appendix A shows the integral worth curve for the regulating rod in the SU core; its calculated value, 0.57 ± 0.05 %Δk/k ($0.75), in good agreement with the measured value. For the EOC case, Fig. 3-30 shows a value of 0.46 ± 0.05 %Δk/k ($0.61).

Figure 4.5.21 is a plot of calculated vs. 'measured' differential shim bank reactivity. The calculated values, Series 2, are from a fifth-order polynomial fit of MCNP results from the BNL

analysis of the EOC core, converted into units of equivalent inches of travel for the regulating rod. The data points of Series 1 are the measured values of regulating rod travel required to offset the shim movement. The measurements are actually numerous reactor operating log entries of shim arm withdrawals and the offsetting regulating rod insertions for the first 18 reactor cycles with the shim safety arms installed in January, 2000. Adjustments are required about every two days to keep the regulating rod within its automatic operating limit. The units of reactivity are equivalent inches of regulating rod travel, assuming that the worth of the rod is a constant, 0.020 %Δk/k per inch. While there is some scatter in the points because the data were collected for other purposes, nearly all of the recorded values for the regulating rod insertions are on, or just below, the curve of calculated differential worths of the shim arm bank. The points below the curve are from the later cycles, and are indicative of the decrease in the worth of the shim bank as the cadmium is depleted. These data serve as a benchmark for the MCNP shim arm reactivity worths.

4.5.1.6 Reactivity of Fuel Elements and Beam-Tube Flooding

4.5.1.6.1 Fuel Reactivity Worth

Without major modifications, it is impossible to load more than 30 FEs into the NBSR core because there are only 30 unoccupied positions in the two grid plates. It is impossible to insert an FE into the core while the reactor is operating. Therefore there is no need to know the reactivity worth of a FE from the standpoint of a transient initiating event. A fuel-loading accident, in which two elements are mistakenly positioned in each other's location, does not result in a large reactivity insertion because the total fuel load is the same.

The worth of a given FE was calculated by omitting it from the hexagonal array in the MCNP input file, and determining the new value of k_{eff}. The calculations, labeled "minus1" and "minusc" in Table 4.5.2 represent the cases where FEs A-4, in the outer core, and F-5, in the inner core, were omitted. Removing A-4 resulted in a worth of $\Delta\rho = -0.86 \pm 0.06$ %Δk/k (-$1.1), and removing F-5 resulted in a worth of $\Delta\rho = -1.05 \pm 0.06$ %Δk/k (-$1.4). The A-4 FE contains 350 grams of ^{235}U, so the reactivity per unit mass is 2.5 %Δρ/kg. The fuel mass in F-5 is just 138 g, so the normalized worth is 7.6 %Δρ/kg. As expected, a unit mass will be much more important in the inner core than in the outer core. An estimate of the average worth of a kilogram of fuel in the NBSR core can be obtained by dividing the excess reactivity, 6.57 %Δρ, by the mass of fuel consumed in an average cycle, 0.97 kg, yielding 6.8 %Δρ/kg.

4.5.1.6.2 Flooding of Beam Tubes

Since the beam tubes in the NBSR vessel introduce large voids in the core reflector, the filling of a beam tube with D_2O will result in a positive insertion of reactivity. A crack in a beam tube thimble, or a failure of a D_2O-cooled experiment installed in a beam tube, could cause the tube to be filled. The cryostat assembly of the cold neutron source is an example of a D_2O-cooled experiment. These scenarios were analyzed in the BNL report, Appendix A, and the resulting

reactivity insertions are listed in Tables 3-3 and 3-4 of Appendix A for the SU and EOC cores, respectively.

The largest single reactivity insertion from such a failure would be the flooding of the moderator chamber and insulating vacuum of the liquid hydrogen CNS, installed in 2002. The results for the CNS and individual beam tubes are:

CNS Cryostat Assembly	0.49 %Δk/k ($0.53)
Average Radial Beam Tube	0.21 %Δk/k ($0.28)
1 Tangential Beam tube	0.38 %Δk/k ($0.50)

All of these reactivity insertions are much smaller (and would occur more slowly) than the maximum reactivity insertion case, 1.3 %Δk/k in 0.5 sec, analyzed in Chapter 13.

4.5.1.7 Core Configuration Management

Physical and administrative constraints combine to preclude a reactivity insertion exceeding the cases described in Chapter 13, Accident Analyses. As mentioned previously in this section, all 30 of the fuel locations are occupied whenever the reactor is operating. The reactor is sealed during operation, making it impossible to introduce another FE, or change the core configuration in any way. There is only a vacant fuel position during refueling, which is done with the reactor shutdown and the shim safety arms fully inserted. Only one FE is moved at any given time, the one being moved, or its replacement.

There are only three means of adding positive reactivity to the reactor while it is critical: (1) withdrawing the shim safety arms, (2) lowering the inlet D_2O temperature, and (3) rapidly removing experiments. Changing the moderator temperature is a slow process, allowing plenty of time for the operators to compensate by inserting the shim safety arms. The startup accident, in which the shim safety arms are continuously withdrawn adding positive reactivity at the maximum possible rate has been analyzed in Section 13.2.2.2.1 and shown to be bounded by the withdrawal of experiments worth 1.3 %Δρ in just 0.5 sec. This maximum reactivity insertion requires an incredible scenario, namely, three operators removing three experiments at the same instant. Nevertheless, it is shown in Section 13.2.2.2.2 that it will not result in fuel failure.

The Safety Evaluation Committee and the reactor operations staff, review proposed experiments for conformance to technical specifications, listed in Section 4.5.3.2. No single experiment may be worth more than 0.5 %Δρ, and a total worth of 2.6%Δρ for all experiments in the core at one time. In addition, no explosives or hazardous materials may be present in the NBSR such that an experiment failure can damage the core.

Although the excess reactivity limit is 15 %Δρ, strict control of experiments assures that there can be no reactivity insertion beyond the maximum insertion analyzed in Chapter 13. The TS concerning the excess reactivity, shutdown margin, experiments, and the moderator dump are presented in Section 4.5.3.

4.5.2 Reactor Core Physics Parameters

4.5.2.1 Delayed Neutron Fraction and Neutron Lifetime

The value used for the effective delayed neutron fraction, β_{eff}, is unchanged from the 1980 Addendum to the original safety analysis, NBSR-9. The prompt neutron lifetime, l_p, has been calculated by simulating a subcritical, pulsed neutron source die-away "experiment" using MCNP in a time-dependent mode.

4.5.2.1.1 Effective Delayed Neutron Fraction

Table 4.5.5 lists the delayed neutron groups and their decay constants. Photoneutrons, created in the D_2O from high-energy gamma rays interacting with deuterium nuclei, supplement the delayed neutrons emitted from fission products. The neutrons are divided into 14 groups, 6 groups from fission products, and 8 groups of photoneutrons, for input into the RELAP5 coupled thermal-hydraulics/point-kinetics code. The code is described in Section 4.6 of this Chapter, and in Chapter 4 of Appendix A. At a steady reactor power, the fraction of all the neutrons that are delayed is $\beta_{eff} = .007574$.

4.5.2.1.2 Prompt Neutron Lifetime

In principle, the prompt neutron lifetime can be calculated by dividing the neutron density in the core by the rate of production of neutrons from fission. While this sounds straightforward, it is quite complicated in a heterogeneous core such as the NBSR. MCNP provides values of the prompt neutron lifetime during standard criticality calculations (Bretscher, 1997). However, these numbers are believed to over-estimate the prompt neutron lifetime. Heavy water moderated and reflected research reactors typically have prompt neutron lifetimes reported to be on the order of 700 μs (GTRR: 770 μs; expanded SPERT-II core: 750 μs; HFBR: 672 μs) (Bretscher, 1997), (Grund, 1963), (Hendrie, 1964).

In NBSR-9 Supplement 1, values of the prompt neutron lifetime, calculated using two-group diffusion theory and a homogenized core model, varied from 500 μs to 800 μs, depending on the core volume and the fuel loading. The value of 400 μs was chosen as a conservative value for that safety analysis. In the current analysis, a more precise calculation was performed using the exact geometry and the SU and EOC fuel loads.

Prompt neutron lifetimes were calculated at BNL (Hanson et al, 2004) using MCNP simulations of a pulsed neutron source in the subcritical NBSR. The response of a subcritical assembly following a neutron pulse was described by Bell (Bell et al, 1970). The prompt neutron lifetime is related to the decay constant, α, which is the slope of the logarithm of the decaying neutron population. Time dependent tallies of neutron population were therefore calculated with MCNP. The neutron population, P, decays as:

$$P(t) = Q\, e^{\alpha t} = Q \exp[(\rho-\beta)t/l_p], \text{ where}$$

Q = source strength
$\alpha = (\rho - \beta)/l_p$ = decay constant
ρ = reactivity
β = effective delayed neutron fraction
l_p = prompt neutron lifetime

A 10-μsec pulse of 14-MeV neutrons was introduced in the center of the core, and detector tallies were made at a variety of locations to check for geometry effects. (Only the detectors near the shim safety arms of the SU core were inconsistent with the others.) Many values of ρ were sampled to determine the asymptotic behavior of α as k_{eff} approached 1.000. The following values of the prompt neutron lifetime were obtained for the NBSR:

Startup: 780 ± 50 μs
End-of-Cycle: 810 ± 50 μs.

4.5.2.2 Reactivity Coefficients

4.5.2.2.1 Moderator Temperature Reactivity Coefficient

The bulk temperature coefficient for the D_2O moderator, coolant, and reflector has been calculated for SU, BOC, middle-of-cycle (MOC) and EOC cores. The details of the calculations are presented in Section 3.5.1 and Table 3-1 of Appendix A. While it is easy to reduce the D_2O density from 1.0966 g/cm^3 at 319 K (115°F) to 1.0635 g/cm^3 at 373 K (212°F) continuously in MCNP, the thermal neutron scattering cross sections, S(α,β), are discrete data sets evaluated at either 300 K or 400 K. Therefore, separate calculations were performed to obtain Δρ for each contributor. These calculated values of Δρ were divided by the appropriate ΔT to obtain two components of the coefficient. The components were then summed together for the overall temperature coefficients. The results are given in Table 4.5.6.

In each case, both components of the coefficient are negative. A comparison between results that use both the density and the scattering kernel singly and together verified that the coefficient is indeed the linear, un-weighted sum of the two components. The measured value of the moderator temperature coefficient for the NBSR is –0.016 %Δk/k/°F, or (-0.029 %Δk/k/°C). The calculations using the BNL model are in excellent agreement with the measurements.

4.5.2.2.2 Void Reactivity Coefficients

Although the FEs in the reactor core are widely spaced, the NBSR is an under-moderated reactor. A decrease in the D_2O density anywhere in the reflector, the moderator, or the coolant inside the FEs, results in a negative reactivity insertion**.** The magnitude of the void coefficient depends on the location of the void.

Figures 3-30 and 3-31 in Appendix A show a large decrease in k_{eff} as the level of D_2O above the core is reduced to zero. It is intuitive that neutrons will be lost to leakage if the density or volume of the reflector is reduced. Since the curves drop sharply as the level approaches zero, the reactivity worth of a liter of D_2O close to the core is greater than a liter far from the core.

The void coefficient in the moderator region between the FEs was calculated using the BNL model by voiding the cells inside the six 3.5-inch (8.9-cm) vertical thimbles in the core. The results for the SU and EOC cores are listed in Table 3-2 of Appendix A, and discussed in Section 3.5.2, of Appendix A. The coefficients are recomputed and shown in Table 4.5.7.

The total volume of the void was used even though a liter of D_2O near the core is worth much more than a liter near a grid plate. The values calculated for NBSR-9 for the upper and lower cores are -0.038 %Δk/k/l (-$0.05) and –0.043 %Δk/k/l (-$0.06), respectively.

A single vertical thimble is approximately the same size as one of the tangential beam tubes. The voiding of one single thimble has a reactivity insertion of -0.34 %Δk/k (-$0.45). This is almost identical to the reactivity insertion for flooding one tangential beam, 0.38 %Δk/k ($0.50).

The updated MCNP model was used to calculate the effect of voiding the coolant channels inside the FEs. To obtain the reactivity change that would occur if the coolant channels were empty of D_2O, presumably due to boiling or a blockage, all of the D_2O in the FEs were voided, above the level of the lower fuel plates. For both the SU and EOC cores, the reactivity insertion so calculated is approximately Δρ = -4.5 %Δk/k (-$5.9). The volume of the coolant channels between the plates is about 93 liters, so the calculated void coefficient is –0.048 %Δρ/liter (-$0.06/l). Finally, from the BNL analysis, if somehow only the unfueled regions between the upper and lower fuel sections were to be voided, the coefficient would be -0.025%Δρ/l, further evidence that the removal of D_2O anywhere in the core adds negative reactivity.

4.5.2.2.3 Light Water Ingress

Section 3.5.7 of Appendix A shows that light water contamination of the NBSR coolant will result in a negative insertion of reactivity. If the D_2O becomes contaminated with 10% H_2O, the reactivity insertion is -16% or -$21 for the SU core.

4.5.2.3 Neutron Flux Distributions

The radial and axial power distributions have been described previously in Section 4.5.1.4. In this section, the thermal and fast neutron flux distributions along the vertical and horizontal axes are presented. In addition, the power distributions are analyzed further to obtain the location of core hot spots, required for the thermal analysis in Section 4.6.

4.5.2.3.1 Axial Flux Distribution

The calculated fast and thermal neutron fluxes in the central thimble as a function of elevation are shown in Fig. 4.5.22. The maximum thermal flux, 3.5 x 10^{14} n/cm^2/s, occurs very close to the core mid-plane, in the unfueled region between the upper and lower cores. The fueled regions are between –36.8 cm and –8.9 cm, in the lower core, and between +8.9 cm and 36.8 cm, in the upper core. For these calculations, a thermal neutron has energy less than 1 eV, and the remainder is considered fast. The fluxes were tallied inside the 3.5-in (8.9 cm) diameter aluminum hold down tube, in 2-cm thick intervals. At its peak, the thermal neutron flux is over four times the fast neutron flux. The calculated values are in good agreement with the measured peak thermal neutron flux in the central thimble of 3.5x10^{14} n/cm^2/s, at 20 MW.

From the asymmetry of the SU curves in Fig. 4.5.22, the impact of fuel burnup and shim motion is obvious. At the start of the cycle, two shim safety arms cross, one on each side of the central thimble, at an elevation of 41 cm. As a result, both the thermal and fast fluxes in the upper core are reduced and skewed toward the lower core. At the end of the cycle, when the bottom of the shim safety arms are at 70 cm, far above the upper core, the axial fluxes are nearly symmetric about the core mid-plane. The value of the peak thermal flux hardly changes during the cycle, but its location shifts from -4 cm to +2 cm.

4.5.2.3.2 Radial Flux Distribution

A plot of the calculated fast and thermal neutron fluxes along the mid-plane as a function of the distance from the core centerline is shown in Fig. 4.5.23. The 2-cm thick tally cells for these calculations lie along the center row of FEs running from the center to the east. The regions were in the unfueled region of FEs I-4, K-4, and M-4. The fast neutron flux is nearly constant at approximately 10^{14} n/cm^2/s through the core at this elevation, after a dip at the centerline. At the edge of the last FE, M-4, about 55 cm, the fast flux drops an order of magnitude in 20 cm. The thermal flux drops more slowly through the core and beyond. The slight increases or waves in the curve correspond to the regions between FEs. Since the FEs are widely spaced, there is no thermal neutron peak in the reflector region.

There is very little difference in the radial flux distributions between the SU core and the EOC core, as can be seen in Fig. 4.5.24. The thermal neutron flux at a point 54 cm from the core centerline, increases from 1.9x10^{14} n/cm^2/s, in the SU core, to 2.1x10^{14} n/cm^2/s at EOC, during a typical cycle.

The fluxes have been calculated for all of the beam tube (BT) tips and pneumatic tube ends. The average thermal flux at the BT tips is 1.5x10^{14} n/cm^2/s, whereas the average fast flux is about 7x10^{12} n/cm^2/s.

4.5.2.3.3 Hot Channels and Hot Spots from the Updated MCNP Model

To determine the peak-to-average heat generation in the core, the energy deposited in each channel was calculated using the MCNP results for the SU and EOC cores. Each channel was subdivided into 8 axial slices, to obtain the axial distribution of the heat input. Channels in the hottest elements were further divided into 17 stripes to obtain the lateral peaking factors. Hot spots, needed for the thermal-hydraulic analysis, were obtained by combining these factors.

Hot Channels:

Using the updated MCNP model of the NBSR core, the heat deposited in all 1080 coolant channels (upper and lower cores) has been determined. The input file used to obtain the data for the SU core had the shim safety arms withdrawn 22.7 degrees, and the regulating rod fully inserted. Inserting the regulating rod slightly enhances power production in the north side of the core. The shim safety arms were fully withdrawn for the EOC case, but the regulating rod was again inserted. Table 128 of the MCNP output lists the number of fissions in each cell, or fuel plate, in the problem. Since the calculation was run for 20 million starting particles, each fission event recorded corresponds to 1 watt, assuming that the fission distribution and the power distribution are identical.

To obtain the heat deposited in the coolant channels, it is assumed that each channel receives half of the heat generated in the two plates defining the channel. The upper core and lower core were computed separately because the coolant mixes in the unfueled region. The hot channels are always either #2 or #17, where #1 is the west-most channel, and #18 the east most. Sums of all these data represent the heat produced in the 30 elements; normalization reproduces the fuel element power factors. Element H-1 produces the most power (769.5 kW) in the SU core; its power factor is 1.154. There are, however, five coolant channels in the lower core with heat input greater than the hot channel in H-1. Element L-3 has the highest power (738.4 kW, power factor 1.108) in the EOC core, and again there are channels in other elements with more heat. The hot channels for some of the highest power elements are shown in Tables 4.5.8 and 4.5.9. The core-average heat input for the 1080 channels is 18,520 W.

Hot Slices:

The distribution of the heat into the hot channels as a function of elevation was determined by dividing all of the fuel plates axially into eight 3.49-cm slices. The raw fission data from Table 128 was used to obtain the axial heat input into each slice of each channel for all of the elements. Again the heat input to a channel slice is half of the heat generated in each of the two plates defining the channel. By dividing each ΔQ by the core average, 2315 W per slice, we have the axial channel peaking factors in Tables 4.5.8 and 4.5.9. In the SU core, the hottest slice of the hot channel is always at the top of the lower fuel section. In the EOC core, most of the hottest slices are at the bottom of the upper fuel section, but there are notable exceptions, such as A-4, in which the hottest slice of the hot channel is at the top of the lower fuel. *Since the axial channel*

peaking factors are directly determined, they combine the fuel element, plate-wise, and axial power factors.

Hot Spots:

To locate the hottest spots in the core, the lateral power distribution of the hottest elements was determined by dividing the hot slices adjacent to the unfueled region, south-to-north, into 17 vertical stripes with widths of $\Delta y = 0.36$ cm. Again, drawing the raw fission data from MCNP Table 128, the heat deposited into each stripe was obtained from the two adjacent plates. These lateral peaking factors are also listed in Tables 4.5.8 and 4.5.9. The local hot stripe peaking factors are the products of the axial channel and the lateral peaking factors. For the lower core, the maximum lateral peaking factor from the top slice of the hot channel is listed. For the upper fuel section, the highest lateral peaking factor for either channel 2 or channel 17 is listed, regardless of which was hottest in the lower section, because the coolant mixes prior to entering the top section.

Uneven Burnup Correction of EOC Hot Spot Factors:

The burnup analysis using MONTEBURNS produces a set of MCNP materials in which the concentrations of ^{235}U are determined from the *average* fission rates in a pair of fuel elements over the course of each cycle. These materials fill all the fuel meat cells in an element *uniformly*. It is impossible for MONTEBURNS to generate a sufficient number of MCNP materials to track the uneven burnup within a given fuel element. Since the fission rate at a hot spot may be well over twice the average rate, according to the MCNP power distributions cited above, it is clear that the ^{235}U atom density at a hot spot at EOC will be lower than the average value characteristic of the MCNP material for the element. Because the hot spots are always at the edges of the fuel sections adjacent to the unfueled center, the uneven burnup is compounded cycle after cycle. As a result, the hot spot factors determined from MCNP power distributions will be increasingly distorted, large over-estimates, with each sequential cycle in core. MCNP power distributions in elements burned more than 4 cycles indicate hot spots (near the unfueled region) *where there would be no fuel remaining* if the power distributions in earlier cycles were correct.

A correction factor for uneven burnup can be estimated by calculating the ^{235}U density at the hot spot at EOC, and its ratio to the EOC material average density. Since the neutron flux in the unfueled region is nearly constant through a cycle, the fission rate is proportional to the estimated ^{235}U atom density. The core average fission rate is obtained from the fact that 667 kW is produced per element in 296 cm^3. Since approximately 3.1×10^{10} fissions/sec is required per watt, the average fission rate is 7.0×10^{13} fis/cm^3/s. The rate of consumption of ^{235}U is 1.17 times the fission rate, or 7.1×10^{18} fis/cm^3/day. We define 'a' as the fractional daily consumption rate, which for a fresh fuel element is given by

$$a = (7.1 \times 10^{18} \text{ fis/cm}^3\text{/day})/(3.03 \times 10^{21} \text{ atoms/cm}^3)$$

$$a = 0.0023 \text{ day}^{-1}.$$

At any time, t, the loss rate is

$$dN/dt = -a\,N(t).$$

The solution is the atom density as a function of time

$$N_{35}(t) = N_{SU} \exp(-at),$$

where, N_{SU} is the ^{235}U atom density at startup. For a hot spot with an average peaking factor of <pf> over a 38-day cycle,

$$N_{EOC} = N_{SU} \exp(-0.088 \langle pf \rangle), \text{ where } a*t = 0.088.$$

From the MCNP fuel constituents, the EOC density is

$$N_{EOC,\,MCNP} = (w_{EOC}/w_{SU})\, N_{SU},$$

where the w's are the weight fractions of ^{235}U in the SU and EOC MCNP materials. The ratio of the hot spot U density to the MCNP material composition will be the correction factor for the EOC peaking factor:

$$\eta = N_{EOC}/N_{EOC,MCNP} = (w_{SU}/w_{EOC}) \exp(-0.088 \langle pf \rangle).$$

For example, the peaking factors for both fuel sections of A-4 for the SU and EOC cores are 2.485, 2.092, 2.254, and 2.175, so <pf> = 2.25. Its ^{235}U weight fractions are $w_{SU} = 0.3274$ and $w_{EOC} = 0.3007$, and the hot spot correction factor is

$$\eta_{A\text{-}4} = (1.09) \exp[(-0.088)(2.25)] = 0.89.$$

The fuel density is only 89% of the MCNP value at the hot spots of A-4 at EOC, and, therefore, the EOC hot spot peaking factors are reduced by this factor. For element M-4, the factor is 0.90, and the hot spot factors for H-1 were reduced in the SU core because the M-4 element is moved to H-1 for the start of the following cycle. The last columns of Tables 4.5.8 and 4.5.9 show these corrections.

Uneven burnup, cycle after cycle, has a profound effect on the power distribution within the fuel elements. Hot spot and axial peaking factors are reduced as the fuel on the edges of the elements is preferentially consumed. As the heat generation moves toward the interior of the fuel element it is more evenly distributed among the plates, and subsequent hot spots and hot channels are never as large as the MCNP calculated results. Values for η in subsequent cycles have been

estimated, and new peaking factors generated. These compounded approximate corrections grow increasingly uncertain, but the semi-quantitative behavior can be seen in Figure 4.5.25.

The correction factors used for the tables are as follows: 0.9, for a one-cycle correction, $(0.92)^2$ for the two-cycle correction, and $(0.92)^3$ for the three (or more) cycle correction. The hot channel factors were not changed: this is conservative, resulting in an overestimate of the heat deposited in those channels. When the hot spot values in Tables 4.5.8 and 4.5.9 are corrected this way for uneven burnup, element A-4 is the limiting EOC case for the response to transients in Chapter 13; H-1 is limiting for the determination of safety limits in Section 4.6 (SU core).

Finally to obtain the hot spot heat flux, the local hot stripe peaking factor was multiplied by the local hot plate to hot stripe power ratio, which varies from 1.00 to 1.05 (H-1 is the largest). This final factor accounts for the fact that the hot stripe factors were obtained from the average of two adjacent plates, not the hottest plate. The maximum local heat flux is the product of the core-average heat flux, 57.2 W/cm^2, and the hot spot peaking factor. The axial power factors for the hot channels, and the hot spots for the local heat fluxes, used in the thermal analyses are listed in Tables 4.5.10 and 4.5.11.

4.5.3 Operating Limits

This section contains the safety limits, limiting safety system settings, and limiting conditions for operation, for NBSR core parameters. None of the Technical Specifications (TS) have been changed, though some of the bases have been updated to refer to this SAR. The complete set of TS is in NBSR-15 (NIST, 2004), a companion document to this SAR.

4.5.3.1 Reactivity

These are the TS concerning the shutdown margin, excess reactivity and the moderator dump. Section 4.5.1.3 describes the numerous calculations of these parameters, and demonstrates the substantial shutdown margins for combinations of 1, or even 2, shim safety arms stuck in their fully withdrawn positions. The shim safety arm worths and the maximum reactivity insertion rate were calculated in Section 4.5.1.5, and shown to be in excellent agreement with measured values. Void coefficients and the moderator temperature coefficient were calculated in Section 4.5.2.2, and again shown to agree well with measurements. The limiting conditions for operation relating to reactivity have not changed.

4.5.3.1.1 Shutdown Margin and Excess Reactivity

Technical Specification 3.3, Reactor Core Parameters:

This specification applies to the core grid positions and core loading. The objective is to ensure that the core grid positions are correctly filled and the core is properly loaded.

(l) The reactor shall not be operated unless all grid positions, except the six corner positions in the outer hexagonal ring, are filled with full-length core assemblies. The six corner positions must be plugged in the lower grid, if not filled with such assemblies.

(2) The core shall not be loaded so that:
   a) it cannot be shut down with the highest-worth shim arm withdrawn at ambient temperatures, or
   b) the excess reactivity at normal operating temperatures exceeds 15 %Δρ.

Basis:

The NBSR employs shim safety arm stops to prevent a broken shim arm from dropping from the reactor core. The proper operation of these stops depends on adjacent fuel elements or experimental thimbles being in place to prevent the broken arm from falling from the core lattice. The six corner positions, although not required as part of the shim arm stops, must be plugged at the bottom to prevent cooling flow from bypassing the fuel elements.

To allow shim arm testing and to provide for the possibility of a stuck arm, the reactor must be subcritical with the highest-worth shim arm fully withdrawn.

The excess reactivity limit was established to ensure a substantial shutdown margin and to accommodate postulated reactivity accidents. The selected value of 15 %Δρ is based on the following:

1. The shutdown margin with the most reactive rod fully withdrawn is adequate.
2. The design-basis reactivity accident, which assumes the insertion of 1.3 %Δρ into a just critical core, is not affected by the total core excess reactivity.
3. The startup accident, which assumes constant withdrawal of all control rods until a scram occurs, is terminated by scram action after an insertion of reactivity, which is small compared to the total core excess reactivity.

4.5.3.1.2 Moderator Dump

In Section 4.5.1.3.3, it was shown that the moderator dump provided sufficient negative reactivity to make the SU core subcritical, even with all four shim safety arms fully withdrawn. Its operability is a limiting condition for operation:

Technical Specifications 3.4, Reactor Control and Safety Systems:

The reactor shall not be operated unless :

(1) all four shim safety arms are operable

(2) the reactivity insertion rate, using all four shim safety arms, does not exceed 5.0 x 10^{-4} $\Delta\rho$ / sec
(3) the Scrams and Major Scrams are operable in accordance with Table 3.1 of the Technical Specifications.
(4) the moderator dump system is operable

Basis:

Although the NBSR could operate and could maintain a substantial shutdown margin with less than the four installed shim safety arms, flux and rod worth distortions could occur by operating in this manner. Furthermore, operation of the reactor with one shim arm know to be inoperable would further reduce the shutdown margin that would be available if one of the remaining three shim arms were to suffer a mechanical failure that prevented its insertion.

A rod withdrawal accident for the NBSR is analyzed (SAR, NBSR 14, Chapter 13 and appendix A) using the maximum insertion rate, corresponding to the maximum beginning-of-life rod worths with the rods operating at the design speed of their constant speed mechanisms. The analysis showed that the most sever accident, a startup from source level, is bounded by the maximum reactivity insertion accident, and will not result in core damage.

In the unlikely event that the shim safety arms cannot be inserted, an alternate means of shutting down the reactor is provided by the moderator dump. The moderator dump provides a shutdown capability for any core configuration. Hence, it is also considered necessary for safe operation. It is shown (FSAR, NBSR 14, chapter 4) that the moderator dump provided sufficient negative reactivity to make the normal Start-Up (SU) core subcritical even with all four shim arms fully withdrawn.

4.5.3.2 Experiments

These are the TS governing the reactivity of experiments, and imposing additional restrictions concerning the use of hazardous materials inside the NBSR. As stated in Section 4.5.1.7, the rapid removal of experiments could result in a positive reactivity insertion, so experiments are strictly controlled:

Technical Specification 3.12, Experiments:

This specification applies to any experiments to be installed within the NBSR. The objectives are to establish criteria for placing experiments in the NBSR and to establish limits on these experiments.

Any experiment installed in the reactor shall meet the following criteria:

(1) The absolute reactivity of any experiment shall not exceed 0.5 %$\Delta\rho$.

(2) The sum of the absolute values of reactivity of all experiments in the reactor and experimental facilities shall not exceed 2.6 %Δρ.
(3) No experiment malfunction shall affect any other experiment so as to cause its failure. Similarly, no reactor transient shall cause an experiment to fail in such a way as to contribute to an accident.
(4) Explosive or metastable materials capable of significant energy releases shall be irradiated in double walled containers that have been satisfactorily prototype tested with at least twice the amount of the material to be irradiated.
(5) Each experiment containing materials corrosive to reactor components or highly reactive with reactor or experimental coolants shall be double contained.

Basis:

The individual experiment reactivity limit is chosen so that the failure of an experimental installation or component will not cause a reactivity increase greater than can be controlled by the regulating rod. Because the failure of individual experiments cannot be discounted during the operating life of the NBSR, failure should be within the control capability of the reactor. This limit does not include such semi-permanent structural materials such as brackets, supports, and tubes that are occasionally removed or modified, but which are positively attached to reactor structures. When these components are installed, they are considered structural members rather than part of an experiment.

The combined reactivity allowance for experiments was chosen to allow sufficient reactivity for contemplated experiments while limiting neutron flux depressions to less than 10%. Included within the specified 2.6 %Δρ is a 0.2 %Δρ allowance for the pneumatic irradiation system, 1.3 %Δρ for experiments that can be removed during reactor operation, and the remainder for semi-permanent experiments that can only be removed during reactor shutdown. Even if it were assumed that all of the allowed 1.3 %Δρ for removable experiments were removed in 0.5 sec, analysis has shown that this ramp insertion into the NBSR operating at 20 MW would not result in any fuel failure releasing fission products (Chapter 13 of this SAR). The 0.2 %Δρ for the combined pneumatic irradiation systems is well below this referenced accident as well as being within the 0.5 %Δρ capability of the regulating rod.

In addition to all reactor experiments being designed not to fail from internal overheating or gas buildup, they must also be designed to be compatible with their environment in the reactor. Specifically, their failures must not lead to failures of the core structure or fuel, or to the failure of other experiments. Also, reactor experiments must be able to withstand, without failure, the same transients that the reactor itself can withstand, without failure (i.e., loss of reactor cooling flows, startup accident, and others where the reactor safety system provides the ultimate protection).

The detonation of explosive or metastable materials within the reactor is not an intended part of the experimental procedure for the NBSR; however, the possibility of a rapid energy release must be considered when these materials are present. Because the analytical methods used for designing containers for very rapid energy releases are not well developed, full prototype testing

of the containment design is specified. The requirement for testing twice the amount of material to actually be irradiated provides a safety margin of at least a factor of two to allow for possible experimental uncertainties.

Experiments containing materials corrosive to reactor components or highly reactive with reactor or experimental coolants, although limited by item (3) of this specification, provide the potential for reducing the integrity of the fuel elements. For this reason, an added margin of safety is required to prevent the release of these materials to the reactor coolant system. This margin of safety is provided by the double encapsulation, each container being capable of containing the materials to the irradiated.

4.5.3.3 Safety Limits and Limiting Safety System Settings

4.5.3.3.1 Safety Limits

The safety limits for the NBSR consist of a series of plots of reactor power versus primary flow for six coolant inlet temperature values for both the inner and outer plenums (NBS, Nov. 1980). The Safety Limits plots are also shown in NBSR-15 (NIST, 2004). The curves represent the maximum power allowed for a given inlet temperature and flow that will not cause the Critical Heat Flux Ratio, CHFR, to drop below 1.00 (corresponding to Departure from Nucleate Boiling, DNB), or the Onset of Flow Instability, OFI. Power distributions and hot spot factors from Sections 4.5.1 and 4.5.2 of this SAR have been used to verify that the 1980 limits are appropriate (see Section 4.6). In all cases, the maximum power in the present analysis for a given temperature and flow, is greater than or equal to the 1980 limit.

Technical Specification 2.1, Safety Limit:

This specification applies to reactor power and reactor coolant system flow and temperature. The objective is to maintain the integrity of the fuel cladding and prevent the release of significant amounts of fission products.

(1) Reactor power, coolant system flow, and inlet temperature shall not exceed the limits shown in Figures 2.1 and 2.2 in NBSR 15 (NIST, 2004b).
(2) The reactor may be operated at power levels of up to 10 kW with reduced flow (including no flow) if decay heat is insufficient to cause significant heating of the reactor coolant.

Basis:

Maintaining the integrity of the fuel cladding requires that the cladding remain below its blistering temperature (450 °C). For all plant operating conditions that avoid either a departure from nucleate boiling (DNB) or the onset of flow instability (OFI), cladding temperatures remain substantially below the blister temperature. Conservative calculations (Section 4.6 of this SAR) have shown that limiting combinations of reactor power and reactor coolant system flow and temperature to values more conservative than the safety limits will prevent cladding failure.

4.5.3.3.2 Limiting Safety System Settings

The Limiting Safety System Settings are also unchanged.

Technical Specification 2.2, Limiting Safety System Settings:

This specification applies to limiting settings for instruments monitoring safety limit parameters. The objective is to ensure protective action if any of the principal process variables should approach a safety limit.

The limiting safety system trip settings shall be:

Reactor power, % (max)	130
Reactor outlet temperature, ^{o}F (max)	147 (rundown)
Coolant flow, gpm/MW (min)*	60 inner plenum
	235 outer plenum

Basis:

At the values established, the safety system settings provide a significant margin from the safety limits. Even in the extremely unlikely event that all three parameters, reactor power, coolant flow, and outlet temperature simultaneously reach their Limiting Safety System Settings, the burnout ratio is at least 1.3. For all other conditions the burnout ratio is considerably higher (Section 4.6 of this SAR). This will ensure that any reactor transient caused by equipment malfunction or operator error will be terminated well before the safety limits are reached. Overall uncertainties in process instrumentation have been incorporated in limiting safety system setting values.

*May be bypassed during periods of reactor operation (up to 10 kW) when a reduction in safety limit values is permitted (see Section 4.5.3.3.1).

4.6 Thermal Hydraulic Design

The thermal hydraulic design of the NBSR is described in this section. The reactor is operated with forced convection cooling for all powers greater than 10 kW.

4.6.1 Design Basis

The design basis of the thermal hydraulic design of the NBSR is that there shall be: no fuel damage during normal operation; and no fuel damage resulting in release of fission products from any credible accident (see Chapter 13). In order to ensure that the design basis is met, NIST followed the procedures of NBSR-9, Addendum 1, using results obtained from detailed MCNP calculations as described earlier in this section. For consistency with NBSR-9, Addendum 1, NIST calculated a parametric set of limiting conditions for operation, based upon

fuel clad temperature. The cladding on U_3O_8 dispersion fuel such as that used in the NBSR will begin to blister at 450 ºC, and during the blistering process, cracks will develop that can release gaseous fission products (Snelgrove et al, 1994). Thus, for normal operating conditions, the criterion chosen was that the heat transfer to the primary coolant shall not exceed Departure from Nucleate Boiling (DNB) conditions, including any excursive instability. These two limiting conditions are discussed separately below.

a) Departure from Nucleate Boiling

There are many different correlations described in textbooks and in the literature for prediction of DNB. However, all come with the caution that they should not be used far outside of the range of conditions for which they were determined, including pressure, degree of sub-cooling, coolant velocity and flow geometry. The IAEA Research Reactor HEU to LEU Core Conversion Guidebook, TECDOC-233 (IAEA, 1980) discusses various correlations in use as of 1980, and makes recommendations for the appropriate choices for various reactor and fuel conditions. The most appropriate selection for the NBSR fuel is the Mirshak correlation (Mirshak et al, 1959), which was determined for plate type fuel in conditions very similar to those encountered in routine operation of the NBSR. This choice also has the merit of having been used in NBSR-9, Addendum 1.

b) Onset of Flow Instability

As for DNB or burnout, many different authors have treated the onset of flow instabilities, and many correlations have been proposed. The most relevant instability for the NBSR, the Ledinegg (4.6.6) static instability, has its origin in a simple effect. As water flow in a heated channel is reduced, a point will be reached where boiling will occur. At a later point significant amounts of vapor will be present in the channel. The presence of this vapor will increase the pressure drop, and when this effect is large enough, this increase will overwhelm the decrease in pressure drop arising from the flow decrease. At this point, the overall pressure drop in the hot channel of a fuel element will increase, and flow will be reduced (if the channel spans an inlet and outlet header, with other, lower power channels in parallel). This condition causes a flow instability, which will result in rapid loss of adequate cooling for that channel.

4.6.1.1 Flow Distribution in the Core

The flow geometry for the NBSR is discussed in detail in the Appendix A, where critical dimensions, elevations and other pertinent data are given. The core consists of 30 fuel assemblies that are fed by two plenums that enter at the bottom of the vessel. The inner core consists of 6 assemblies in the innermost area of the core (Figure 4.2.2), while the outer consists of the remaining 24 assemblies. The primary coolant flow is distributed between these two plenums by the inherent flow resistance of the two different paths, and has been measured at a total flow of 560 l/s (8700 gpm) as 148 l/s (2300 gpm) for the inner plenum and 412 l/s (6400 gpm) for the outer plenum. Approximately 4% of the flow bypasses the core; this is treated

conservatively in the next sections by reducing both flows to 95% when calculating the flow through any element.

4.6.1.2 Power Distribution in the Core

The power distribution in the core is assumed to be given by the fission density as calculated by the computer code MCNP. This is a very conservative assumption, as 14% of the energy is in the form of γ-rays and neutrons, and will be deposited much more uniformly throughout the core. As discussed earlier, many calculations were done to determine the fission rate in the fuel plates as a function of shim arm position and core depletion throughout the cycle. The model used represents the geometry of the system in great detail, and has been shown to give excellent agreement with several benchmarks, including startup shim arm positions and liquid hydrogen cold source performance. The limiting case for the thermal hydraulic design is the SU core. With four new FEs criticality occurs when the shim safety arms are inserted furthest into the core. This insertion results in flux compression into the bottom half of the fuel. For each assembly in the core, the power produced in each plate is used to calculate a hot channel, which is the cooling channel into which the most heat is deposited from the fuel. Further, the power distribution within the hot plates is also calculated both for the axial and transverse directions by subdividing each plate first into 8 horizontal strips, then into 16 vertical strips, calculating the fission rate for both, and assuming that the effects are multiplicative. This allows definition of a "hot spot," the point with the highest heat flux.

4.6.2 Major Correlations Used

In order to estimate the limits of operation, several empirical correlations were used to determine different heat transfer and flow regimes. The basis for selection of the particular correlations used, and the details of each, are given below.

4.6.2.1 Onset of Nucleate Boiling

In NBSR-9, Addendum 1, the nominal settings of flow and inlet temperature were selected by the requirement that there be no nucleate boiling at the hot spot. This was conservatively estimated by the requirement that the fuel clad temperature at the hot spot remain below the saturation temperature T_s for D_2O at the appropriate pressure. In order to test this condition, a heat transfer coefficient must be defined, and used to calculate the fuel clad temperature. While there are several possibilities, we have chosen to use the Dittus-Boelter correlation (Dittus and Boelter, 1930):

$$Nu=0.023(Re)^{0.8}(Pr)^{0.4}$$

Where:

Nu = Nusselt number = hDe/k
Re = Reynolds number=DeG/μ
Pr = Prandtl number = $\mu C_p/k$
h = heat transfer coefficient ($W\text{-}m^{-2}\text{-}s^{-1}$)
k = Thermal conductivity ($W\text{-}m^{-1}\text{-}K^{-1}$)
De = Hydraulic Diameter for hot channel (m)
G = mass flux density ($kg\text{-}m^{-2}\text{-}s^{-1}$)
μ = Viscosity ($kg\text{-}m^{-1}s^{-1}$)
C_p = Specific heat at constant pressure ($J\text{-}kg^{-1}\text{-}K^{-1}$)

The temperature of the fuel cladding is given by:

$$T_c = T_b + q_m/h$$

where:
T_b = Bulk coolant temperature at hot spot
q_m = heat flux at hot spot.

This correlation was used to calculate the clad temperature required to remove the hot spot heat flux by convective heat transfer, after calculating the water temperature rise from the entrance to the hot spot.

In order to test for the onset of nucleate boiling, we use the correlation of Bergles and Rohsenow (Bergles and Rohsenow 1964) for incipient boiling:

$$T_{W\text{-}ONB} = T_{sat} + \frac{5}{9}\left(\frac{9.23q''}{p^{1.156}}\right)^{\left(\frac{p^{0.0234}}{2.16}\right)}$$

$T_{W\text{-}ONB}$ = the clad temperature at which incipient boiling occurs
q´´ = the local heat flux in $W\text{-}cm^{-2}$ (note units)
p = pressure in bars.

4.6.2.2 Departure from Nucleate Boiling

As stated above, the Mirshak correlation was chosen to test for Departure from Nucleate Boiling, based upon the close similarity of the conditions for which it was determined to those in the NBSR fuel. The correlation is given by:

$$q_c = 1.51x10^6 (1+0.1198v)(1+0.00914(T_s - T_b))(1+0.19P)$$

where

q_c = the critical heat flux (W-m^{-2})
v = coolant velocity (m-s^{-1})
T_s = saturation pressure of coolant (ºC)
T_b = Bulk temperature of coolant at hot spot (ºC)
P = Pressure (bar)

4.6.2.3 Onset of Flow Instability

Once again there are many correlations to choose from. The Costa correlation (Costa, 1969), which was also used for the HFIR at Oak Ridge National Laboratory, has been chosen. This correlation will be limiting only at low flow and low sub-cooling, where significant amounts of vapor are generated before the DNB flux is attained. The correlation was developed exactly as a predictor of the point of significant vapor product, and is thus a conservative choice for the Onset of Flow Instability (OFI), which arises from the presence of significant amounts of vapor at the exit of a channel.

The correlation is (note units):

$$q_c = (T_s - T_b)\, v^{0.5}/1.28, \text{ where}$$

q_c = the critical heat flux (W-cm^{-2})
v = coolant velocity (cm-s^{-1})
T_s = saturation pressure of coolant (ºC)
T_b = Bulk temperature of coolant at hot spot (ºC).

4.6.3 Determination of Limiting Conditions

As stated earlier, extensive calculations of fission rates were completed for the NBSR for the Startup (SU), Beginning of Cycle (BOC) and End of Cycle (EOC) cores. For establishment of thermal hydraulic limits, the SU conditions are limiting, as they provide a power distribution that is concentrated in the lower half of the core. For some accident analyses (reactivity excursions) examined in Chapter 13, the EOC conditions are limiting, as a result of the rate of insertion of negative reactivity after a reactor trip. In all cases, the hot element is in the outer plenum, the hot channel for each assembly is one between two fuel plates nearest the fuel assembly edge, and the

hot stripe is closest to the edge of a plate. The latter two results are readily understood by considerations of moderation – the hot channel and hot stripe are located where they view the most D_2O, as the core is under moderated. Detailed results for some of the hottest elements can be found in Section 4.5.2.3.3. For the purposes of thermal limit analysis, the SU cases for the outer and inner plenums are listed in Tables 4.5.8 and 4.5.10. The results are summarized below:

Outer Plenum:

Limiting element H-1
Total Element Power = 770 kW; radial peaking factor = 1.154
Lower Fuel Section = 412 kW
Upper Fuel Section = 358 kW
Hot Channels: Lower Section = 30.0 kW
Upper Section = 22.9 + 26.1 = 49.0 kW*
Hot Spot Peaking Factor= 2.47, relative to core
Heat Flux at Hot Spot = $q_m = 1.41 \times 10^6$ W-m^{-2} (at top of lower core, edge of plates)
Peaking Factor at Upper Hot Channel Exit = 1.63, relative to the core
Heat Flux at Upper Hot Channel Exit = 9.32×10^5 W-m^{-2}

Inner Plenum:

Limiting element H-3
Total Element Power = 707 kW; radial peaking factor = 1.059
Lower Fuel Section = 416 kW
Upper Fuel Section = 291 kW
Hot Channels: Lower Section = 27.9 kW
Upper Section = 23.1 + 19.8 = 42.9 kW*
Hot Spot Peaking Factor = 1.83, relative to core
Heat Flux at Hot Spot = $q_m = 1.05 \times 10^6$ W-m^{-2} (at top of lower core, edge of plates)
Peaking Factor at Upper Hot Channel Exit = 0.694, relative to core
Heat Flux at Upper Hot Channel Exit = 3.97×10^5 W-m^{-2}

*The hot channel in the upper fuel is obtained from the average channel in the lower fuel plus the upper fuel hot channel, consistent with complete mixing in the unfueled region.

In order to calculate the minimum flows required to remain below ONB, one must also know the saturation temperature of the coolant, which is a function of pressure. The pressure at the hot spot is conservatively estimated as the static head, which is 3.34 m of D_2O, or 138.5 kPa, or 1.37 bar. At this pressure, the saturation temperature of the coolant is 110.3º C. The data given here, along with the correlations given in 4.6.2.1 can be used to show that the nominal operating conditions shown in Table 4.6.1, analogous to those derived in NBSR-9, Addendum 1, satisfy the condition that there shall be no region undergoing nucleate boiling. This table shows that the values derived in NBSR-9, Supplement 1 were conservative.

Having determined nominal flows, the limits of safe operation must be determined using the criteria of DNB and OFI, whichever is limiting. This has been done using the correlations given

above, Mirshak and Costa, for both the inner and outer plenums, at both the hot spot and the hot channel exit of the upper fuel section. The results are given in Figures 4.6.1 and 4.6.2 respectively. The following conditions were used in the analysis:

- The most severe condition occurs at startup, when the flux is most compressed.
- All effects were calculated for the hot channel, using geometry for that channel (gap = 0.002730 m), rather than the average channel (gap = 0.002906 m).
- Coolant within a single channel mixes completely.
- It is sufficient to test at the top of the bottom plates and the top of the upper plates (the first follows as this is always the hot spot, while the second follows since the end of the plate will reflect anything that happens earlier; its coolant temperature is greatest).
- The coolant mixes completely in the unfueled gap between the upper and lower core.
- The heating profiles follow from the MCNP calculations of fission rates.
- The statistics for thermal hydraulic factors are the same as those derived for the Mirshak correlation in Appendix A, so that equating the heat flux ratios to 1.3 represents the probability of no DNB to be greater than 95%, as shown in Appendix A. For a discussion of the uncertainties (power measurement, power distributions, channel dimensions, velocity profiles, flow rate measurements, fuel loading tolerances) leading to this result, see the details in that section.

These calculations are conservative for the following reasons:

- The peaking factors were determined with the assumption that all of the energy from fission is deposited locally, whereas about 14% of the energy (from prompt and delayed photons, neutrons, and capture gamma rays) is widely distributed throughout the core and the moderator.
- The hot channel and hot stripe are always close to the edges of plates and assemblies, which will substantially reduce peaking (heat will diffuse outside the fueled region, and divide so as to reduce peaking into the channel heated from only one side).
- The friction factors for the hot channel will be less than for the other channels, so that more coolant would actually flow in this channel, reducing the effects of peaking.
- The correlations used are themselves conservative.
- The limits derived here are representative of the situation at 20 MW immediately after startup; at any later time, the margin will increase substantially as the shim safety arms are withdrawn.

The power limits shown on Figures 4.6.1 and 4.6.2 were compared to the values on the Safety Limit curves for power, primary flow, and coolant inlet temperature, calculated in NBSR-9, Addendum I (NBS, 1980). For the bounding primary flows and inlet temperatures, the power limits calculated in the above analysis were greater than or equal to those calculated in the 1980 Addendum. The current analysis confirms the adequacy of the existing Safety Limits.

The results just derived allow determination of the Safety Limits for the third variable when two are at the Safety System Setting (SSS), and when two variables are at the normal condition.

These limits are listed in Tables 4.6.2 and 4.6.3. Again, the current results are less limiting than the 1980 values in Tables 3.2-3 and 3.2-4 of Addendum I (NBS, 1980). That is, the allowed power is greater, or the required flow is lower, than the existing Safety Limits.

4.6.4 Shutdown Cooling

The NBSR is equipped with shutdown cooling (as described in Chapter 5), which provides ample cooling for all shutdown conditions. One of the accidents analyzed in Appendix A includes loss of off-site power (and hence main primary pumps), followed by failure of both redundant shutdown pumps. This scenario results in no damage to the fuel, showing that natural convection cooling is adequate to provide cooling of the fuel in the shutdown condition, even immediately following a scram due to loss of all primary pumps.

4.6.5 Operation With Natural Convection

The analysis in Appendix A, pp. E1-E4 shows that the NBSR fuel can be cooled from the top for powers up to 1.2 MW with no flow (i.e. the case of complete flow blockage at the bottom of an element. The derivation of this flooding-limited power is fully described in Appendix A. The result shows that power up to 1 MW would be allowable with no forced flow, even without any natural convection (but boiling would occur).

The RELAP code has been used to analyze operation at 500 kW with natural convection allowed, and shown to be completely safe. The analysis shows that the core coolant flow is stable and subcooled. The peak fuel centerline temperature is about 25 degrees C below the saturation temperature. The peak heat flux is at least an order of magnitude below the calculated CHF and the wall heat flux corresponding to the OFI condition.

4.6.6 Summary of Thermal Hydraulic Design

The operating limits developed here are based upon well tested correlations, are conservative, and provide ample margin to ensure that there will be no damage to fuel during normal operations. In addition, as shown in Chapter 13 and in Appendix A, the operating conditions provide ample margin for all credible accident scenarios to assure that there will be no fission product release.

4.7 References

Bell, G. I. and Glasstone S. (1970). *Nuclear Reactor Theory*. Robert E. Krieger Publishing Company: Malabar, Florida.

Bergles, A. E. and Rohsenow, W. M., (1964). "The Determination of Forced Convection Surface Boiling Heat Transfer," Trans. ASME, J. Heat Trans. **86,** 365.

Bretscher, M. M. (1997). *Perturbation-Independent Methods for Calculating Research Reactor Kinetic Parameters*. ANL/RERTR/TM-30, Argonne National Laboratory: Argonne, Illinois.

Briesmiester, J. F. (1997) (Ed.). *MCNP – A General Monte Carlo N-Particle Transport Code, Version 4B*. LA-12625, Los Alamos National Laboratory: Albuquerque, New Mexico.

Carew, J., Cheng, L., Hanson, A., Xu, J., Rorer, D., and Diamond, D., (2003). *Physics and Safety Analysis for the NIST Research Reactor.* BNL-NIST-0803, Brookhaven National Laboratory: Upton, New York.

Costa, J., (October, 1969). "Mesure de Coefficient de Frottement en Ecoulement Turbulent Simple Phase avec Transfert de Chaleur dans un Canal Rectangulaire," Note CEA N 1142.

Croff, A. G., (1980). *A User Manual for the ORIGEN2 Computer Cod*e. ORNL/TM-7175, Oak Ridge National Laboratory: Oak Ridge, Tennessee.

Dittus, F. W. and Boelter, L. M. K., (1930). University of California Publs. Eng., Vol.2, 443.

Grund, J. E., (1963). *Self-Limiting Excursion Tests of a Highly Enriched Plate-Type D_2O-Moderated Reactor: Part 1. Initial Test Series*. IDO-16891, Phillips Petroleum Company:

Hanson, A. L., Brookhaven National Laboratory, memo of July 17, 2003.

Hanson, A.L., Ludewig, H. and Diamond D., *Calculation of Neutron Lifetime in the NBSR,* (February, 2004).

Hendrie, J. M., (1964). *Final Safety Analysis Report on the Brookhaven High Flux Beam Reactor*. BNL 7661, Brookhaven National Laboratory: Upton, New York.

IAEA, (1980). "Research Reactor Core Conversion From the Use of Highly Enriched Uranium to the Use of Low Enriched Uranium Fuels," IAEA-TECDOC-233, 1980.

Ledinegg, M., (1954). "Instability of Flow During Natural and Forced Convection," Die Warme 61:8, AEC-tr1861.

Mirshak, S., Durant, W. D. and Towell, R. H. (1959). "Heat Flux at Burnout," DuPont, DP-355.

National Bureau of Standards (November, 1980). *Addendum 1, Final Safety Analysis Report,* NBS Research Reactor Radiation Division.

National Bureau of Standards, (1966a). *FSAR on the National Bureau of Standards Reactor*, NBSR-9, U.S. Department of Commerce.

National Bureau of Standards, (December 1966b). *Supplement B of the FSAR on the National Bureau of Standards Reactor*, NBSR-9B, U.S. Department of Commerce.

NIST Center for Neutron Research (1989). *NIST Reactor Logs*.

NIST Center for Neutron Research (2004a). "Specification for Aluminum Clad Fuel Elements for the National Institute of Standards and Technology Research Reactor," NCNR-ACFESpec-01.

NIST Center for Neutron Resarch (s004b). "Technical Specifications for the National Bureau of Standards 20 Megawatt Test Reactor," (NBSR 15).

Ougouag, A. M. et al, (1993). *MCNP Analysis of the Foehn Critical Experiment*. ORNL/TM-12466, Oak Ridge National Laboratory: Oak Ridge, Tennessee.

Sitarman, S., (1992). *MCNP: Light Water Reactor Critical Benchmarks*. General Electric Nuclear Energy, NEDO-32028.

Snelgrove, J. L. and Hofman, G. L., (1994). "Dispersion Fuels," in *Materials Science and Technology, A Comprehensive Treatment, Volume 10A, Nuclear Materials*, Part I, Brian R. T. Frost, Volume Editor, ed. by R. W. Cahn, P. Haasen, and E. J. Kramer, VCH, New York.

Trellue, H.R., (December 1998). *Development of MONTEBURNS: A Code that Links MCNP and ORIGEN in an Automated Fashion for Burnup Calculations*. LA-13514-T, Los Alamos National Laboratory: Albuquerque, New Mexico.

Whalen, Daniel J. et al, (1991). *MCNP: Neutron Benchmark Problems*. LA-12212, Los Alamos National Laboratory: Albuquerque, New Mexico.

Weeks, J. R. et al, (1993) "Effects of High Thermal Neutron Fluences on Type 6061 Aluminum," in Effects of Radiation on materials: 16th International Symposium, ASTM STP 1175, A. S. Kumar, D. S. Gelles, R. K. Nanstad, and E. A. Little, Eds., American Society for Testing and Materials, Philadelphia.

Table 4.1.1: Major Reactor Parameters

Steady-State Operating Power:	20 MW thermal
Total Primary Coolant Flow Rate	8700 gpm
Inner Plenum	2300 gpm
Outer Plenum	6400 gpm
Primary Coolant Outlet Temperature:	114 ^{o}F (45.5 °C)
Limiting Safety System settings	
Power:	130 %
Flow:	60 gpm/MW inner plenum
	235 gpm/MW outer plenum
Temperature:	147 ^{o}F (63.9 °C) (Rundown)
Coolant, Moderator and Reflector:	Heavy Water
Reactor Type:	Tank
Fuel Type:	MTR
Fuel Geometry:	Curved Plate

Table 4.2.1: Chemical Requirements for Aluminum Powder Melting Stock

Element	Weight (%)
Aluminum (metals)	99.300
Cadmium	0.002
Copper	0.200
Lithium	0.008
Silicon and Iron	0.250
Zinc	0.100
Other (single)	0.050
Al_20_3	0.700
Boron	0.001

Table 4.2.2: Material and Physical Properties of NBSR Fuel

Property	Value
Aluminum Clad (6061-T6)	
Melting Point	1080-1200 °F (580-650 °C)
Softening Point	840 °F (450 °C)
Heat Capacity	640 J/kg °C
Thermal Conductivity	155 W/m °C
Fuel	
^{235}U	350 gm/element
Enrichment	93% (minimum)

Table 4.2.3: Fuel Element Operating Conditions
(in High Power Density Research and Test Reactors)

	NBSR	ORR	MTR	ETR	HFBR
Core Inlet Water Temperature, °F(°C)	100 (37.8)	120 (48.9)	115 (46.1)	120 (48.9)	120 (48.9)
Water Velocity in fuel Element Channels (ft/sec) (m/sec)	12 (3.66)	30 (9.14)	33 (10.1)	35 (10.7)	35 (10.7)
Core Pressure Drop (psi) (kg/cm^2)	12 (0.84)	25 (1.76)	40 (2.81)	45 (3.16)nominal 55 (3.87) maximum	31 (2.18)
Nominal Water Channel Thickness (in) (cm)	0.116 (0.295)	0.104 (0.264)	0.116 (0.295)	4 at 0.119 (0.302) 2 at 0.115 (0.292) 12 at 0.105 (0.268)	2 at 0.129 (0.328) 2 at 0.116 (0.295) 2 at 0.108 (0.274) 12 at 0.102 (0.259)
Fuel Plate Thickness (in) (cm)	0.050 (0.127)	.050 (0.127)inside .065 (0.165)outside	.050 (0.127)inside .065 (0.165)outside	0.050 (0.127)	0.050 (0.127)inside 0.140 (0.356) outside
Fuel Meat thickness (in) (cm)	0.020 (0.051)	0.020 (0.051)	0.020 (0.051)	0.020 (0.051)	0.020 (0.051)inside 0.010 (0.025) outside
Weight %U in Fuel Alloy	35	18	18	22	30
Width of Fuel Plates Between Side Plates (in) (cm)	2.415 (6.134)	2.512 (6.380)	2.622 (6.660)	2.624 (6.665)	2.446 (6.213)
Plates	Curved	Curved	Curved	Straight	Curved
Radius of Curvature (in) (cm)	5.5 (13.97)	5 (12.7)	5.5 (13.97)	na	6 15.24)
Max. Heat Flux (BTU/hr-ft)	4.35E05 (1.54E05)	7.5E05	9E05	1.35E06	1.6E06 (first core) 1.48E06 (Equilibrium)
Hot Spot Surface temp (F) (°C)	248 (120) at low-flow trip point	240 (115)	312 (155)	400 (204)	359 (182)first core 344 (173)equilibrium
Avg U-235 burnup, %	70	35-40	20-25	17	20.4

Table 4.4.1: Radiation Entering and Exiting the Biological Shield

Energy Level in MeV	Neutron Flux in n/cm^2-sec	Gamma Flux in mW/cm^2
Entering the Shield		
Thermal	3×10^5	
Thermal - 1	5.6×10^9	
1 - 5	3×10^7	
5 - 10	8×10^6	
10 – 15	2.6×10^6	
~ 6 (Average)		11.2
Exiting the Shield		
Average	2.8×10^{-3}	2×10^{-7}

Table 4.4.2: Shielding Coefficients of NBSR Magnetite Concrete

Energy Level in MeV	Attenuation Coefficients in cm^{-1}
Neutron	
Thermal - 1	0.194
1 - 5	0.132
5 - 10	0.126
10 - 15	0.112
Gamma	
~ 6	0.107

Table 4.5.1: Summary of Core Nuclear Characteristics

Moderator and Coolant	D_2O
Reactor Power	20 MWt
Core Volume	
Fueled Region	542 liters
Gap	174 liters
U-235 Operating Mass (30 Elements)	
SU Core	7400 grams
End of Cycle	6430 grams
Average Metal Volume Fraction	0.066
Core Dimensions	
Diameter	111 cm
Top Fueled Height	28 cm
Gap Height	18 cm
Bottom Fueled Height	28 cm
Reactivity, Clean*, Cold, All Shim Arms Withdrawn	6.91%
Reactivity with Equilibrium Xe and Sm, All Shim Safety Arms Withdrawn	
Beginning of Cycle	3.83%
End of Cycle	0.0%
Total Reactivity Worth, All Shim** Arms	-23.7%
Minimum Shutdown Margin, All Shim Arms	-17.1%
Minimum Shutdown Margin, Three Shim Arms	-9.42%
Minimum Shutdown Margin, Two Shim Arms	-3.06%
Void Coefficient of Reactivity	
Average Coolant	-0.049%/liter
Gap Region	-0.025%/liter
Moderator (Minimum)	-0.024%/liter
Temperature Coefficient of Reactivity	
Beginning of Cycle	-0.017%/ºF
End of Cycle	-0.014%/ºF
Prompt Neutron Lifetime	800 μs
Effective Delayed Neutron Fraction	.00757
Average Power in 30 Fuel Elements	667 kW

* Clean is defined as having no short-lived fission product poisons, i.e. no Xe. The SU core includes 26 partially burned FEs that contain long-lived poisons, such as Sm.

**Shim arm worths for the SU core with normal Cd density, i.e. no depletion.

Table 4.5.2: Results of MCNP Calculations Using the Updated Model

Input File	Description of Modeled Core Configuration	k_{eff}	$\Delta\rho$ ($)
kstd1	Benchmark criticality of March 10, 2000. Shims at 23.5° withdrawn, regulating rod withdrawn 14.6 in (37 cm), 1 MW, operating temperature, Unit 1 CNS	1.00726 ± 0.00060	
suref	Same as kstd1 benchmark, but Unit 2 CNS	1.01289 ± 0.00026	
su183	SU reference core, shims 22.7° withdrawn, regulating rod 50%, normal operation	1.00732 ± 0.00027	
surefx	Maximum reactivity case, all shims and regulating rod fully withdrawn, operating temperature	1.07870 ± 0.00060	+8.67
susdm	Shutdown reactivity with SU core, shims at full insertion, regulating rod withdrawn	0.85929 ± 0.00060	-22.6
	SU Shim Bank Worth		-31.3
sucold	SU reactivity at ambient temperature, 20 ^{o}C, otherwise like su183	1.01077 ± 0.00032	+0.45
sureg	Like "su183" but regulating rod fully inserted	1.00455 ± 0.00019	-0.36
noreg	Like "su183" but regulating rod fully withdrawn	1.00925 ± 0.00038	+0.25
sucns	Like "su183" but NO liquid hydrogen in Unit 2 CNS	1.00561	-0.22
dumpxs	Most reactive SU core, "surefx" but with moderator dump (D_2O at dump level, 2.96 cm above upper fuel)	0.99847 ± 0.00042	-1.16
dump2	Like "dumpxs" but D_2O at dump level inside FEs	0.99225 ± 0.00039	-1.99
dump18	Like "dumpxs" but shims 22.7° withdrawn	0.97668 ± 0.00028	-4.11
minus1	Like "su183" but A-4 FE replaced by D_2O	0.9987 ± 0.0005	-1.13
minusc	Like "su183" but F-5 FE replaced by D_2O	0.9968 ± 0.0006	-1.38
susdm1	SU core with shims 2,3,4 fully inserted; shim #1 and regulating rod withdrawn, ambient temperature	0.9033 ± 0.0009	-15.1
susdm2	SU core with shims 1,3,4 fully inserted; shim #2 and regulating rod withdrawn, ambient temperature	0.9200 ± 0.0009	-12.4
susdm3	SU core with shims 1,2,4 fully inserted; shim #3 and regulating rod withdrawn, ambient temperature	0.9178 ± 0.0009	-12.8
susdm4	SU core with shims 1,2,3 fully inserted; shim #4 and regulating rod withdrawn, ambient temperature	0.9062 ± 0.0009	-14.6
susdm1	Susdm1 insertion worth, compared to shutdown. Measured value = $8.5	0.9033 ± 0.0009	+7.49

Table 4.5.2: Results of MCNP Calculations Using the Updated Model (Cont.)

susdm2	Susdm2 insertion worth, compared to shutdown. Measured value = $9.5	0.9200 ± 0.0009	+10.14
susdm3	Susdm3 insertion worth, compared to shutdown. Measured value = $7.5	0.9178 ± 0.0009	+9.80
susdm4	Susdm4 insertion worth, compared to shutdown. Measured value = $7.5	0.9062 ± 0.0009	+7.95
susd12	SU core with shims 3 and 4 fully inserted, shims 1 and 2, and regulating rod withdrawn, ambient temperature	0.9772 ± 0.0012	-4.04
susd34	SU core with shims 1 and 2 fully inserted, shims 3 and 4, and regulating rod withdrawn, ambient temperature	0.9749 ± 0.0012	-4.36
drop1	Max. reactivity case, "surefx," but shim #1 fully inserted	1.01271 ± 0.00075	-7.98
drop2	Max. reactivity case, "surefx," but shim #2 fully inserted	1.02400 ± 0.00074	-6.54
drop3	Max. reactivity case, "surefx," but shim #3 fully inserted	1.02265 ± 0.00076	-6.71
drop4	Max. reactivity case, "surefx," but shim #4 fully inserted	1.00969 ± 0.00080	-8.37
eqlib	Like su183 but with "equilibrium" concentration of ^{135}Xe, ^{105}Rh, and ^{149}Sm, operating temperature (BOC core), shims at 22.7°, regulating rod 50%	0.97911 ± 0.00037	-3.78
eqi13	BOC core like "eqlib," but shim safety arms at 28.0° withdrawn and regulating rod fully inserted	1.00724 ± 0.00027	
eqixe	Like eqi13 but no Xe-135	1.0477 ± 0.0006	+5.08
ecref	EOC core (38 day burnup), all shims and regulating rod withdrawn fully, operating temperature	1.00362 ± 0.00025	
eccold	EOC core but cold and "clean" (no ^{135}Xe or ^{105}Rh, ^{149}Sm at SU concentration), ambient temperature	1.03197 ± 0.00042	+3.61
eocreg	Like ecref but regulating rod fully inserted	0.99910 ± 0.00025	-0.60
ecsdm	Like ecref but all four shims fully inserted	0.7931 ± 0.0008	-35.4
dumpec	Like ecref but D_2O at moderator dump level	0.9284 ± 0.0006	-10.7
ecsdm1	Like ecref but shim #1 dropped to scram position	0.9416 ± 0.0008	-8.67
ecsdm2	Like ecref but shim #2 dropped to scram position	0.9518 ± 0.0008	-7.16
ecsdm3	Like ecref but shim #3 dropped to scram position	0.9504 ± 0.0009	-7.37
ecsdm4	Like ecref but shim #4 dropped to scram position	0.9372 ± 0.0008	-9.32

Table 4.5.3: Nuclear Properties of Short-Lived Fission Product Poisons

Poison	Cross Section (barns)	Half-life (hours)	Precursor	Half-life (hours)	Mass Yield (%)
Xe-135	2.6×10^6	9.10	I-135	6.57	6.54
Sm-149	40,000	∞	Pm-149	53.1	1.08
Rh-105	16,000	35.4	Ru-105	4.44	0.96

Table 4.5.4: Calculated Shim Arm Reactivity Worths

Shim-arm "drop" worth	SU core ($)	EOC core ($)	Average ($)		Insertion Worth ($)	Measured Worth ($)
Shim #1	-7.98	-8.67	-8.33		+7.49	8.5
Shim #2	-6.54	-7.16	-6.85		+10.14	9.5
Shim #3	-6.71	-7.37	-7.04		+9.80	7.5
Shim #4	-8.37	-9.32	-8.85		+7.95	7.5
Sum	-29.6	-32.5	-31.5		35.4	
Calc. Bank BNL	-30.5	-35.4				
Updated Model	-31.3	-35.4				
Measured (9/95)	-31.3					

Table 4.5.5: Delayed Neutron Groups

Group	β_i	β_i/β	Decay Constant (sec^{-1})
1	0.0276	0.03644	0.0127
2	0.1546	0.2041	0.0317
3	0.1364	0.1801	0.115
4	0.2954	0.3900	0.311
5	0.0929	0.1227	1.40
6	0.0189	0.02495	3.87
Photo Neutrons			
7	0.023	0.02680	0.278
8	0.0065	0.008582	0.0169
9	0.00223	0.002944	0.00490
10	0.00107	0.001413	0.00152
11	0.00066	8.714×10^{-4}	4.27×10^{-4}
12	0.00074	9.770×10^{-4}	1.16×10^{-4}
13	0.00010	1.320×10^{-4}	4.41×10^{-5}
14	0.000033	0.4357×10^{-4}	3.65×10^{-6}

$\beta_{eff} = \Sigma \beta_i = 0.007574$ (0.7574 %)

Table 4.5.6: Calculated Moderator Temperature Coefficients

Core Model	%Δk/k/°C	%Δk/k/°F
SU	-0.031 ± 0.002	-0.017 ± 0.001
BOC	-0.031 ± 0.002	-0.017 ± 0.001
MOC	-0.028 ± 0.002	-0.015 ± 0.001
EOC	-0.025 ± 0.002	-0.014 ± 0.001

Table 4.5.7: Calculated Moderator Void Coefficients

Core Model	%Δk/k	Volume of Void (liters)	Void Coefficient (%Δρ/liter)
SU	-2.05 ± 0.06	59.56	-0.034 ± 0.001
EOC	-1.45 ± 0.06	59.56	-0.024 ± 0.001

Table 4.5.8: Hot Channel and Hot Stripe Peaking Factors SU Core

(Upper (U) and Lower (L) Sections of Several Fuel Elements in the SU Core. The values were calculated from the MCNP fission distributions.)

FE Ch# Power Factor*	U or L	Fuel Section Power (W)	Hot Channel Heat Input (W)	Maximum Axial Heat Input (W) Δz=3.5 cm	Axial Channel Peaking Factors*	Lateral Peaking Factor Δy=3.6mm	Hot Stripe Peaking Factor*	Hot Spot With Un-even BU Factors*
H-1 #2	U	357,920	26,136	4,526	1.96	1.27	2.49	2.24 (1)
1.154	L	411,580	29,957	4,837	2.09	1.25	2.61	2.35
I-2 #2	U	307,463	22,486	4,423	1.91	1.12	2.14	1.66 (3)
1.102	L	427,779	30,503	4,880	2.11	1.12	2.35	1.83
A-4 #17	U	207,508	16,217	3,949	1.71	1.23	2.09	-
0.938	L	418,032	30,783	4,886	2.11	1.18	2.49	-
K-2 #2	U	261,745	19,754	4,073	1.76	1.23	2.17	1.83 (2)
1.008	L	410,508	29,903	4,753	2.05	1.26	2.59	2.20
M-4 #2	U	208,979	16,264	3,948	1.71	1.24	2.11	-
0.925	L	407,487	30,023	4,736	2.05	1.10	2.26	-
J-7 #2	U	338,007	24,975	4,441	1.92	1.21	2.32	2.08 (1)
1.062	L	370,012	27,099	4,493	1.94	1.22	2.36	2.13
F-3 #17	U	292,021	19,840	4,042	1.75	1.12	1.96	1.53 (3)
1.063	L	416,391	27,814	4,499	1.94	1.13	2.19	1.70
H-3 #17	U	290,760	19,782	3,973	1.72	1.11	1.91	1.49 (3)
1.059	L	415,736	27,870	4,530	1.96	1.16	2.28	1.77
F-1 #17	U	343,961	25,670	4,327	1.87	1.29	2.41	2.17 (1)
1.102	L	390,879	28,818	4,644	2.01	1.23	2.46	2.21
C-2 #17	U	305,616	22,622	4,086	1.76	1.26	2.22	1.88 (2)
1.064	L	403,816	29,478	4,650	2.01	1.28	2.58	2.18
B-3 #17	U	239,788	18,843	4,006	1.73	1.26	2.18	1.85 (2)
0.979	L	413,211	31,557	4,821	2.08	1.15	2.39	2.02
L-3 #2	U	231,443	18,145	4,127	1.78	1.17	2.09	1.78 (2)
0.968	L	414,161	31,074	4,950	2.14	1.14	2.43	2.06

* All power factors are with respect to the core average. *The axial channel peaking factors are directly determined; they combine the fuel element, plate-wise, and axial power factors.* The uneven burnup corrections are as follows:

(1) x 0.90
(2) x $(0.92)^2$
(3) x $(0.92)^3$

Table 4.5.9: Hot Channels and Hot Stripe Peaking Factors EOC Core
(Upper (U) and Lower (L) Sections of Several Fuel Elements in the EOC Core. The values were calculated from the MCNP fission distributions.)

FE Ch# Power Factor*	U or L	Fuel Section Power (W)	Hot Channel Heat Input (W)	Maximum Axial Heat Input (W) Δz=3.5 cm	Axial Channel Peaking Factors*	Lateral Peaking Factor Δy=3.6mm	Hot Stripe Peaking Factor*	Hot Spot With Un-even BU Factors*
L-3 #2	U	384,829	28,721	4,690	2.03	1.16	2.34	1.83 (3)
1.108	L	353,572	26,515	4,460	1.93	1.12	2.15	1.68
I-2 #2	U	385,110	27,277	4,346	1.88	1.19	2.24	1.74 (3)
1.095	L	345,220	24,141	4,172	1.80	1.23	2.22	1.74
K-2 #2	U	382,975	27,841	4,440	1.92	1.19	2.28	1.78 (3)
1.091	L	344,577	24,784	4,101	1.77	1.22	2.17	1.69
H-1 #2	U	392,030	28,270	4,370	1.88	1.21	2.28	1.93 (2)
1.087	L	332,437	24,049	4,042	1.75	1.28	2.24	1.89
M-4 #2	U	363,564	26,773	4,413	1.91	1.19	2.28	2.05 (1)
1.072	L	351,436	25,769	4,535	1.96	1.11	2.17	1.95
A-4 #17	U	358,158	26,675	4,406	1.90	1.14	2.17	1.96 (1)
1.068	L	353,682	26,038	4,614	1.99	1.13	2.25	2.03
B-3 #17	U	356,651	27,278	4,320	1.87	1.12	2.09	1.63 (3)
1.048	L	342,265	25,994	4,428	1.91	1.18	2.07	1.61
C-2 #17	U	356,615	26,026	4,040	1.75	1.27	2.23	1.74 (3)
1.030	L	329,990	24,085	4,048	1.75	1.20	2.10	1.64
F-3 #17	U	353,741	23,683	3,833	1.62	1.08	1.75	1.36 (3)
1.014	L	321,984	21,369	3,604	1.55	1.11	1.71	1.33
H-3 #17	U	356,981	23,750	3,816	1.65	1.14	1.87	1.46 (3)
1.021	L	323,580	21,459	3,633	1.57	1.12	1.75	1.36
F-1 #17	U	368,200	27,081	4,181	1.81	1.32	2.39	2.02 (2)
1.020	L	311,493	22,911	3,952	1.71	1.27	2.17	1.84

* All power factors are with respect to the core average. *The axial channel peaking factors are directly determined; they combine the fuel element, plate-wise, and axial power factors.* The uneven burnup corrections are as follows:

(1) x 0.90
(2) x $(0.92)^2$
(3) x $(0.92)^3$

Table 4.5.10: Limiting Cases for Thermal-Hydraulic Analyses of the SU Core
(Hot spots are adjacent to the unfueled region in the hot stripe/channel.)

Relative Power Factors Used to Generate Safety Limits (SU Core):

Outer Plenum:			Inner Plenum:	
Use H-1		Hot Spot in	Use H-3	Hot Spot in
	Hot	Hot Stripe	Hot	Hot Stripe
Elevation	Channel:	Test Case	Channel	Test Case
-35.08	1.509	1.509	1.407	1.407
-31.59	1.395	1.395	1.331	1.331
-28.1	1.473	1.473	1.358	1.358
-24.61	1.415	1.415	1.430	1.430
-21.11	1.606	1.606	1.489	1.489
-17.62	1.668	1.668	1.502	1.502
-14.13	1.785	1.785	1.626	1.626
-10.64	2.089	2.470	1.957	1.829
10.64	1.955	2.343	1.716	1.537
14.13	1.593	1.593	1.350	1.350
17.62	1.422	1.422	1.217	1.217
21.11	1.356	1.356	1.078	1.078
24.61	1.259	1.259	0.891	0.891
28.1	1.213	1.213	0.785	0.785
31.59	1.214	1.214	0.677	0.677
35.08	1.278	1.626	0.540	0.694

Table 4.5.11: Limiting Cases for Thermal-Hydraulic Analyses of the EOC Core
(Hot spots are adjacent to the unfueled region in the hot stripe/channel)

Relative Power Factors Used to Generate Safety Limits (EOC Core):

Outer Plenum			Inner Plenum (no uneven BU)	
Use A-4		Hot Spot	Use H-3	Hot Spot
	Hot	Hot Stripe	Hot	Hot Stripe
Elevation:	Channel:	Test Case	Channel:	Test Case
-35.08	1.341	1.341	1.022	1.022
-31.59	1.200	1.200	1.003	1.003
-28.1	1.180	1.180	0.994	0.994
-24.61	1.251	1.251	1.046	1.046
-21.11	1.341	1.341	1.168	1.168
-17.62	1.393	1.393	1.145	1.145
-14.13	1.549	1.549	1.324	1.324
-10.64	1.993	2.084	1.569	1.981
10.64	1.903	2.125	1.649	1.963
14.13	1.617	1.617	1.403	1.403
17.62	1.421	1.421	1.307	1.307
21.11	1.317	1.317	1.217	1.217
24.61	1.270	1.270	1.177	1.177
28.1	1.286	1.286	1.109	1.109
31.59	1.287	1.287	1.152	1.152
35.08	1.421	1.859	1.246	1.457

Table 4.6.1: Derived Nominal Operating Conditions for the NBSR

(These are the minimum flows to assure that there be no nucleate boiling at any point in the core.)

Inlet Temperature (ºF)	Inner Plenum Flow (gpm)	Outer Plenum Flow (gpm)	Total Flow (gpm)
105	1100	5300	6400
110	1150	5400	6550
115	1200	5500	6700

Table 4.6.2: Safety Limits for One Variable with other two at the Safety System Settings

Inner Plenum			Outer Plenum		
Inlet Temp. ºF	Flow gpm	Total Power MW	Inlet Temp. ºF	Flow gpm	Total Power MW
130 (SSS)	1200 (SSS)	45 (SL)	130 (SSS)	4700 (SSS)	39 (SL)
130 (SSS)	500 (SL)	26 (SSS)	130 (SSS)	2800 (SL)	26 (SSS)
>170 (SL)	1200 (SSS)	26 (SSS)	>150 (SL)	4700 (SSS)	26 (SSS)

Table 4.6.3: Safety Limits for One Variable with other two at Normal Settings

(Note that 115 ºF is higher than the usual inlet temperature.)

Inner Plenum			Outer Plenum		
Inlet Temp. ºF	Flow gpm	Total Power MW	Inlet Temp. ºF	Flow gpm	Total Power MW
115 (N)	1450 (N)	52 (SL)	115 (N)	6850 (N)	49 (SL)
115 (N)	350 (SL)	20 (N)	115 (N)	1850 (SL)	20 (N)
>170 (SL)	1450 (N)	20 (N)	>170 (SL)	6850 (N)	20 (N)

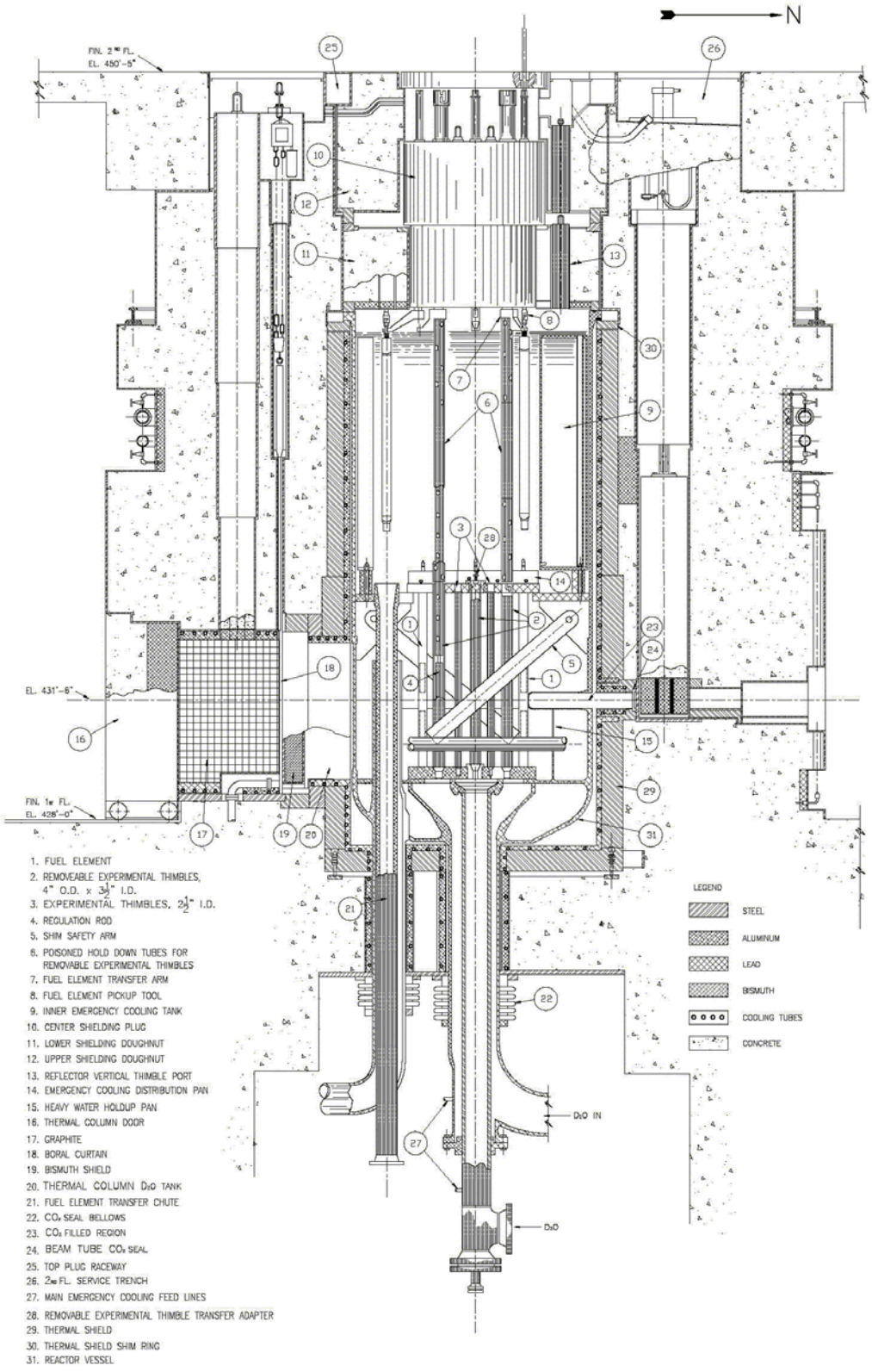

Figure 4.2.1: Reactor Elevation

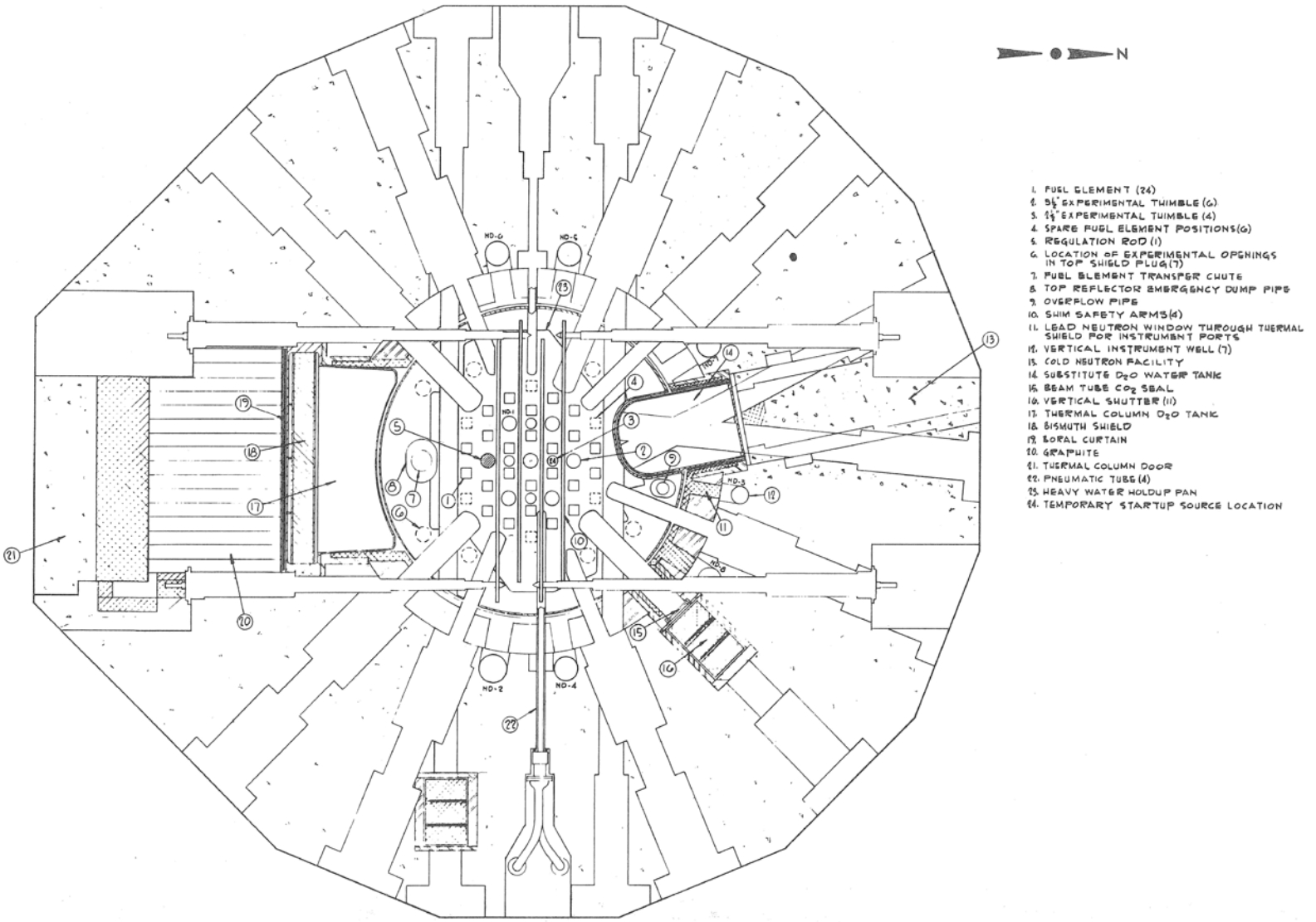

Figure 4.2.2: Reactor Plan View

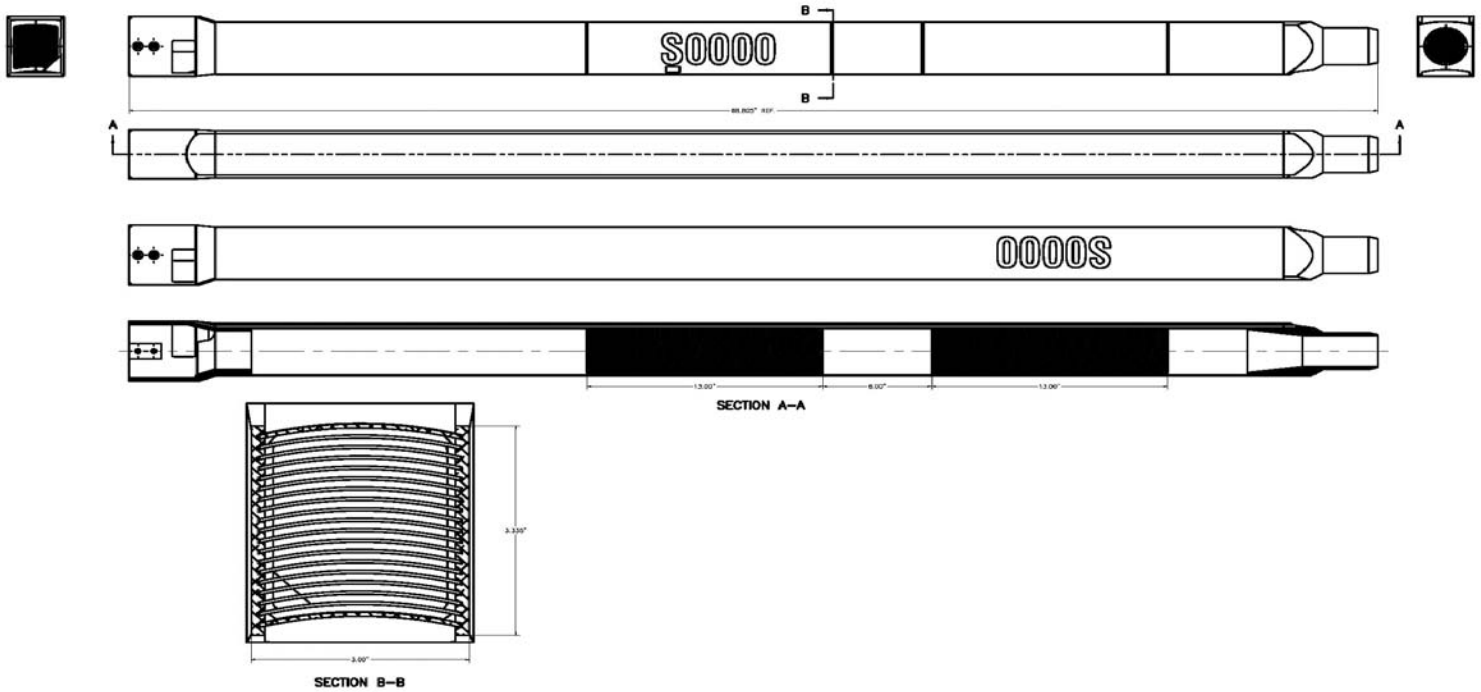

Figure 4.2.3: Fuel Element Assembly

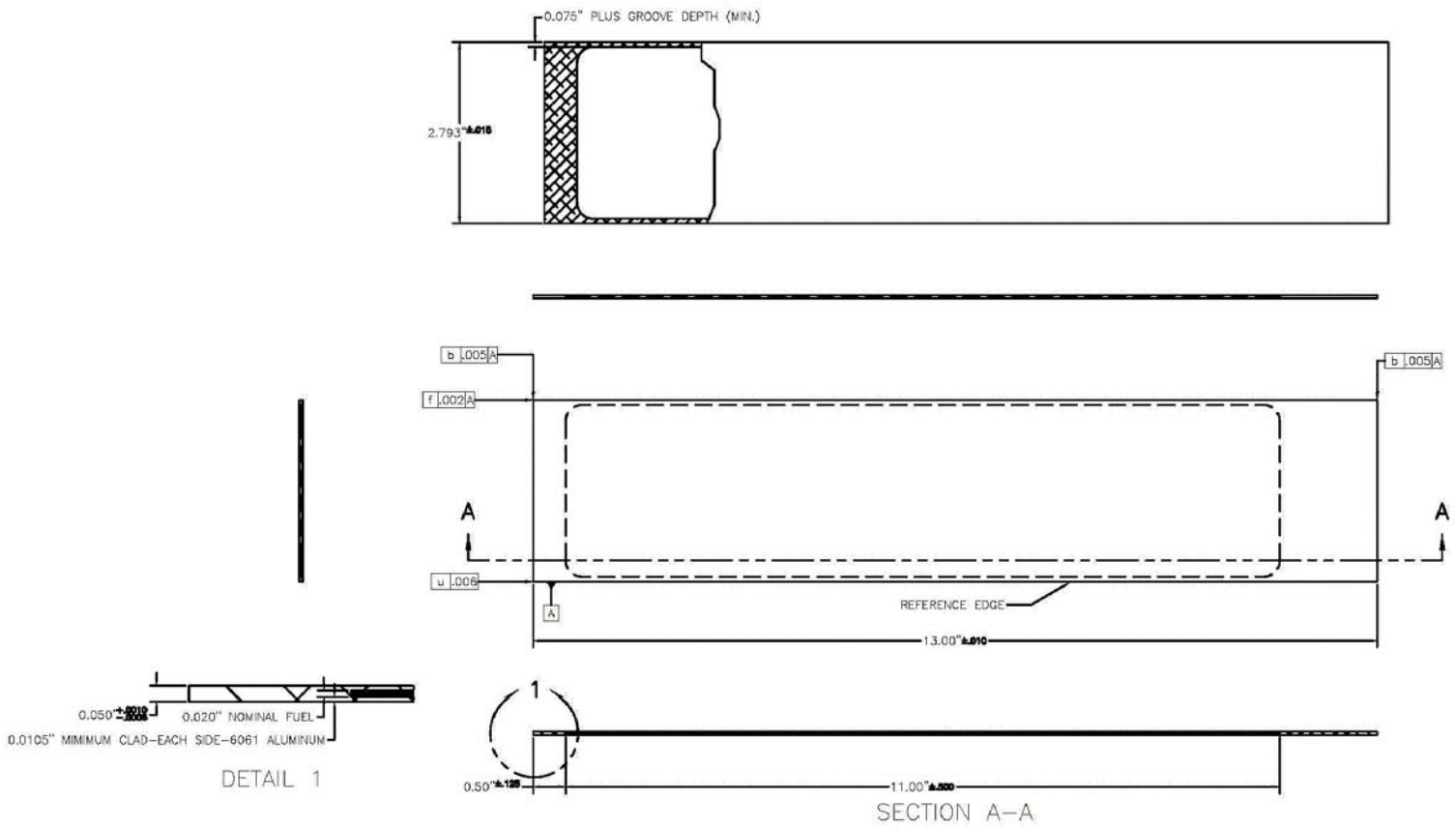

Figure 4.2.4: Typical Top and Bottom Flat Fuel Plate

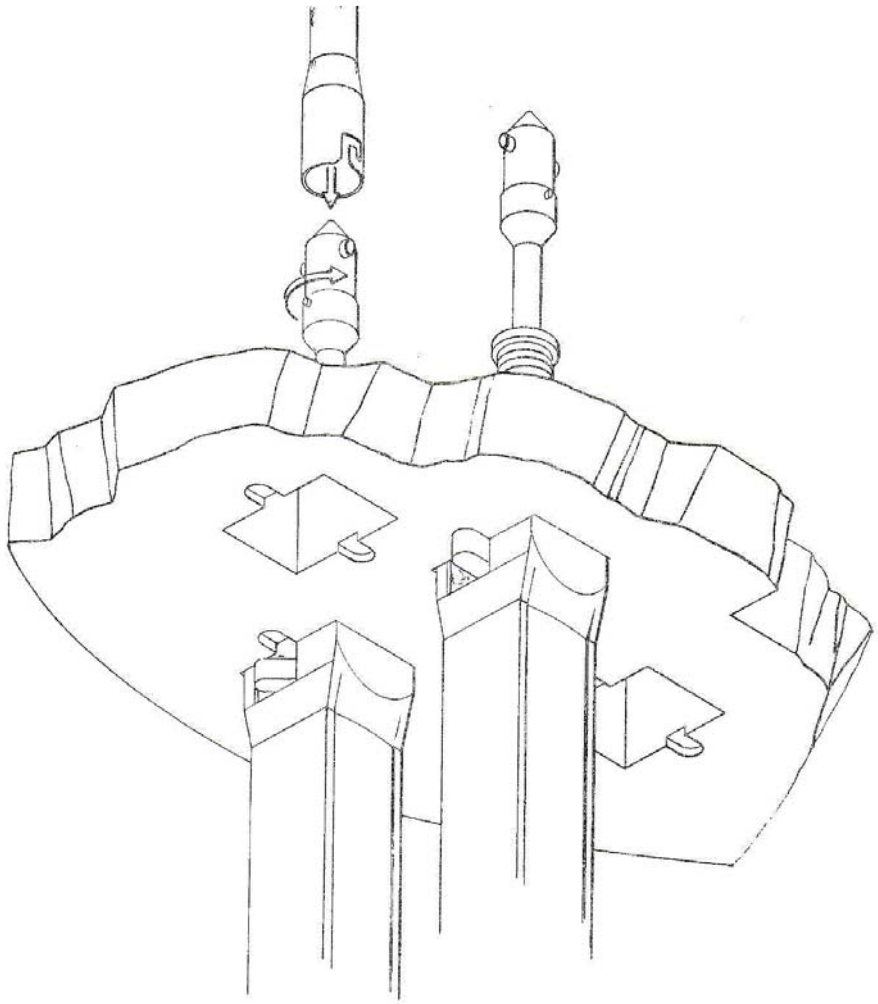

Figure 4.2.5: Isometric Of Fuel Element Locking Mechanism

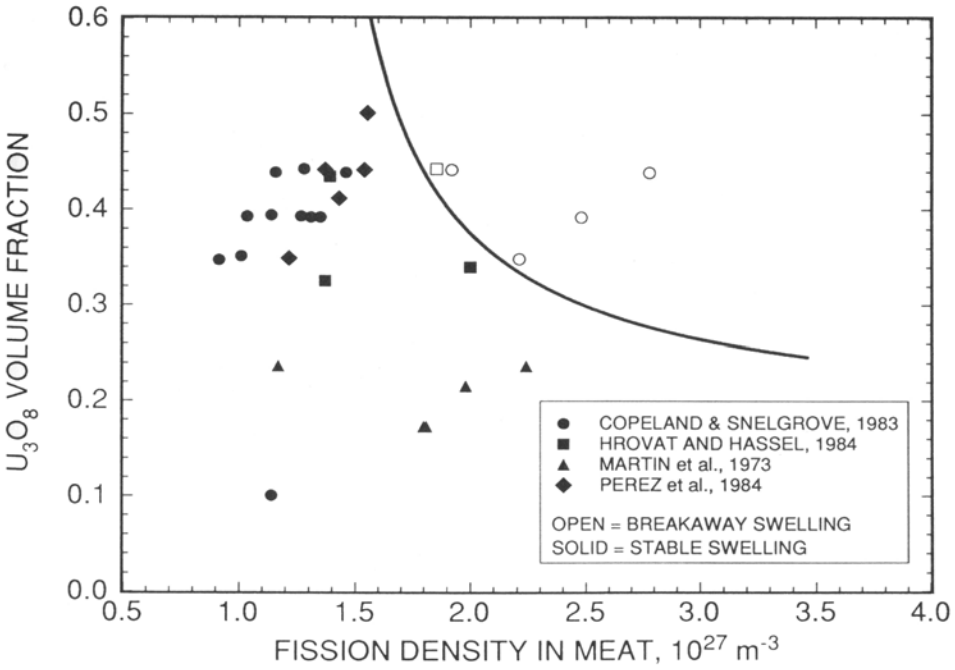

Figure 4.2.6: Burnup Failure Diagram For U_3O_8 – Al Plate

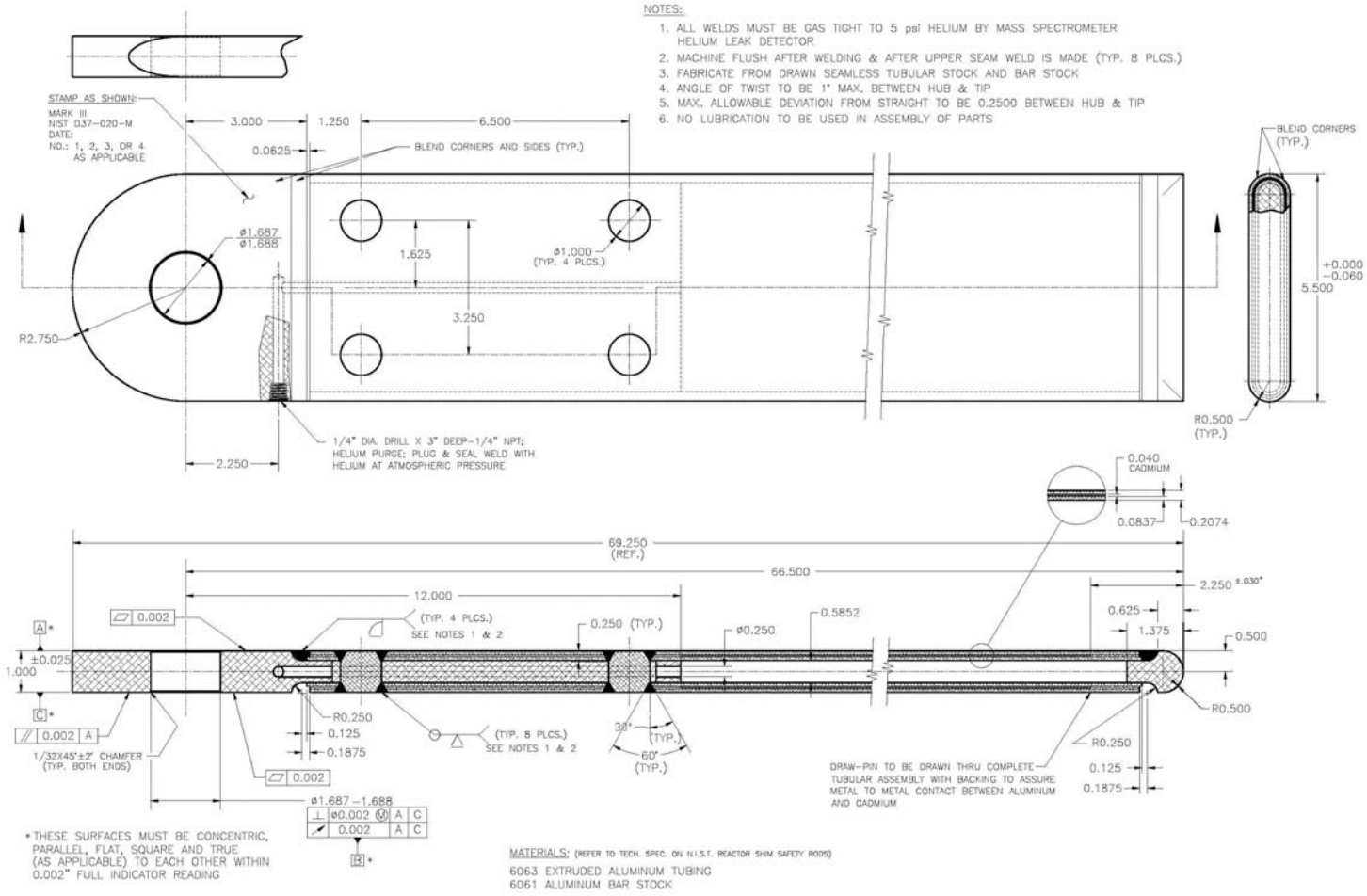

Figure 4.2.7: Shim Safety Arm – Detailed Design

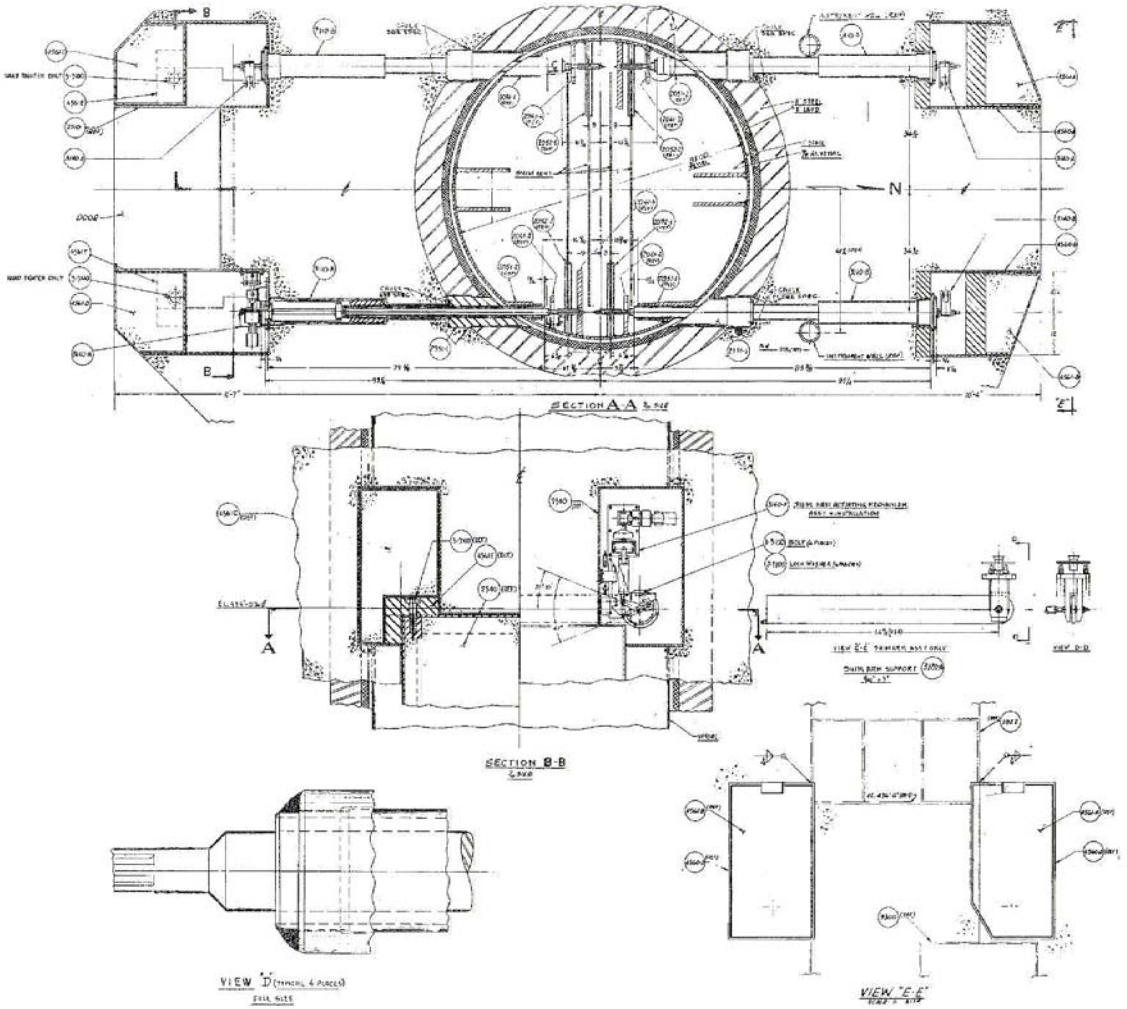

Figure 4.2.8: Shim Safety Arm System Assembly

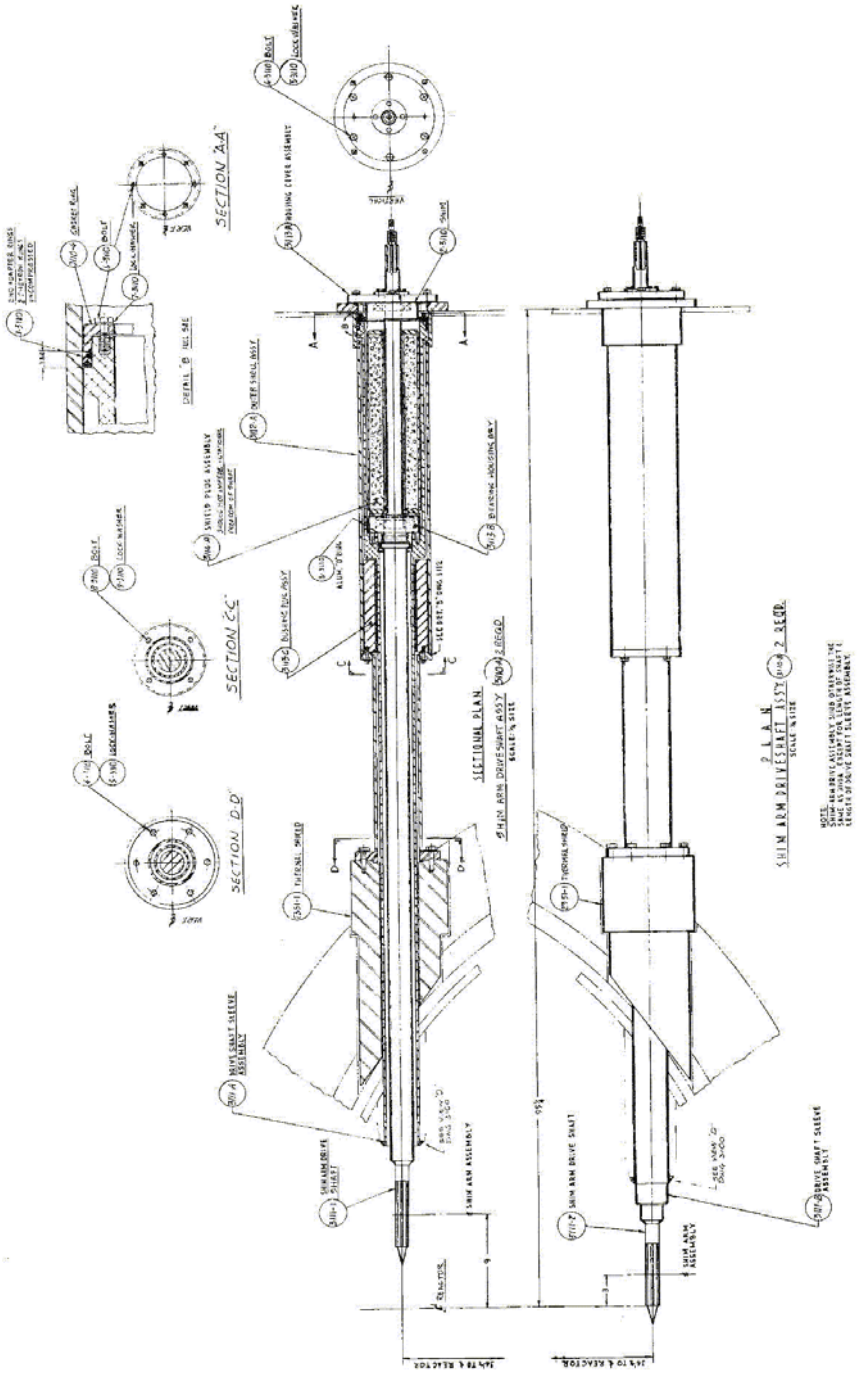

Figure 4.2.9: Shim Safety Arm Drive Shaft Assembly

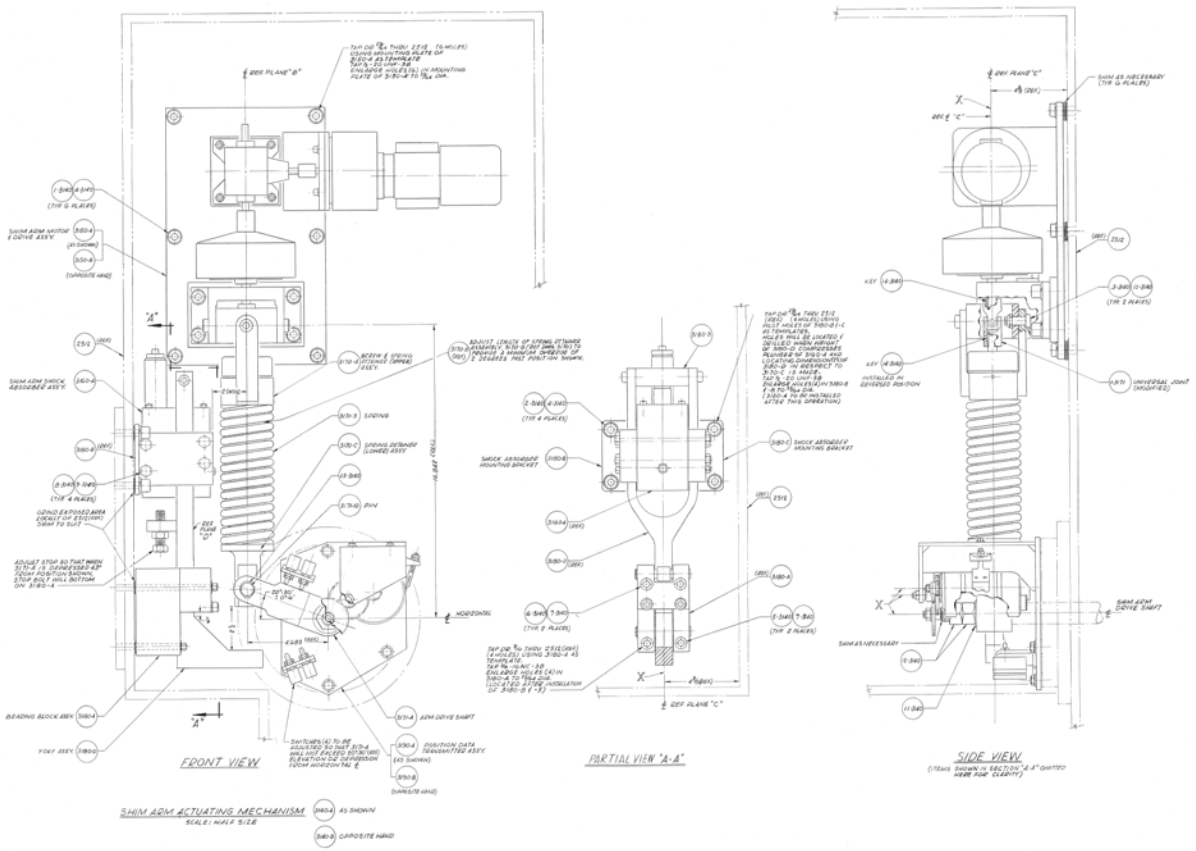

Figure 4.2.10: Shim Safety Arm Drive Mechanism

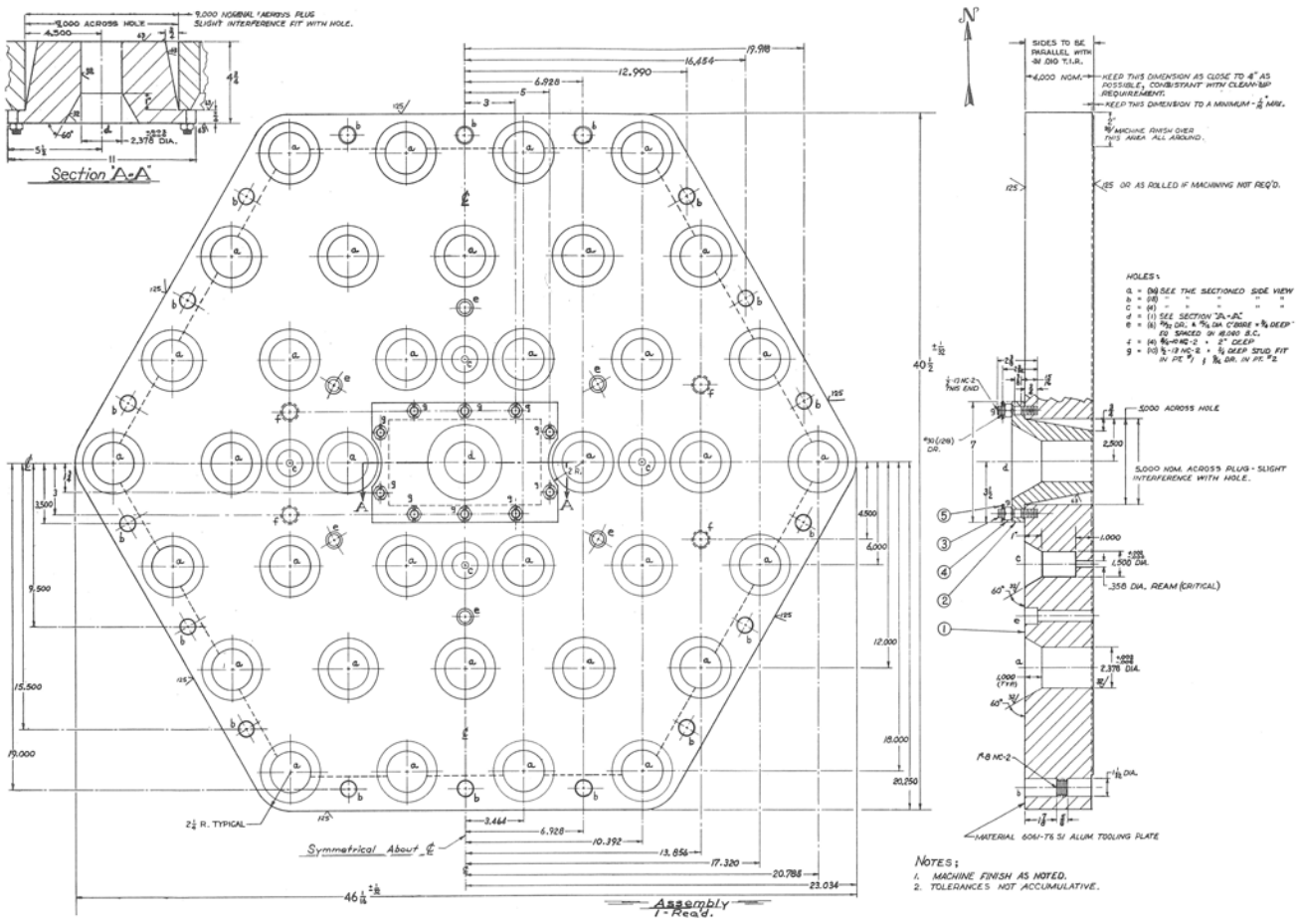

Figure 4.2.11: Lower Grid Plate

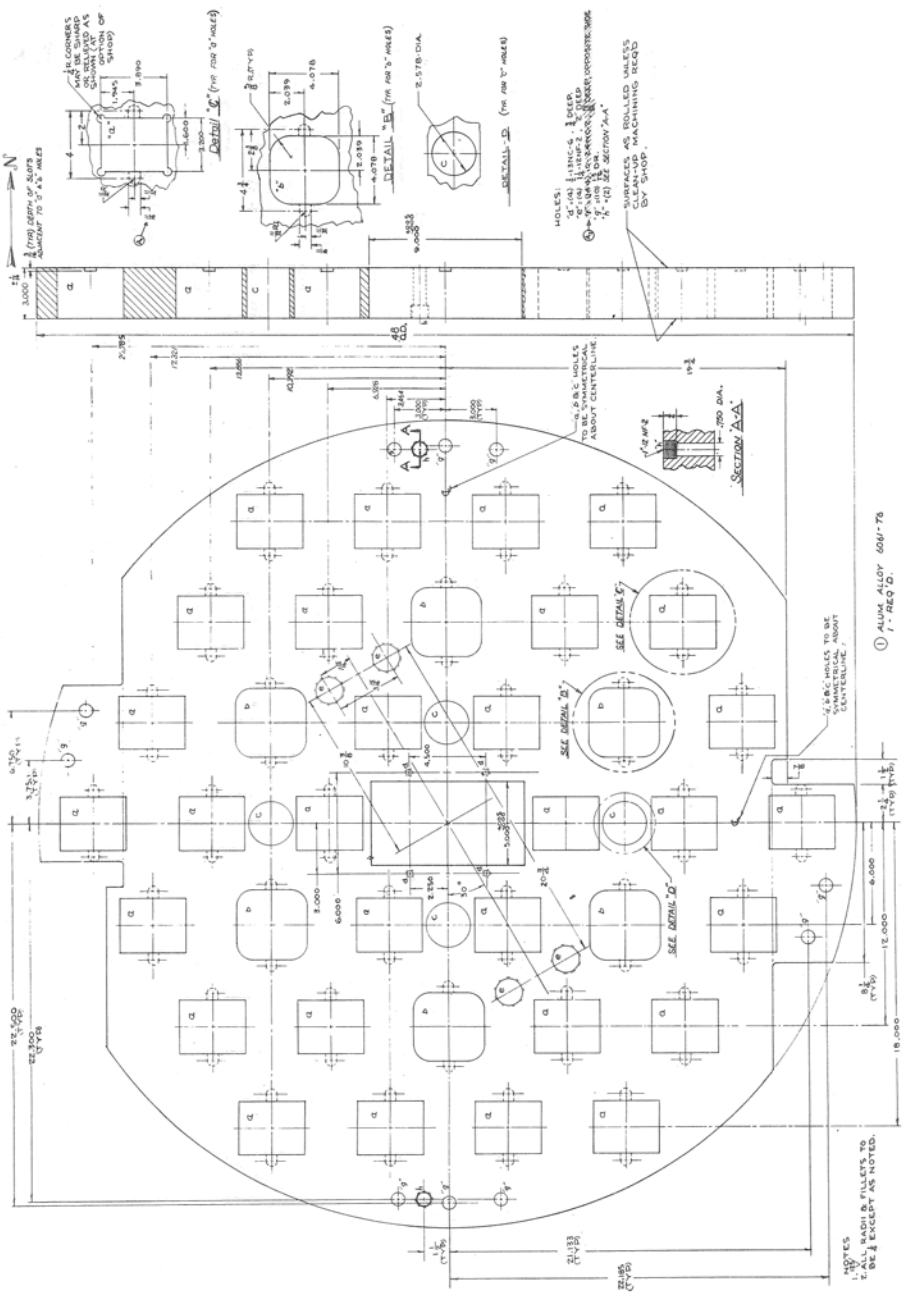

Figure 4.2.12: Upper Grid Plate

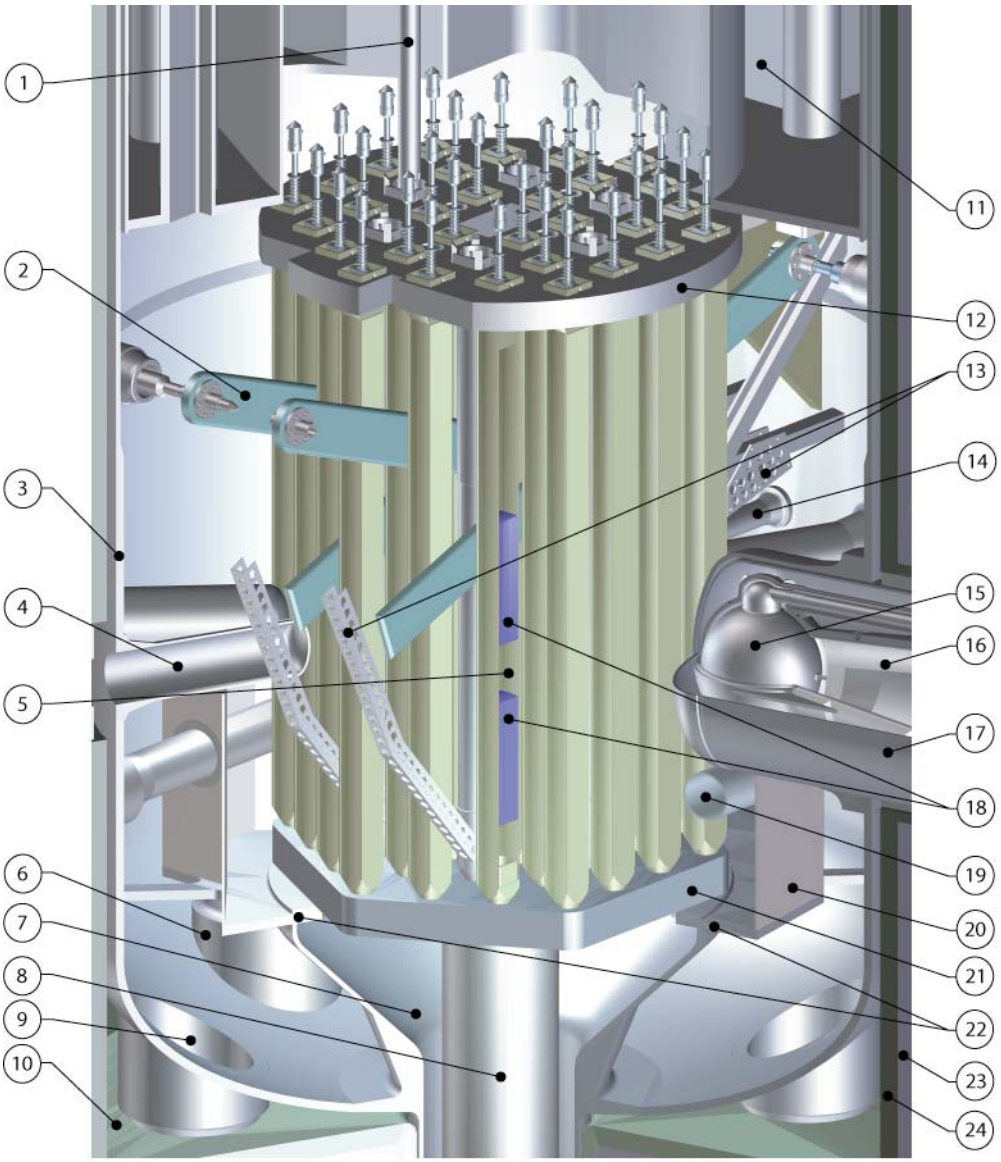

1 Poisoned Hold Down Tube (1 of 7)
2 Shim Arm #2
3 Reactor Vessel
4 BT-2 Thimble
5 Element Unfueled Gap
6 D_2O Outlet (1 of 2)
7 D_2O Inlet - Outer Plenum
8 D_2O Inlet – Inner Plenum
9 Fuel Transfer Chute Opening
10 CO_2 Filled Region
11 Inner Reserve Tank
12 Upper Grid Plate w/30 Elements
13 Shim Arm Guide Extension # 3
14 RT-3 Pneumatic Tube
15 Cold Source Moderator Chamber
16 Cold Source Insulating Vacuum
17 Cold Source D_2O Cooling Jacket
18 Fuel Plates, Upper and Lower Sections
19 Through Tube (North)
20 Heavy Water Holdup Pan
21 Lower Grid Plate
22 Outer Plenum Flange
23 Steel (Thermal Shield)
24 Lead (Thermal Shield)

Figure 4.3.1: Reactor Vessel Internal Structure

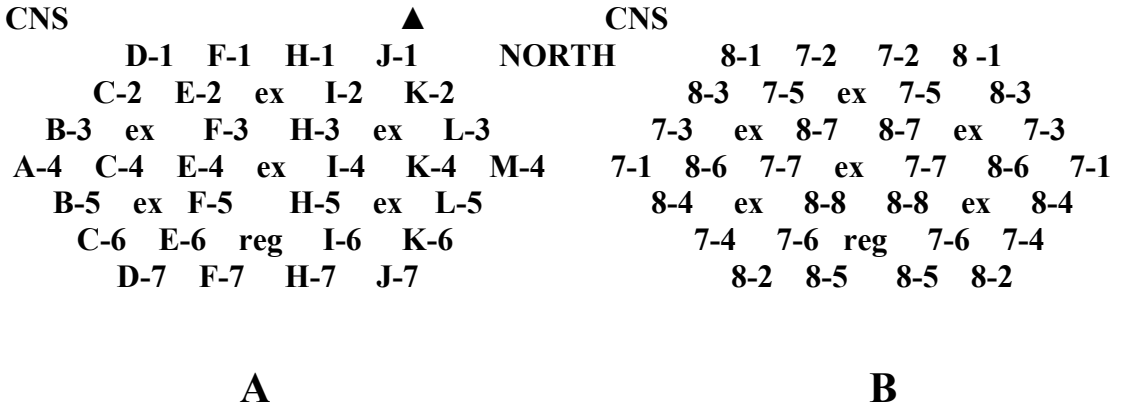

Figure 4.5.1A: Map of the Locations of the FEs

Figure 4.5.1B: Diagram of the Fuel Management Scheme

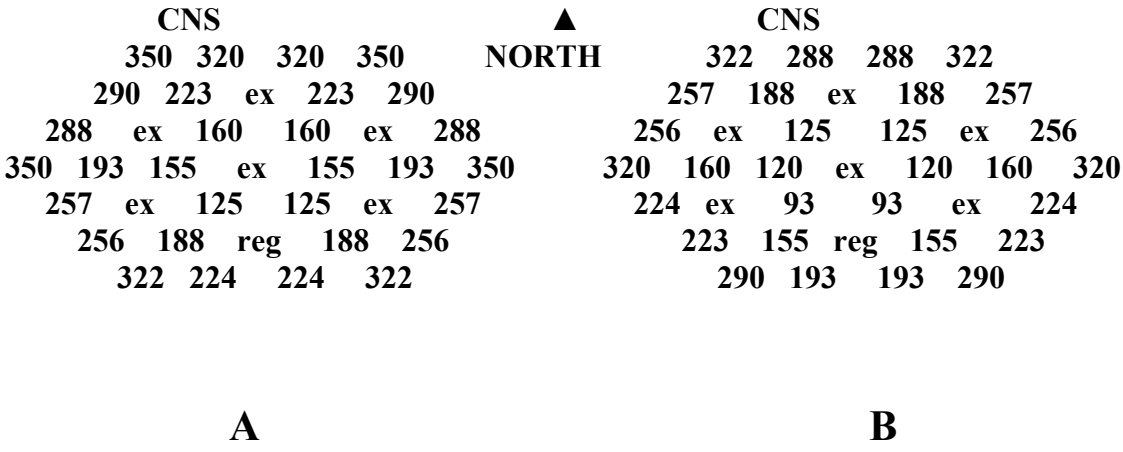

Figure 4.5.2A: Map of the Expected ^{235}U Masses (grams) in Each FE in the Startup Core

Figure 4.5.2B: ^{235}U Masses End-of-Cycle Core of a Typical, 38-Day Reactor Cycle

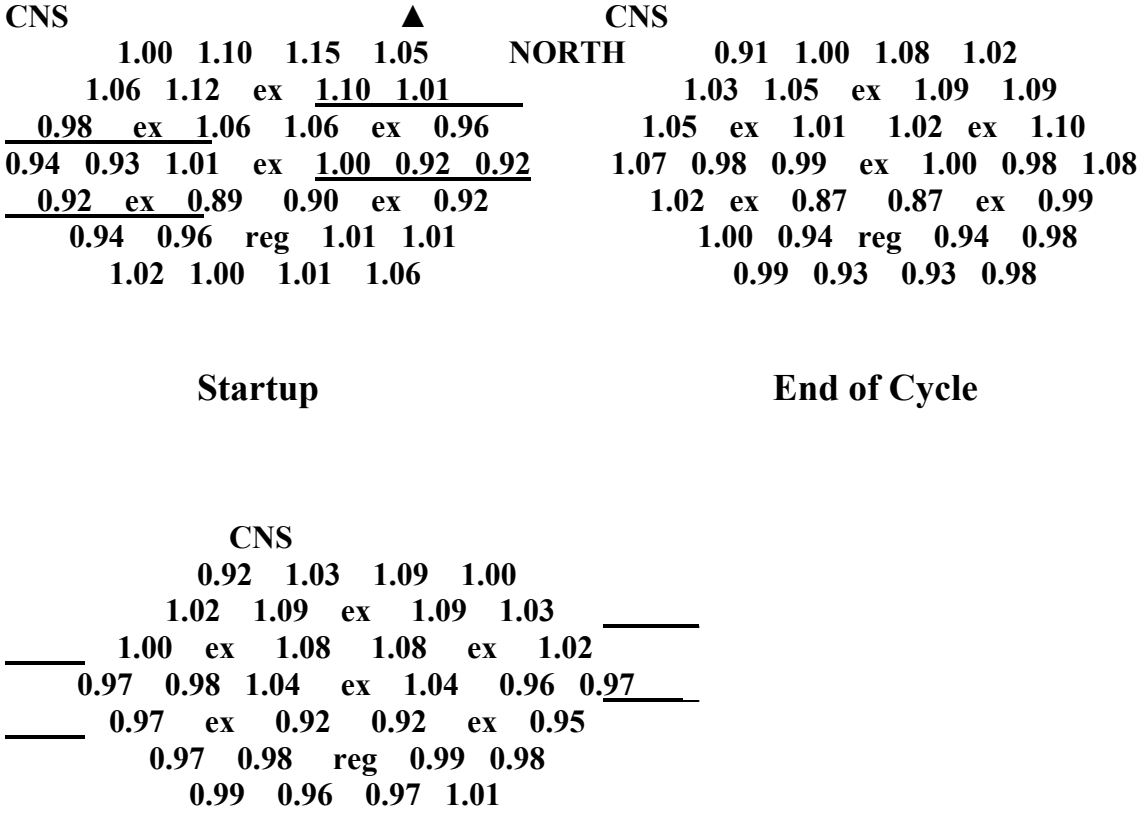

Figure 4.5.3: Relative Fission Power in the SU, EOC, and BOC Cores

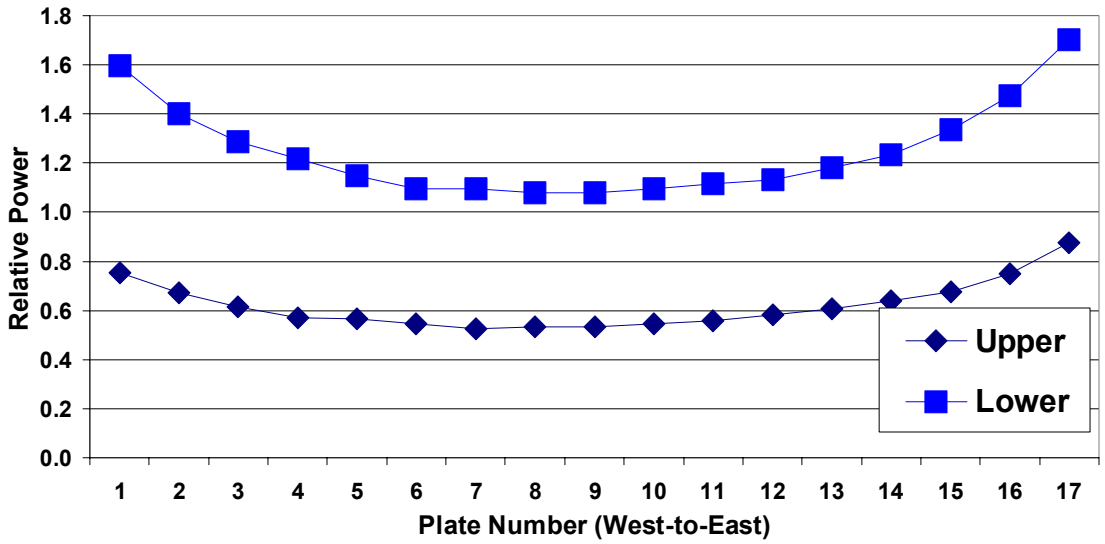

Figure 4.5.4: Plate-Wise Relative Power Distribution in the A-4 FE in the SU Core
(Updated MCNP model)

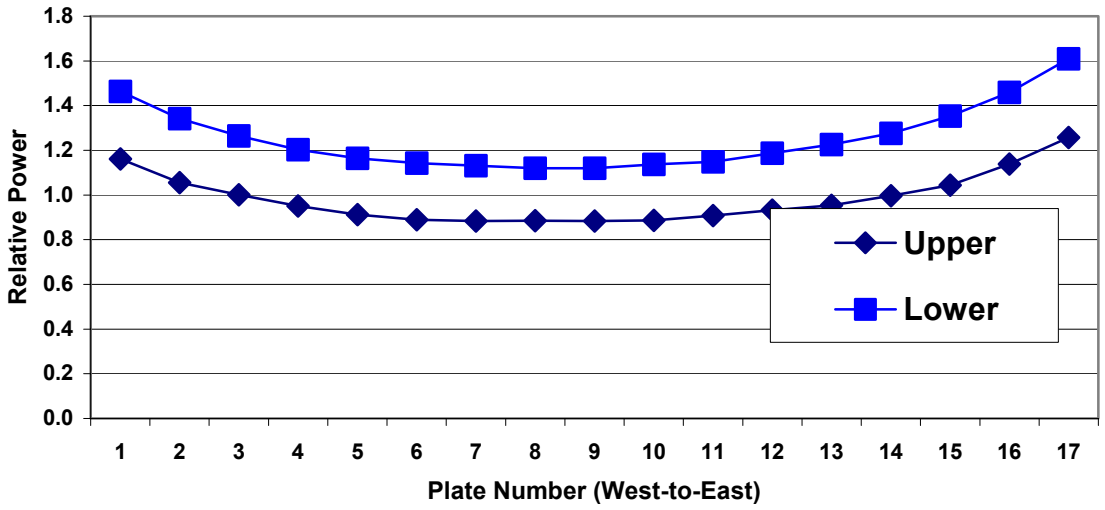

Figure 4.5.5: Plate-Wise Relative Power Distribution in the E-2 FE in the SU Core
(Updated MCNP model)

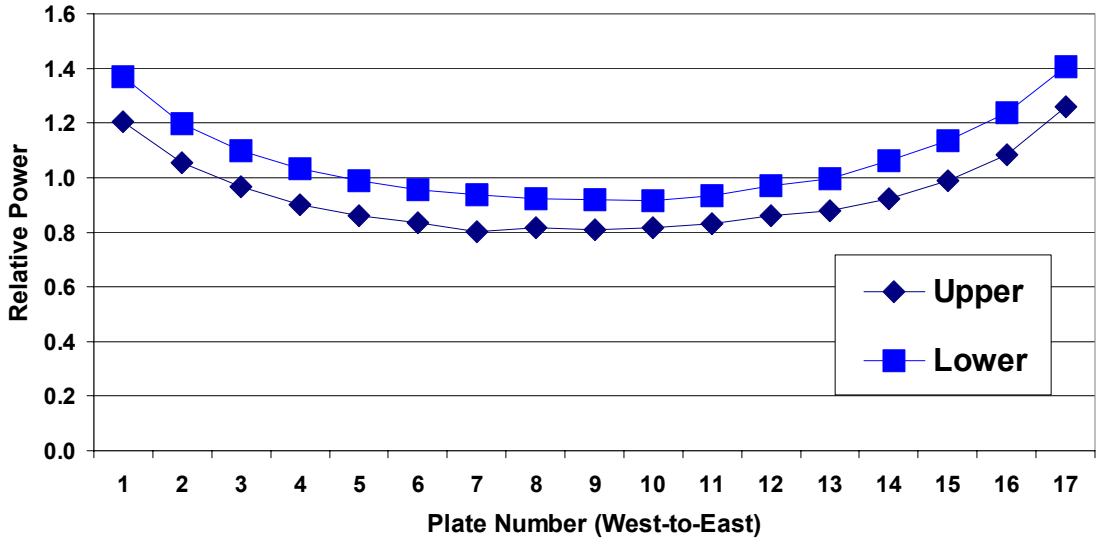

Figure 4.5.6: Plate-Wise Relative Power Distribution in the D-1 FE in the SU Core
(Updated MCNP model)

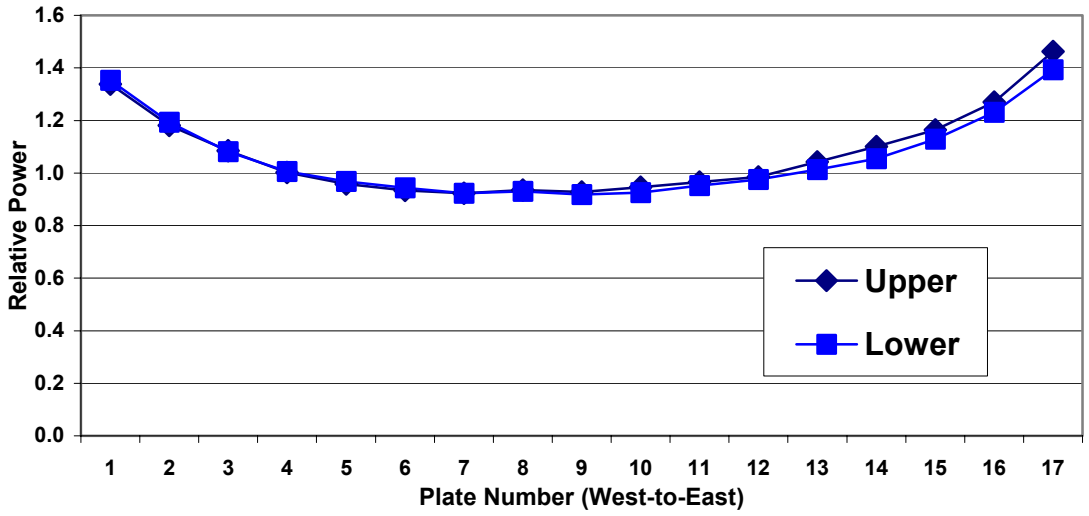

Figure 4.5.7: Plate-Wise Relative Power Distribution in the A-4 FE in the EOC Core
(Updated MCNP model)

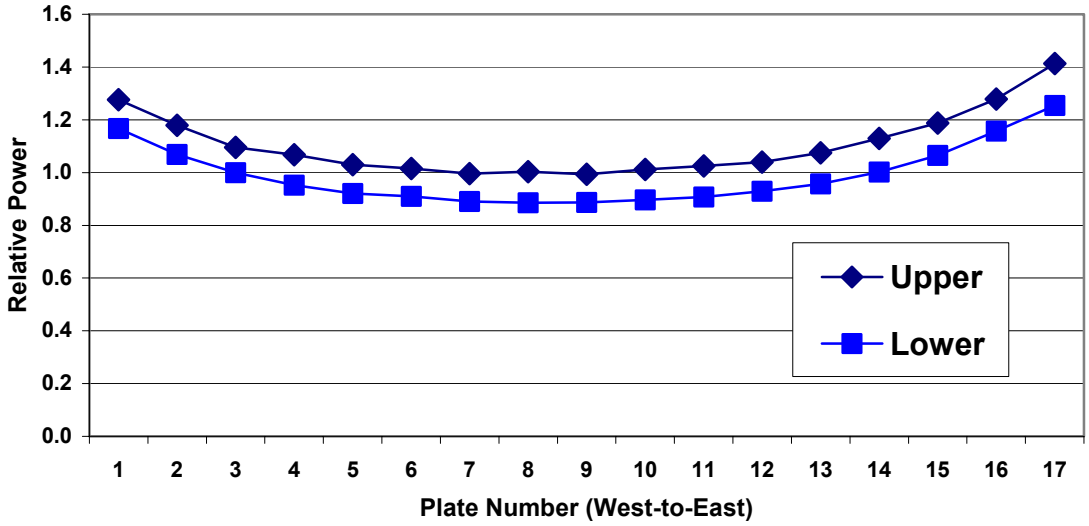

Figure 4.5.8: Plate-Wise Relative Power Distribution in the E-2 FE in the EOC Core
(Updated MCNP model)

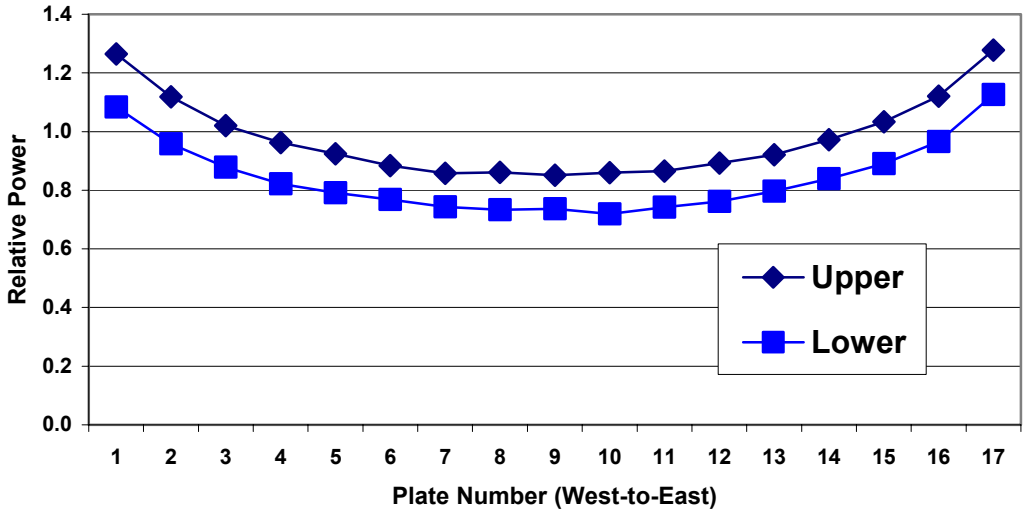

Figure 4.5.9: Plate-Wise Relative Power Distribution in the D-1 FE in the EOC Core
(Updated MCNP model)

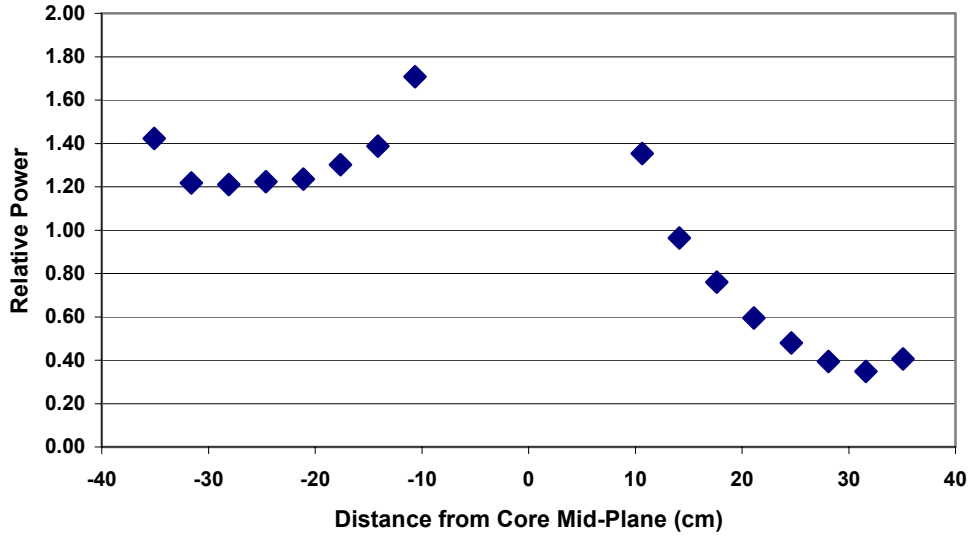

Figure 4.5.10: Relative Power in the FE A-4 vs. Elevation for the SU Core
(Updated MCNP model)

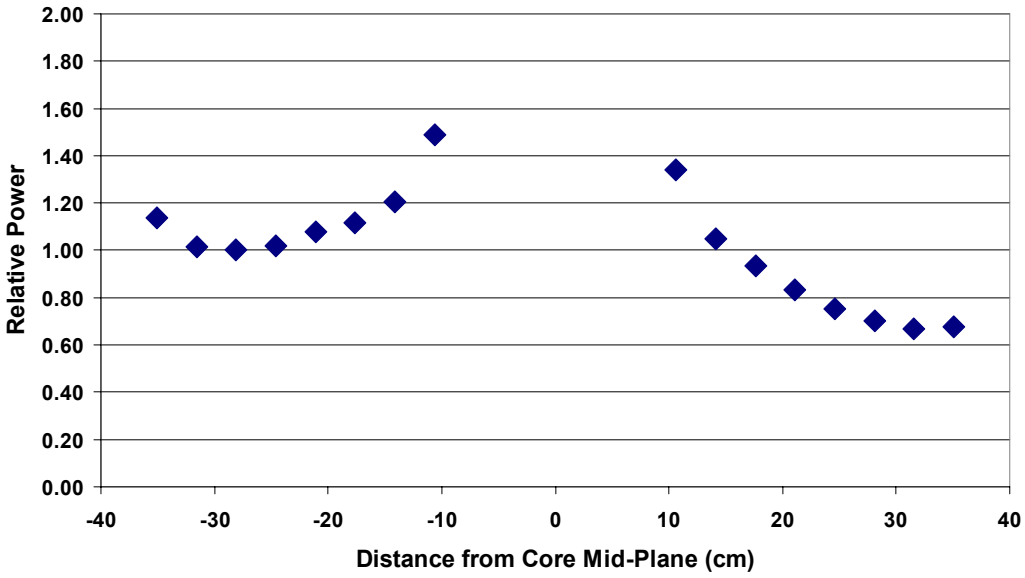

Figure 4.5.11: Relative Power in the FE E-2 vs. Elevation for the SU Core
(Updated MCNP model)

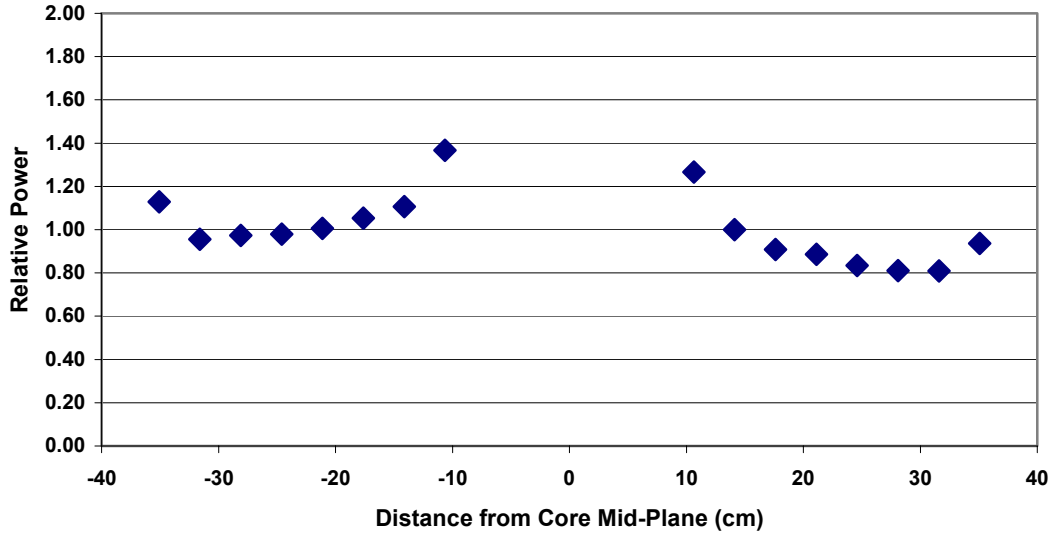

Figure 4.5.12: Relative Power in the FE D-1 vs. Elevation for the SU Core
(Updated MCNP model)

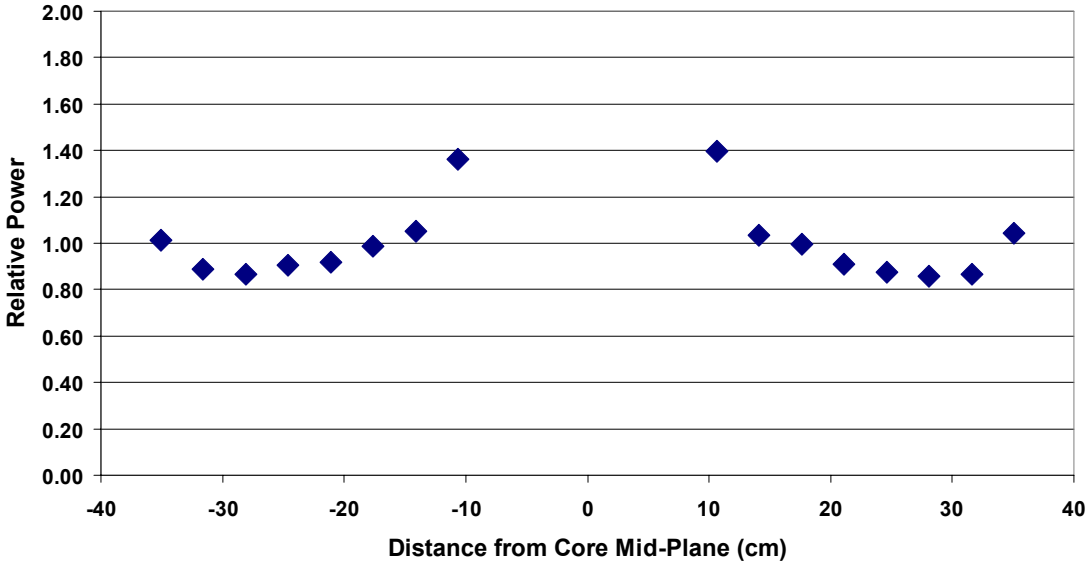

Figure 4.5.13: Relative Power in the FE A-4 vs. Elevation for the EOC core
(Updated MCNP model)

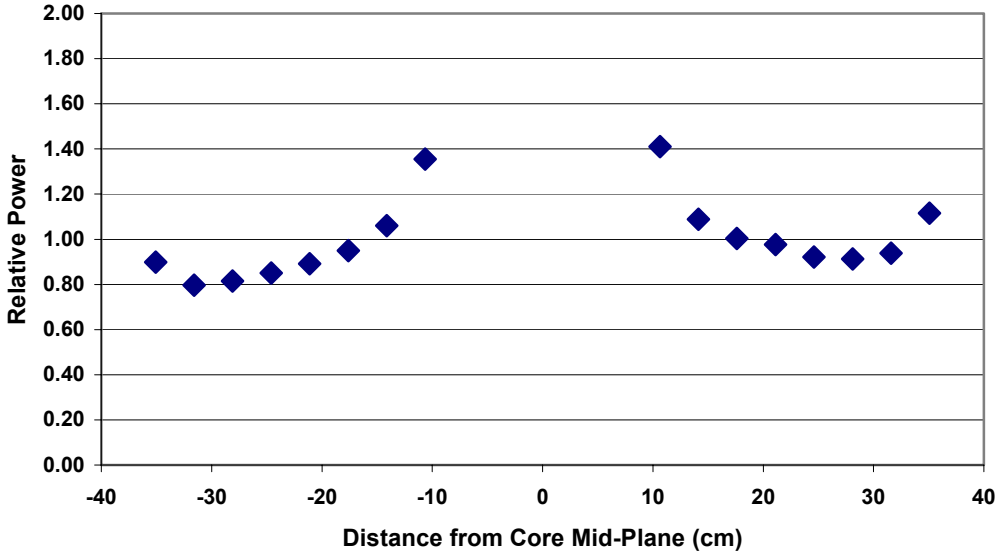

Figure 4.5.14: Relative Power in the FE E-2 vs. Elevation for the EOC core
(Updated MCNP model)

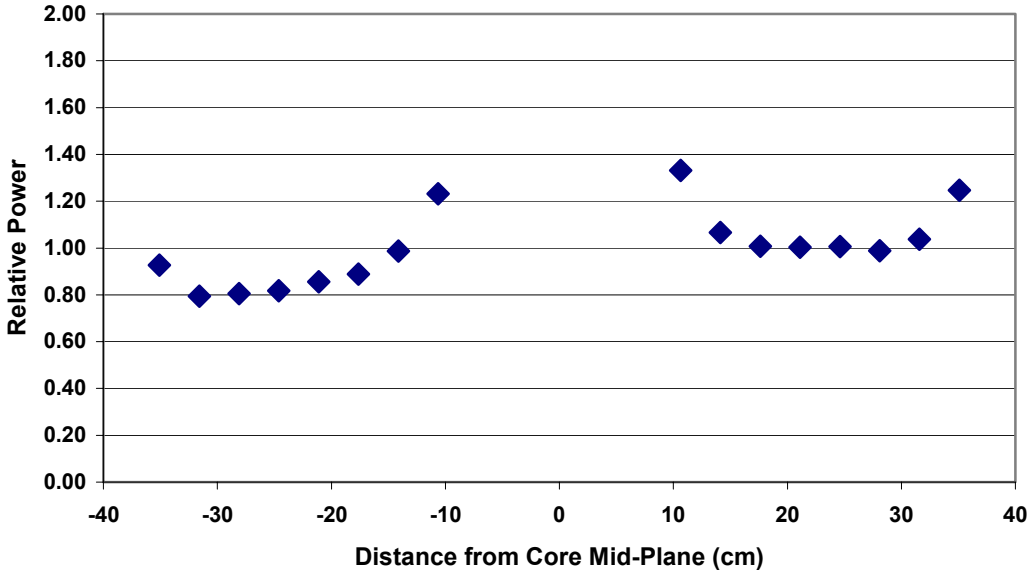

Figure 4.5.15: Relative Power in the FE D-1 vs. Elevation for the EOC core
(Updated MCNP model)

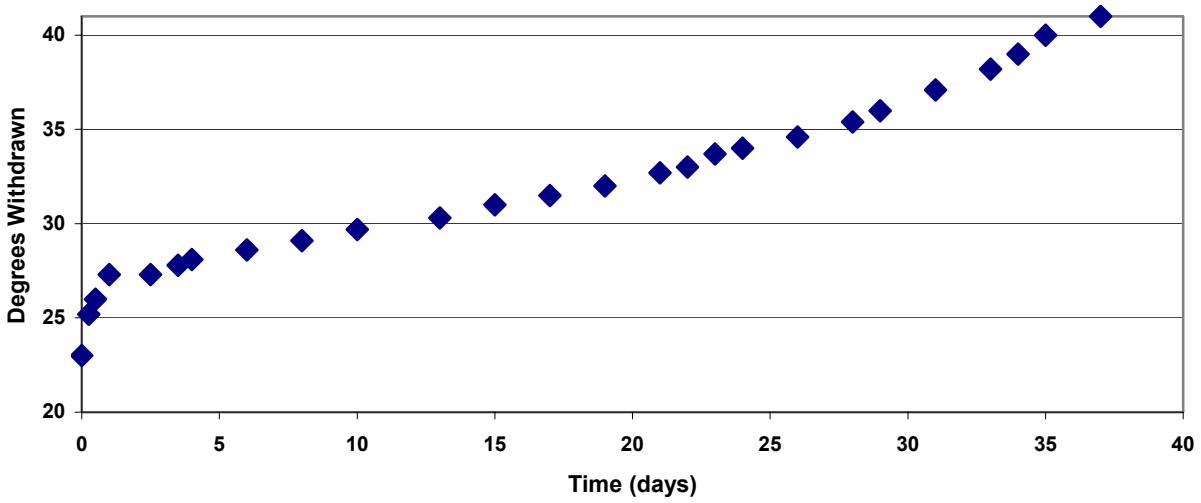

Figure 4.5.16: Position of the Shim Safety Arms during the Reactor Cycle Starting May 2, 2002

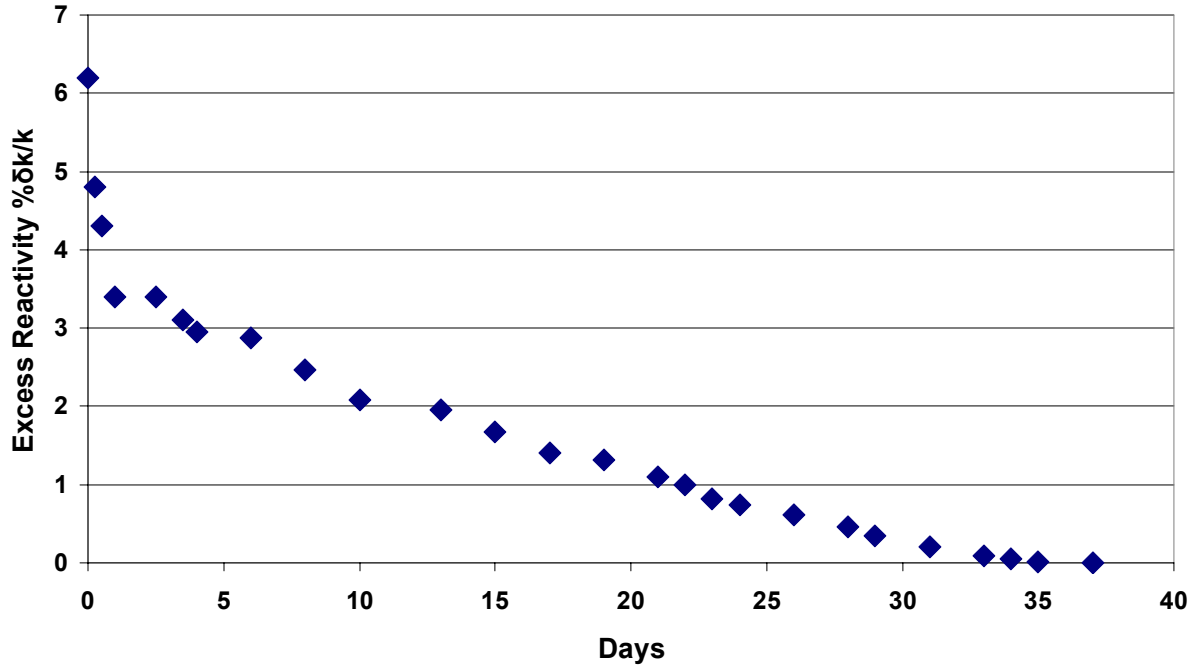

Figure 4.5.17: Excess Reactivity during the Reactor Cycle of May 2, 2002

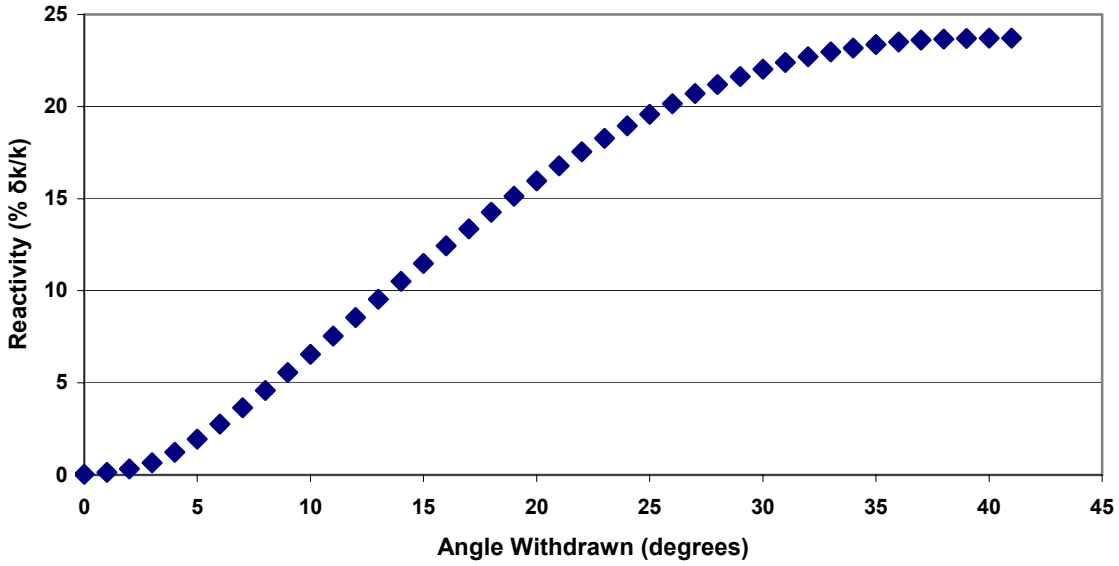

Figure 4.5.18: Measured Integral Worth of the Shim Arm Bank vs. Angle Withdrawn

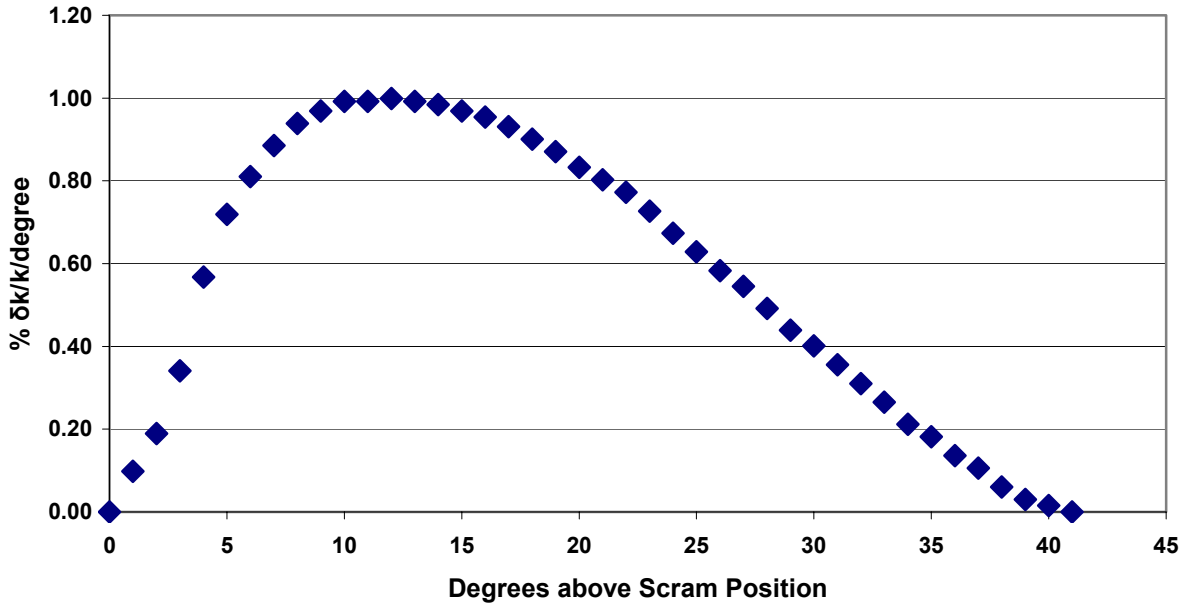

Figure 4.5.19: Measured Differential Shim Bank Reactivity vs. Angle Withdrawn

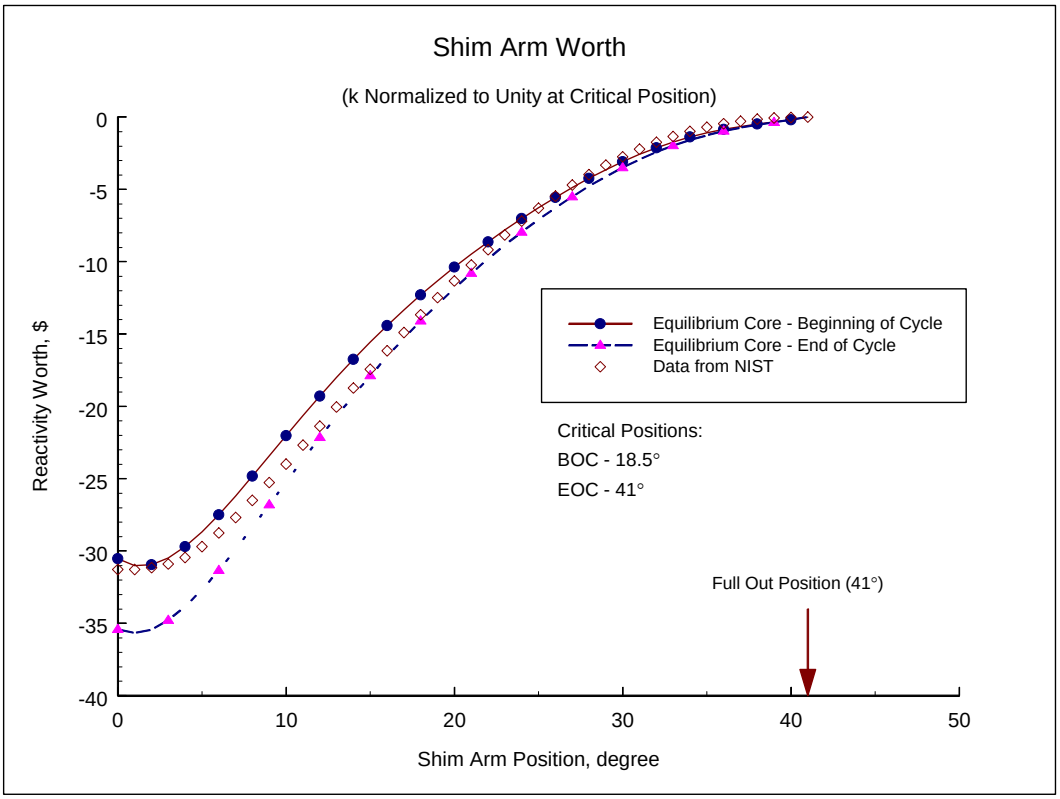

Figure 4.5.20: Fitted Curves of Shim Arm Bank Worth vs. Position

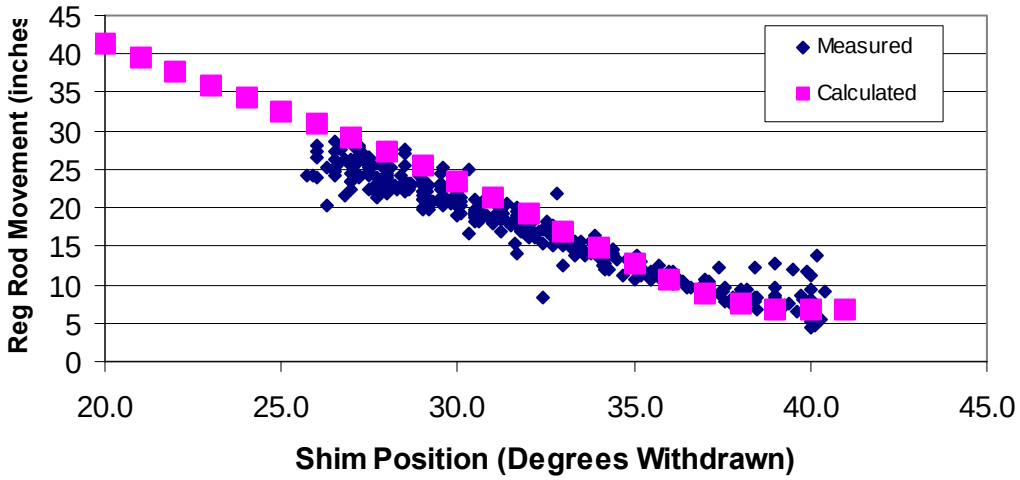

Figure 4.5.21: Calculated Differential Shim Bank Worth vs. Measurements

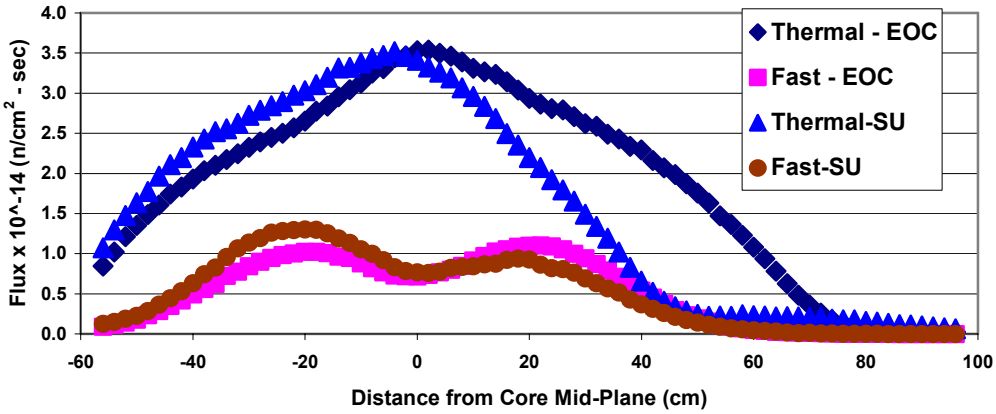

Figure 4.5.22: Calculated Axial Neutron Flux Distributions for the SU (Updated Model) and EOC Cores

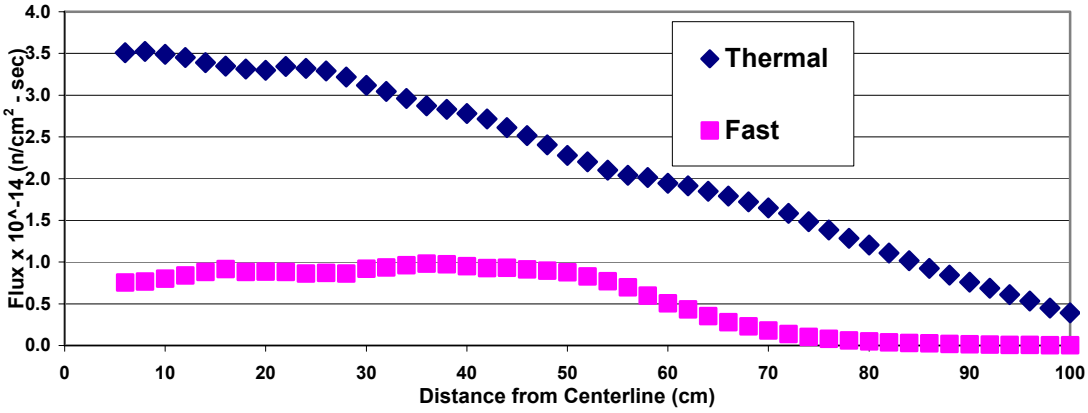

Figure 4.5.23: Calculated Radial Fast and Thermal Neutron Flux Distributions
(Core Mid-Plane)

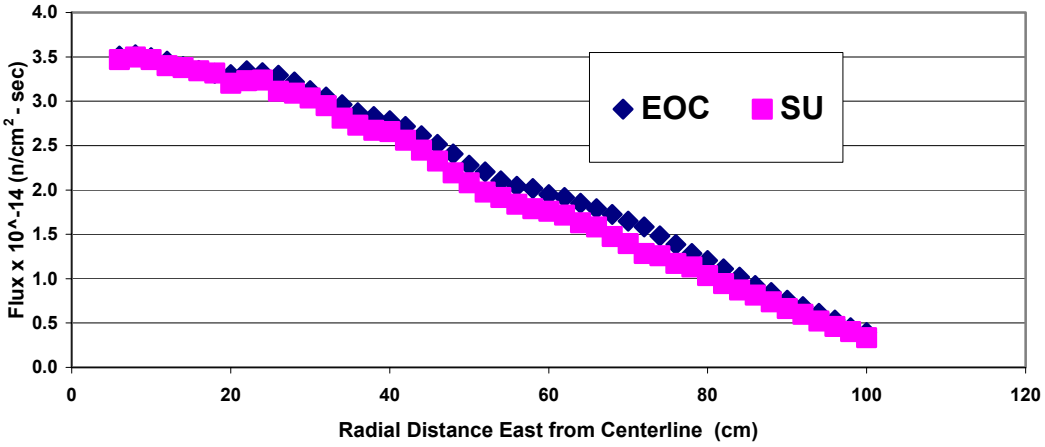

Figure 4.5.24: Comparison of the Radial Thermal Neutron Fluxes for the SU and EOC Cores

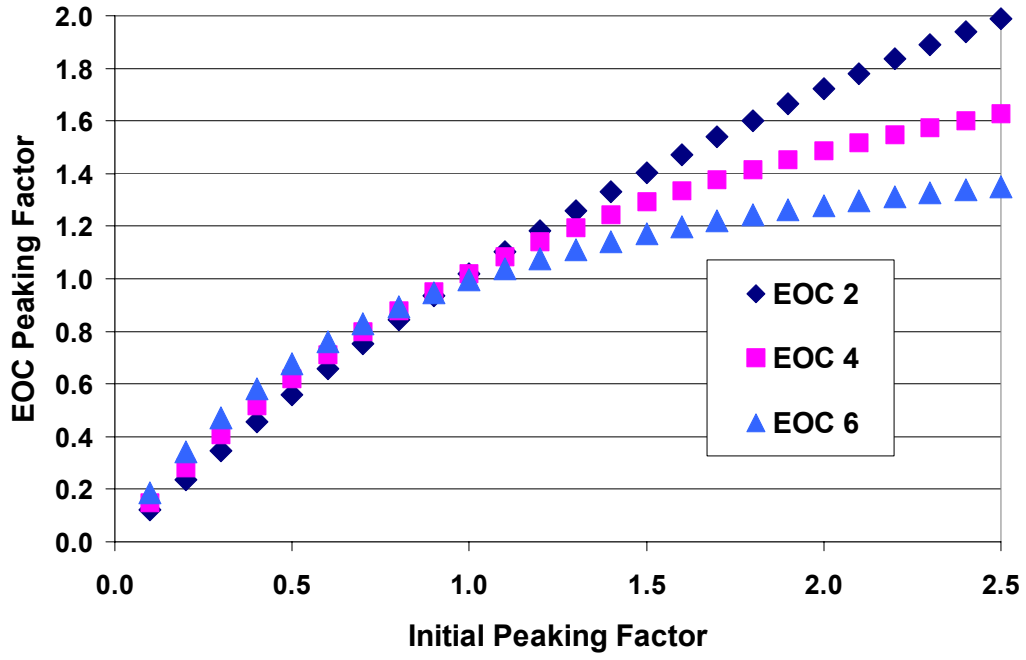

Figure 4.5.25: Generic Behavior of Hot Spot Peaking Factors
(Uneven Burnup Corrections after 2, 4 and 6 Cycles)

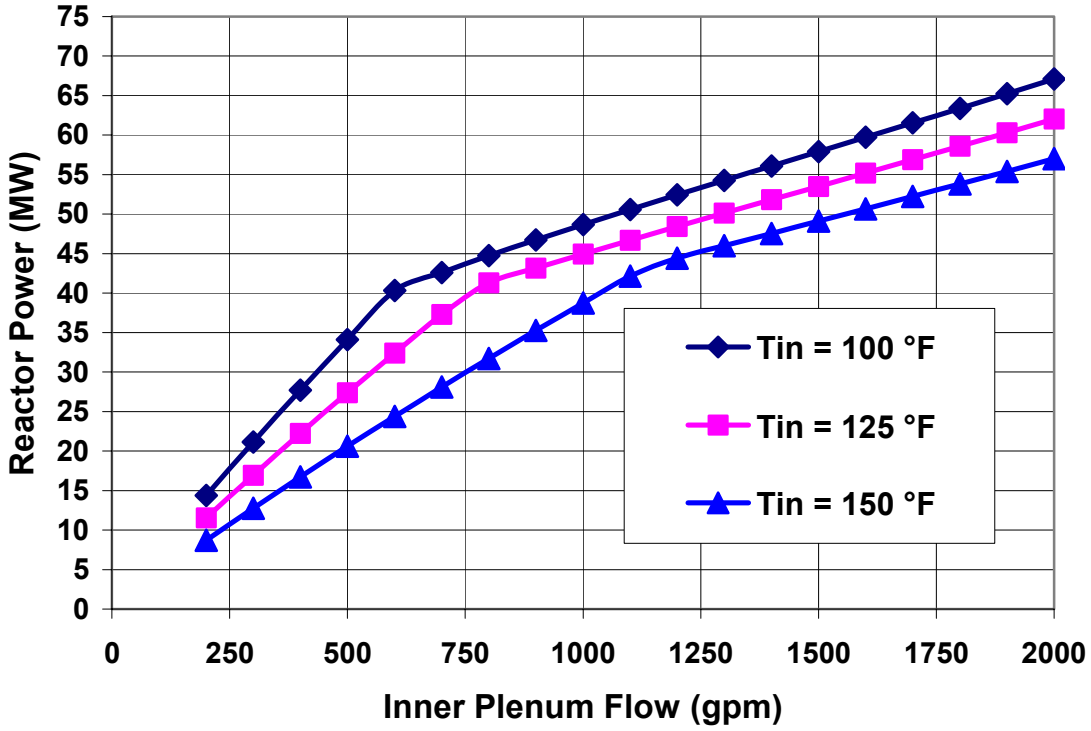

Figure 4.6.1: Safe operating limits for NBSR Inner Plenum
(Determined by the Costa OFI correlation and the Mirshak DNB correlation, using MCNP hot spot data for the inner plenum)

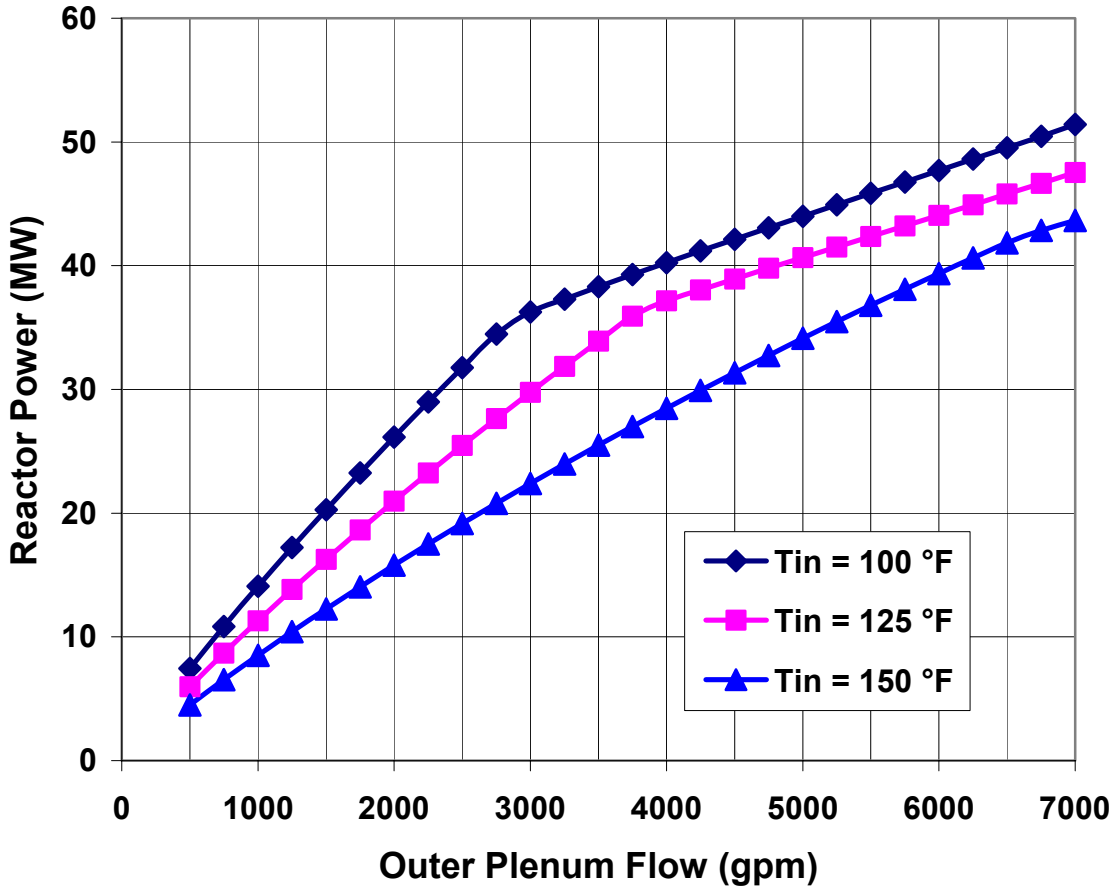

Figure 4.6.2: Safe operating limits for NBSR Outer Plenum
(Determined by the Costa OFI correlation and the Mirshak DNB correlation, using MCNP hot spot data for the outer plenum.)